UNIVERSITÀ DEGLI STUDI DI PADOVA

Dipartimento di Fisica e Astronomia "Galileo Galilei"

Corso di Laurea Magistrale in Fisica

Tesi di Laurea

An Effective Field Theory Approach To Non Standard Neutrino Interactions

Relatore

Prof. Paride Paradisi

Laureando

Francesca Ferranti

Anno Accademico 2017/2018

ABSTRACT

The present work will focus on possible effects due to Non Standard Interactions (NSI) on the observables at stake in atmospherical and reactor neutrino experiments. We worked within an Effective Field Theory approach, where NSI arise from dimension six operators defined at a scale Λ much bigger than the Electroweak scale (m_{EW}). Through Renormalization Group Equation methods the effects of these operators are studied below m_{EW}. As an explicit proof of the correctness of our calculations, we checked the cancellation of the renormalization scale dependence in physical amplitudes. We provided an explicit calculation of the corrections to the oscillation probabilities and to relevant neutrino scattering cross sections, due to NSI. A complete analysis of the most recent and future experimental results is also provided.

CONTENTS

INTRODUCTION

It is nowadays universally acknowledged that the Standard Model of Particle Physics represents the most experimentally and theoretically successful theory describing the physics of fundamental interactions. Despite the great agreement with experimental data and its impressive predictivity, there are still many open issues left. As a consequence, it is widely believed that the Standard Model needs an ultra-violet completion. In other words, it can be thought of as an Effective Field Theory of a more fundamental theory, valid beyond a certain scale $\Lambda \gg m_{\text{EW}}$. This New Physics scale Λ, according to the naturalness hypothesis, should occur already below the TeV scale, which is being directly tested at the LHC, but no signals were found during the first run, that achieved a center of mass energy of 7 TeV.
Nevertheless, the existence of many hints in the flavor sector addressing to New Physics effects represent a strong clue in the search of a high energy completion of the Standard Model.

Among the others, the nature of neutrino masses and mixing represent one of the most compelling. In the beginning, such peculiar properties were identified as the only source of lepton flavor violation but it became clear that it was possible to introduce extra lepton flavor violation sources when introducing new and dimension-six operators in the Lagrangian, using the tools provided by the Effective Field Theory approach. This methodology provides definite predictions in a suitable energy range, where a perturbative expansion is applicable. In that context, the New Physics effects are enclosed in the coefficients associated with the higher dimensional operators, called Wilson coefficients. This enables to set up a model-independent discussion; then a model-dependent analysis can be used to derive the exact expression of such coefficients in specific models.
For what concerns neutrino physics, the introduction of those operators gives birth to many new lepton flavor violating interactions, called Non-Standard Neutrino Interactions, which can affect neutrino oscillation experiments, modifying the propagation of neutrinos in matter. Moreover, they also affect the production and the detection processes, directly at the source and at the detector, producing wrong flavor neutrinos, without oscillation.
This MSc thesis is inserted within this framework: its final aim will be to develop constraints on the strength of those new interactions by analyzing the modification to the observables at stake and verifying their compatibility with current and predicted experimental results.

In order to achieve this goal, this work has been organized as follows. In the first chapter, the reasons that motivate why and at what energies we are looking for an UV completion of the SM, will be briefly reviewed. Consequently, after having briefly recalled the main characteristics of the Electro-Weak sector of the

Standard Model, especially focusing on its flavor structure, a complete overview of neutrino physics main aspects will be provided, analyzing both theoretical and experimental traits. Subsequently, the Effective Field Theory approach will be outlined, introducing the relevant features of Renormalization Group Equation and matching procedure.
In the second chapter the effective New Physics Lagrangian at the scale Λ will be introduced, considering a well-motivated basis of two leptonic and five semi-leptonic operators in order to be able to take into account neutrino Non Standard Interactions but also to be compatible with another compelling hint of New Physics, represented by B anomalies. Then, the low energy Lagrangian will be derived by computing the quantum effects induced at the GeV scale, using the key tool of Renormalization Group Equations.
Then, in the third and last chapter the main experimental results provided by the IceCube Observatory will be discussed, along with an analysis of the future DUNE project. Then, describing and parametrizing the observables at stake in those experiments, modified by New Physics effects, bounds on the involved Wilson coefficients will be obtained and compared with the present status of the art.

1

NEUTRINO PHYSICS: INTRODUCTIVE REVIEW

At present time, the Standard Model (SM) of Elementary Particles represents the most successful theory of fundamental interactions from both a theoretical and an experimental point of view. It has been tested for the past decades at increasing energies and precision, and its predictions were in agreement with the experimental results in a large part of phenomena.
Nevertheless, nowadays it is widely acknowledged that the SM is not the most complete theory of nature, when going to very high energies. In fact, despite the present impossibility to experimentally test the presence of New Physics (NP) signals, there are many hints that suggest that a Beyond the SM (BSM) theory is required.

The most important justification for introducing BSM theories will be discussed in 1.1, in particular by analyzing the most promising channels for searching for NP signals. Among them, the main focus will be on *neutrino interactions*. In order to give a more complete picture of the theory describing those particles, the flavor physics of Electroweak sector of the SM will be briefly reviewed in 1.2. Consequently, the historical discovery of *neutrino masses and oscillation* will be discussed from both an experimental and theoretical point of view in 1.3, pointing out the importance of an *UV-completion* of the SM . In the last section of the chapter, 1.4, the Effective Field Theory (EFT) approach, the theoretical tool used in the present work in order to investigate NP signals, will be introduced.

1.1 GOING BEYOND THE STANDARD MODEL

Among the others, *neutrino masses and mixing* represent one of the most striking and promising channel to investigate the presence of NP.
In the SM, in fact, neutrinos are considered as massless particles, preventing the possibility for them to oscillate. By now a huge amount of experiments confirmed that neutrinos actually oscillate, so this lack of predictivity of the SM in neutrino sector represents one of the possible ways to shed light on NP.
Moreover, new and *non standard neutrino interactions* (NSI) have been implemented nowadays as a natural feature in many BSM neutrino mass models. Such interactions are clearly subdominant but, since they produce modifications to many observables like oscillation probability and its parameters, they represent an important tool in order to put boundaries on the energy scale at which the NP should arise.
Moreover, from an experimental point of view, many oscillation parameters are

yet to be precisely understood: the Dirac CP-violating phase in the U_{PMNS}, the neutrino mass hierarchy and the octant of θ_{23}. Hopefully, the upcoming generation of neutrino experiments should be sensitive to subdominant oscillation effects, helping to test the various neutrino models recently proposed (1).
The present work aims to insert itself in that issue, by means of a model independent way to parametrize NSIs, as will be highlighted in the following chapters.

In addition to neutrino masses and mixing, some of the most important clues that might account for NP signals are briefly listed in the following.
They include both *experimental issues*, i.e. discrepancies between the SM prediction and the experimental data, and more fundamental *theoretical trademarks*, i.e. fine tuning problems affecting many parameters of the theory. There is a striking difference in the nature of the two problems. The experimental one deal with more pragmatic issues of the theory, which is unable to correctly predict some of the observed phenomena. The theoretical one could also appear as philosophical issues since they deal with aspect of the theory that do not fulfill the concept of *naturalness*,[1] which is hard to put into numbers.
Nevertheless, both of them must be resolved in order to obtain a most complete theory of nature.

- *Dark matter* - The strong evidence that 25.6% of the total matter that constitute our universe is non-baryonic, forces a completion of the SM in order to take into account the potential new particle able to explain the amount of Dark Matter in the universe (3).

- *Baryon asymmetry* - Cosmological observations strongly confirmed the exceeding presence of matter with respect to antimatter. In disagreement with such observations, the SM is believed to satisfy an accidental symmetry that is related to the conservation of the Baryon Number. The solution of that friction requires a modification of SM.

- *B anomalies* - In the last few years, various experimental collaborations observed indications of Lepton Flavour Universality Violation (LFUV) in semileptonic B decays. Although such indications are not yet conclusive, the overall pattern of deviations from the SM predictions is very coherent. The anomalous data refer to a number of different interactions: charged-current transitions $b \to c\ell\bar{\nu}$ with τ/e and τ/μ LFUV and neutral-current transitions $b \to s\ell\bar{\ell}$ with μ/e LFUV (42). Interestingly enough, global fit analyses for the angular distributions of the $B^0 \to K_0^*\mu^+\mu^-$ decay reported anomalies which are consistent with LFUV data. For this reasons, semileptonic B decays are one of the most interesting testing-ground searching for NP (4).

- *Muon* $g-2$ - There exists a long lasting discrepancy between the experimental value of the muon anomalous magnetic moment and the SM prediction. From the most recent data, one gets a 3σ difference between the

1 The formulation of naturalness given by 't Hooft reads that a theory is natural if, for all its parameters p, small with respect to their fundamental scale Λ, the limit $p \to 0$ corresponds to an enhancement of the symmetry of the system (2).

two values and this is conceivable as a direction for searching NP. Otherwise, the main limit on the SM predictions results from the computation of the Leading Order hadronic contribution to the muon $g-2$ (5).

- *Strong CP problem* - The existence of a four dimension term arising in the gluon sector of the SM Lagrangian, i.e. $\theta_{QCD}\tilde{G}^{a}_{\mu\nu}G^{a\,\mu\nu}$, leads to CP violation in the strong sector. In order to take into account the cross-section of CP violating processes, one should fix by hand the parameter of named term, $\theta_{QCD} \lesssim 10^{-10}$, which is unnaturally small. Possible ways to dynamically generate such a small coefficient have been proposed, most of which requiring the existence of a new particle, the axion (6).

- *Hierarchy problem* - The Higgs sector of the SM Lagrangian contains one independent parameter, the vacuum expectation value (vev), related to the Higgs mass, of order $v \simeq 10^2$ GeV. From a theoretical point of view, one would have expected a bigger value for this parameter, because the loop correction to m_h are quadratically, instead of logarithmically, divergent. For this reason, a fine tuning is required in order to recollect the experimental value. Possible solution have been proposed, involving Supersymmetry and composite Higgs models.

- *Flavor puzzle* - The huge hierarchy in the mass spectrum of fermions, which spans from the electron mass $m_e \simeq 10^{-3}$ GeV to the top-quark mass $m_t \simeq 170$ GeV, is considered unnatural. A definite explanation of such a spectrum is yet to be proposed.

Taking all those unsatisfactory aspects in mind, it is clear why the SM does not have the characteristic of a really fundamental theory.
In order to build the *UV completion* of the SM, and to take into account NP phenomena, both experimental improvements and advanced theoretical tools are required.

It is possible to underline two complementary strategies in order to experimentally investigates possible effects of NP. The first one aims directly at producing and detecting the supermassive particles that may eventually represent the mediator of some more complete theory, while the second one deals with the investigation of virtual modifications caused by NP in low-energy processes, through high-precision experiments. NSI experiments fits into the second possibility as greatly analyzed, for example in (7) and (8).

From a theoretical point of view, it is possible to identify two main approaches in order to implement NP effects in a more complete model of particle physics. One aims to directly build an explicit BSM theory, gaining in predictivity but being very model-dependent and less general. The other one analyses the NP effects within an EFT approach, which provides a more general description of NP at low energies through a limited number of parameters, but is quite unable to discern between the different high energies scenarios. NSI will be studied by means of the EFT approach, as will be discussed in Chap. 2.
Following that last strategy, if one assumes that the SM correctly describes

physics in the energy range up to the W boson mass, but it must be considered within an EFT approach up to energies of order of some scale Λ, it becomes compelling to put boundaries on that new physics energy scale.

THE Λ SCALE OF NEW PHYSICS Without considering the long standing problem of including gravity interactions in the SM, since such an unification is put by mutual consent at the Planck scale $M_P \simeq 10^{19}$ GeV, which clearly represents an ultimate UV cutoff for the SM, there are many other theoretical and experimental clues able to put boundaries on the scale at which NP should arise (9).
The first indication comes from the Renormalization Group evolution of the gauge coupling of the SM. There exists, in fact, an energy scale where all the running coupling constants seem to converge, nearly at $\Lambda_{\text{GUT}} \simeq 10^{14}$ GeV, in the SM. Such a scale is called scale of *Grand Unified Theory* since suggests that the SM gauge group would be embedded just in a simple group like $SU(5)$ or $SO(10)$, where all gauge forces are unified (10). In that context NP effects should arise approximately around that GUT scale.
Another indication in accord with that result comes from the *see-saw mechanism*, which is able to explain the smallness of neutrino masses without any *fine tuning* issues, as will be treated in 1.3. Without dealing with the details of the mechanism, in order to obtain $m_\nu \simeq 0.1$ eV, the energy scale of new physics must be put around $\Lambda \simeq 3 \cdot 10^{14}$ GeV.
In addition to the mentioned evidences, there are also many cosmological suggestions, related to inflation models, which confirmed that the scale of NP should be around $\Lambda \simeq 10^{14} \div 10^{16}$ GeV.

Such a scale is far beyond the achievable energies of experiments nowadays, explaining why NP signals have not been seen yet. Nevertheless, as already mentioned, NP effects could still give modification to low-energy processes.

1.2 ELECTROWEAK SECTOR OF THE STANDARD MODEL

Neutrinos are one of the main building blocks that constitute the SM. Due to their small cross section, they have been discovered relatively late and most of their characteristics, like masses and mixing parameter, are yet poorly understood.
Nevertheless, in order to give an introductive overview of neutrino physics, the EW sector of the SM will be discussed hereafter. Consequently, possible ways of generating neutrino masses will be treated, along with oscillation probability and the main consequences on Flavor Symmetries. In the end, a short overview of the most important experiments at work nowadays will be provided.

THE STANDARD MODEL The Electro-Weak(EW) sector of the SM is based on the gauge group $SU(2)_L \times U(1)_Y$.
The particle content consists of three leptons (electron, muon, tau) and the associated neutrino; six quarks (up, down, charm, strange, top, bottom), one scalar boson (Higgs) and three vector bosons (photon, Z, W).
The fields describing the matter content are organized in three generations of

doublets and singlets according to their transformation properties under the gauge group.
Denoting the field by $P(T, Y)$ where T and Y are the representations under $SU(2)_L$ and $U(1)_Y$ we get the subsequent matter content

$$L^i\left(2, \frac{1}{2}\right) \quad e_R^i\,(1,1) \quad Q^i\left(2, -\frac{1}{6}\right) \quad u_R^i\left(1, -\frac{2}{3}\right) \quad d_R^i\left(1, \frac{1}{3}\right) \quad \phi\left(2, -\frac{1}{2}\right), \tag{1.1}$$

where $L^i = (\nu_L^i, e_L^i)$ and $Q^i = (u_L^i, d_L^i)$. The index $i = 1, 2, 3$ runs over the different flavours that define each generation.

Therefore, the Lagrangian of the EW sector, in the interaction basis, reads:

$$\begin{aligned}\mathcal{L}_{\text{EW}} = &\underbrace{-\frac{1}{4}W_{\mu\nu}W^{\mu\nu} - \frac{1}{4}B_{\mu\nu}B^{\mu\nu}}_{\text{gauge sector}} + \underbrace{i\sum\nolimits_f(\bar{f}\not{D}f)}_{\text{matter sector}} \\ &\underbrace{+(D_\mu\phi)^\dagger(D^\mu\phi) + \mu^2(\phi^\dagger\phi) - \lambda(\phi^\dagger\phi)^2}_{\text{Higgs sector}} \\ &\underbrace{-y_e^{ij}\bar{L}_i e_{jR}\phi - y_d^{ij}\bar{Q}_i d_{jR}\phi - y_u^{ij}\bar{Q}_i u_{jR}\tilde{\phi} + \text{h.c.}}_{\text{Yukawa sector}},\end{aligned} \tag{1.2}$$

where W_μ^a and B_μ are the vector fields in the interaction basis, $D_\mu f = (\partial_\mu + \frac{i}{2}g_2\tau_a W_\mu^a + ig_1 Y B_\mu)f$ and $D_\mu\phi = (\partial_\mu + \frac{i}{2}g_2\tau_a W_\mu^a - ig_1 Y B_\mu)\phi$ are the covariant derivatives for the fermion and scalar field respectively.

The request of invariance under the gauge symmetry prevents the possibility to write by hand a mass term for fermions and vector bosons. Those masses are generated via the *Spontaneous Symmetry Breaking mechanism* by the appearance of a non-zero vacuum expectation value (vev) of ϕ, being

$$v = \sqrt{-\frac{\mu^2}{\lambda}} = 246 \text{ GeV}. \tag{1.3}$$

The vector boson masses arise from the Higgs kinetic term and are given by

$$M_W^2 = \frac{1}{4}g_2^2 v^2 \qquad M_Z^2 = \frac{1}{4}v^2(g_2^2 + g_1^2) \qquad M_\gamma = 0\,. \tag{1.4}$$

The Higgs mass arises from the Higgs potential and is given by

$$M_\phi^2 = 2\lambda v^2\,. \tag{1.5}$$

The fermion masses, instead, arise from the Yukawa sector and are given by

$$M_f^2 = \frac{1}{2}v^2 y_f^2\,. \tag{1.6}$$

It is important to notice that, since the particle content of the SM does not include the ν_R, it is impossible to generate neutrino masses by means of this mechanism. Since it has been experimentally proven that neutrinos do have

masses, this lack represents one of the main problems of the SM and one of the most important hints of physics beyond SM.

The possible ways of generating neutrino masses that have been proposed along the years will be treated in 1.3, along with their main consequences.

FLAVOR SYMMETRIES In addition to the gauge symmetry, one might wonder whether other symmetries, namely *accidental symmetries*, arise in the SM Lagrangian.
In an ideal case where the non-diagonal Yukawa couplings are turned off, i.e. $y_f^{ij} = 0$, then $\mathcal{L}_{\text{EW}}$ is invariant under a global flavor symmetry

$$G_F(y_f = 0) = U^5(3) = U(3)_Q \times U(3)_d \times U(3)_u \times U(3)_L \times U(3)_e \,. \tag{1.7}$$

This means that both the Lepton and Baryon Numbers are conserved, along with the Lepton Family Number (LFN) and Baryon Family Number (BFN).

This ideal situation is clearly broken in the real case where the Yukawa couplings are non zero, i.e. $y_f^{ij} \neq 0$. In that case, being $U(3) = SU(3) \times U(1)$, all the $SU(3)$ are broken and the residual flavor group is

$$G_F(y_f \neq 0) = U(1)_B \times U(1)_e \times U(1)_\mu \times U(1)_\tau \,. \tag{1.8}$$

Therefore only the LFN and Baryon Number are now conserved. This fact can be seen explicitly by diagonalizing the Yukawa couplings, which corresponds to switch from the *interaction basis* to the *mass basis*.
In order to correctly diagonalize the Yukawa matrices, a biunitary transformation, involving two independent unitary matrices, is needed

$$y_u = R_u y_u^D V_u^\dagger \quad y_d = R_d y_d^D V_d^\dagger \quad y_e = R_e y_e^D V_e^\dagger \,. \tag{1.9}$$

Consequently, the effect on the fields is summarized by the following transformation laws

$$\begin{aligned} u_L^i &= V_u u_L^m \quad d_L^i = V_d d_L^m \quad L_L^i = V_e L_L^m \\ u_R^i &= R_u u_R^m \quad d_R^i = R_d d_R^m \quad e_R^i = R_e e_R^m \,. \end{aligned} \tag{1.10}$$

By performing these transformations the mass terms and the Yukawa sector become diagonal. Instead, as a consequence, the charged current terms are modified, since the different components of the doublets are mixed.
It is important to notice that, since neutrinos have no mass in the SM, their transformation law is completely arbitrary. Then, one is allowed to safely choose $V_\nu = V_e$ so that the transformation law for the two components of the lepton doublet is the same and the mixing matrix reduces to the identity matrix, $V_{\text{PMNS}} = \mathbb{1}$. As a consequence, the Family Lepton Number is not broken.
Conversely, the transformation matrices for the components of the quark doublet,

V_u and V_d, are not arbitrary and *a priori* are different, thus inducing the breaking of the Baryon Family Number through a mixing matrix called $V_{\text{CKM}} = V_u^\dagger V_d$

$$\mathcal{L}_{\text{EW}}^{\text{CC}} = -\frac{g}{\sqrt{2}} W_\mu^+ (\bar{u}_{iL} \underbrace{V_u^\dagger V_d}_{(V_{\text{CKM}})^{ij}} \gamma^\mu d_{jL} - \frac{g}{\sqrt{2}} W_\mu^+ (\bar{\nu}_{iL} \underbrace{V_e^\dagger V_e}_{\mathbb{1}} \gamma^\mu e_{jL}) \tag{1.11}$$

The V_{CKM} is the only source of flavor violation in the SM. It is also important to notice that, at tree level, Flavor Changing arise only in Charged Currents (FCCC) while Flavor Changing Neutral Current (FCNC) processes do not show up at tree level.

It is even more important to stress that the whole discussion above is valid only in the massless neutrino case. On the other hand, it is clear today that LFN is not a symmetry of the SM, since various experiments confirmed that neutrino oscillate. Such phenomenon require LFN breaking. The oscillation arises only if neutrino masses are different from zero and one from another as will be analyzed in due time.

1.3 NEUTRINO OSCILLATION

The phenomenon of Neutrino Oscillation was theoretically predicted in 1968 by Bruno Pontecorvo (*11*), in order to take into account the possibility of lepton flavor violation processes. For the first time, in that pioneering article, the possibility for neutrinos to have non zero masses was proposed in order to generate lepton flavor violation.[2]
However, given the small cross section associated to these processes, of the order $10^{-45} \div 10^{-50}$ m^2, the experimental proof was found only long after, in 1998, while trying to solve an important astrophysical problem: the Solar Neutrino Puzzle.

NEUTRINO MASSES AND MIXING PROBABILITY The existence of three different flavors of neutrinos (ν_e, ν_μ, ν_τ) participating in weak interactions, has been stated in several experiments. In fact, in order to match the theoretical and experimental result for the decay width of the Z boson, the number of non sterile neutrinos must be exactly three (*12*). As a consequence, once discarded the massless neutrino hypothesis, it is straightforward to assume the existence of three mass eigenstates (ν_1, ν_2, ν_3).
Nevertheless, the absence of sterile neutrinos in the *particle content* of the SM, along with the *renormalizability* prescription prevents the generation of neutrino masses. Only by giving up one of this two assumptions it will be possible to give mass to neutrinos, according to (*13*).

Adding sterile neutrinos $\nu_R^i(1,0)$, it is possible to write another Yukawa term *Particle content*

2 It is important to notice that, according to what is the neutrino type (Dirac or Majorana), it would be possible to violate both LFN (Dirac) and lepton number (Majorana) and to generate different mass terms; that is another open problem that will not be analyzed in the present work.

involving this new particle

$$\mathcal{L}_Y^{\nu_R} = y_\nu^{ij} \bar{L}_i \nu_{Rj} \tilde{\phi} + \text{h.c.} \tag{1.12}$$

Via the *Spontaneous Symmetry Breaking Mechanism* the neutrinos acquire a mass of the form 1.6. It is a Dirac mass, hence only the LFN will be violated after diagonalizing the Yukawa matrix.
In fact, after introducing the sterile neutrino, the arbitrariety of choosing the transformation law for ν_L is lost because of the diagonalization of the new Yukawa coupling, $y_\nu = R_\nu y_\nu^D U_\nu^\dagger$, in addition to 1.9. Then, further transformations must be defined

$$e_L^i = V_e e_L^m \quad \nu_L^i = V_\nu \nu_L^m \quad \nu_R^i = R_\nu \nu_R^m \,.$$

As seen in the case of the quarks, the charged current term will be modified by these transformation and a mixing matrix will emerge for leptons too, leading to the violation of LFN

$$\mathcal{L}_{\text{EW}}^{\text{CC}} = -\frac{g}{\sqrt{2}} W_\mu^+ (\bar{\nu}_{Li} \underbrace{V_\nu^\dagger V_e}_{(U_{\text{PMNS}})^{ij}} \gamma^\mu e_{Lj}) + \text{h.c.}$$

The global flavour symmetry would be in this case

$$G_F(m_\nu^D \neq 0) = U(1)_B \times U(1)_L \,.$$

This method, which would seem the most natural one since it does not require any additional theoretical assumption, it's actually affected by a *fine tuning* issue.
In fact, from experimental data, a mass limit of order $m_\nu < 1$ eV must be required. However, being m_ν proportional to the Higgs v.e.v $m_\nu \simeq 175\ \text{GeV} \cdot y_\nu$, the Yukawa coupling must be set by hand to a value, $y_\nu \lesssim 10^{-11}$, which is highly artificious.
In conclusion, even if this method allowed the possibility of neutrino oscillation and mixing, it seems unconvincing to give a Dirac mass to neutrinos from a Yukawa term.

Renormalizability

The other path that can be followed requires the introduction of a dimension $d = 5$ operator involving Majorana neutrinos, the *Weinberg operator*, which introduces a massive scale, spoiling renormalizability:

$$\mathcal{L}_{d=5}^W = \frac{C}{\Lambda_W} \bar{L}_L^c \phi \phi^c L_L + \text{h.c.}$$

Via the *Spontaneous Symmetry Breaking Mechanism* neutrinos acquire a Majorana mass of the form

$$m_\nu = \frac{C}{\Lambda_W} v^2 \tag{1.13}$$

and the experimental limit on that mass allows to find limits on the massive scale $\Lambda_W \simeq 10^{14}\ GeV$. This method is *fine tuning free* since no coupling must be

set by hand in order to replicate experimental results.
In that case the global symmetry of flavor would be just

$$G_F(m_\nu^M \neq 0) = U(1)_B \,. \tag{1.14}$$

The introduction of an effective operator, suggests the existence of a more general theory and of a more massive mediator, with respect to which, the SM represents just the low energy limit. Evidently, the construction of such a theory requires many theoretical tools and therefore other simpler mechanisms have been introduced.

See-Saw Mechanism

Nowadays a third approach is commonly considered as a good alternative option, in order to give mass to neutrinos. The basic idea underlying the See-Saw Mechanism is to give (Majorana) mass to a heavy sterile neutrino N_R emerging at a very high scale ($\Lambda_N \simeq 10^{15}$) via *Spontaneous Symmetry Breaking* on a Yukawa term. The mass of the light (SM) neutrino emerges in the diagonalization of the mass term and it does not require any *fine tuning* of y_ν.
The Lagrangian describing this mechanism is

$$\mathcal{L}^{\text{See-Saw}} = y_\nu \bar{L}_L N_R \tilde{\phi} + B \bar{N}_R^c N_R + \text{h.c.}$$

The key concept of the See-Saw Mechanism is that $B \gg \frac{v}{\sqrt{2}} y_\nu$.
Since the mass eigenstates of the diagonalized mass matrix are

$$\begin{cases} m_{N_R} = B \\ m_{\nu_L} = \dfrac{y_\nu^2 v^2}{B} \end{cases} \tag{1.15}$$

it is clear that it is possible to generate a mass $m_{\nu_L} < 1$ eV naturally, with $y_\nu \simeq 1$, thanks to the high energy scale B. Evidently since this mechanism generates Majorana masses the flavour symmetry would be 1.14.

The exact absolute value of neutrino masses is nowadays still unknown. In fact, experiments are sensible only to *mass differences* so that the mass hyerarchy is yet obscure.
According with the experimental results, there are two options: *normal hyerarchy* having $m_1 \lesssim m_2 \ll m_3$ and *inverted hyerarchy* with $m_3 \ll m_1 \lesssim m_2$.

Δm^2_{12}	$\lvert\Delta m^2_{13}\rvert$	$\lvert\Delta m^2_{23}\rvert$
$8 \times 10^{-5}\text{eV}^2$	$3 \times 10^{-3}\text{eV}^2$	$3 \times 10^{-5}\text{eV}^2$

Table 1.1: Acknowledged values for neutrinos mass differences. Notice that for the oscillations $1 \leftrightarrow 3$ and $2 \leftrightarrow 3$ only the absolute value is known, not the sign.

Whatever the mechanism neutrinos acquire mass with, the diagonalization of the mass matrix will induce a mixing matrix in the charged current term, $(V_{\text{PMNS}})^{ij}$.

If neutrinos are Dirac particles it is possible to parametrize this matrix using three angles $\theta_{12}, \theta_{13}, \theta_{23}$ and a phase δ as following

$$U_{\text{PMNS}}^{\text{Dirac}} = \begin{pmatrix} 1 & 0 & 0 \\ 0 & c_{23} & s_{23} \\ 0 & -s_{23} & c_{23} \end{pmatrix} \begin{pmatrix} c_{13} & 0 & s_{13}\, e^{i\delta} \\ 0 & 1 & 0 \\ -s_{13}\, e^{-i\delta} & 0 & c_{13} \end{pmatrix} \begin{pmatrix} c_{12} & s_{12} & 0 \\ -s_{12} & c_{12} & 0 \\ 0 & 0 & 1 \end{pmatrix},$$

where $c_{ij} = \cos\theta_{ij}$ and $s_{ij} = \sin\theta_{ij}$.
In case neutrinos are Majorana particles, two additional phases α_1, α_2 are present

$$U_{\text{PMNS}}^{\text{Majorana}} = U_{\text{PMNS}}^{\text{Dirac}} \begin{pmatrix} e^{i\alpha_1} \\ e^{i\alpha_2} \\ 1 \end{pmatrix}.$$

It is important to state that the physical observables are not sensible to these two phases, because they cancel when calculating the modulo-squared amplitude.

Taking into account this parametrization and using a quantum-mechanical approach, the oscillation probability in vacuum, between two possible flavor states, can be calculated

$$\mathcal{P}_{\ell\ell'} = |\langle \nu_{\ell'}(0) \,|\, \nu_\ell(t) \rangle|^2 .$$

Writing the relation between the mass and the interaction basis and evolving the mass state, an expression for the flavor state is obtained

$$|\nu_\ell(t)\rangle = \sum_{i=1}^{3} e^{-iE_i t} U_{\ell i} \,|\nu_i(0)\rangle , \tag{1.16}$$

the oscillation probability between two different flavor states becomes then

$$\begin{aligned} \mathcal{P}_{\ell\ell'} = \delta_{\ell\ell'} &- 2\sum_{i>k} \text{Re}(U_{i\ell'}^* U_{\ell' k} U_{k\ell}^* U_{\ell i}) \left(1 - \cos\left(\frac{\Delta m_{ki}^2 L}{2E}\right)\right) \\ &+ 2\sum_{i>k} \text{Im}(U_{i\ell'}^* U_{\ell' k} U_{k\ell}^* U_{\ell i}) \sin\left(\frac{\Delta m_{ki}^2 L}{2E}\right), \end{aligned} \tag{1.17}$$

where $L = ct$ is the distance travelled by neutrinos in the time t, and $E \simeq |\vec{p}|$ their energy.

A couple of brief comments is needed:

- neutrino oscillation is possibile only if neutrinos are massive, so $U_{\text{PMNS}} \neq \mathbb{1}$,
- neutrinos must be non-degenerate in the mass spectrum, so that $\Delta m_{ik}^2 \neq 0$.

Taking that in mind, it is clear that improvements in the theoretical understanding of neutrino physics are required.
From the experimental side, there is an ongoing ambitious program that aims to

precisely determines the *mixing parameter*, discern the correct *mass hyerarchy* and prove the existence of a *Dirac or Majorana phase*.

NEUTRINO OSCILLATION EXPERIMENTS Experiments on solar neutrinos provided the first testing ground for neutrino oscillation. In fact, that hypothesis was invoked in order to solve the *Solar Neutrino Puzzle*[3] and explain the observed flux of electronic neutrinos on Earth. Subsequently, neutrino oscillation was also verified in reactor experiments.
It is important to check neutrino oscillation through experiment involving neutrinos of different origins because they are sensible to different channel of oscillation. In fact, in the case of *solar neutrinos*, having $L \simeq 1$ AU,

$$\frac{|\Delta m_{13}|L}{E} \simeq \frac{|\Delta m_{23}|L}{E} \gg 1 \tag{1.18}$$

and 1.17 reduces to an oscillation probability between $1 \leftrightarrow 2$ only.
Analogously speaking, in the case of *artificial neutrinos* produced in reactor experiments, as well as *atmospheric neutrinos*, having a relatively small L

$$\frac{\Delta m^2_{21} L}{2E} \ll 1 \tag{1.19}$$

and 1.17 reduces to an oscillation probability between only two generations, $1 \leftrightarrow 3$ or $2 \leftrightarrow 3$.

Solar neutrino sector

Solar neutrino analysis began with the historical radiochemical experiments Homestake (*14*), Gallex (*15*), SAGE (*16*), which were sensible only to the number of neutrinos but not to their energy, and Kamiokande, which could also provide information on the direction of the neutrinos. Those experiment were sensible only to charged current (CC) processes; for this reason only with the SNO experiment, which could detect neutrinos through neutral current processes too, it was possible to provide the definitive solution to the Solar Neutrino Puzzle (*17*). The differences observed between the measurements of the neutrino flux obtained in the various experiment was explained by taking into account matter effect in the Sun (*18*).

Nowadays two solar detectors are at work, Super-Kamiokande and Borexino, and also a reactor experiment, KamLAND, which is sensible to the $1 \leftrightarrow 2$ oscillation channel, assuming CPT is conserved.
Fig. 1.1 reports the allowed region in the $(\sin^2\theta_{12}, \Delta m^2_{21})$ plane, according to solar neutrino experiments (in black) and KamLAND (in blue). It is possible to put in evidence the preferred values of Δm^2_{21} by solar experiments and KamLAND

$$\begin{cases} \Delta m^2_{21} = 7.6 \times 10^{-5}\,\text{eV}^2 & \text{KamLAND} \\ \Delta m^2_{21} = 4.96 \times 10^{-5}\,\text{eV}^2 & \text{Solar experiments} \end{cases} \tag{1.20}$$

3 It dealt with the discrepancy between the Solar Standard Model prediction for the solar neutrino flux and its measurements. A second issue dealt with the further discrepancy of the measured flux from an experiment to another.

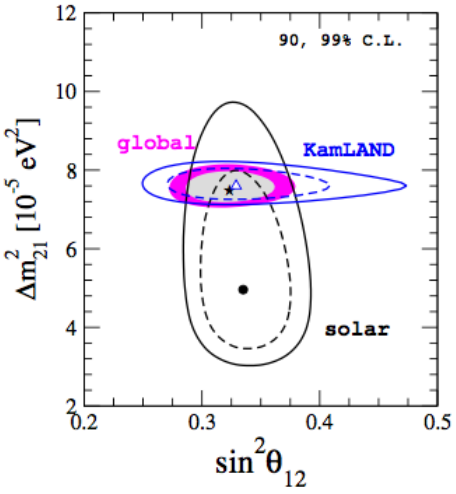

Figure 1.1: Allowed region for the solar oscillation parameters, according to KamLAND and Solar experiments. From (1).

Attempts to explain the observed discrepancy have been made, mostly in the context of non-standard neutrino interactions.
Nevertheless, the best fit point for that global analysis corresponds to:

$$\sin^2\theta_{12} = 0.321^{+0.018}_{-0.016} \quad \Delta m^2_{21} = 7.56 \pm 0.19 \times 10^{-5}\,\text{eV}^2. \tag{1.21}$$

Atmosferic and artificial neutrino sector

After the discovery of neutrino oscillation in the solar flux, many other experiments analysing atmospheric and artificial neutrinos were built up, in order to put constraints on the remaining parameters Δm^2_{13}, $\sin^2\theta_{23}$ and θ_{13}.
Atmospheric neutrino experiments, such as the Super-Kamiokande Collaboration (19), are sensitive in higher range of energy then the solar ones, approximately from 100 MeV to TeV. The best fit for some of the oscillation parameters, obtained with Super-Kamiokande, are

$$\sin^2\theta_{23} = 0.587 \quad |\Delta m^2_{23}| = 2.5 \times 10^{-3}\,\text{eV}^2 \tag{1.22}$$

Recently, many experiments have been designed in order to analyze the atmospheric neutrino flux such as ANTARES and IceCube (20), whose results are compatible with 1.22, as reported in fig.1.2.

Afterwards, also many reactor experiments (both long and short-baseline) have been realized in order to confirm the oscillation phenomenon. Among the long-baseline experiments, T2K and NOνA are still at work nowadays. The best fit obtained in those experiments for the artificial oscillation parameters are

$$\sin^2\theta_{23} = 0.532 \quad |\Delta m^2_{23}| = 2.545 \times 10^{-3}\,eV^2 \tag{1.23}$$

In that case the constraints provided by different experiments are quite in agreement.
For what concerns the short-baseline experiments, such as Daya Bay, RENO and

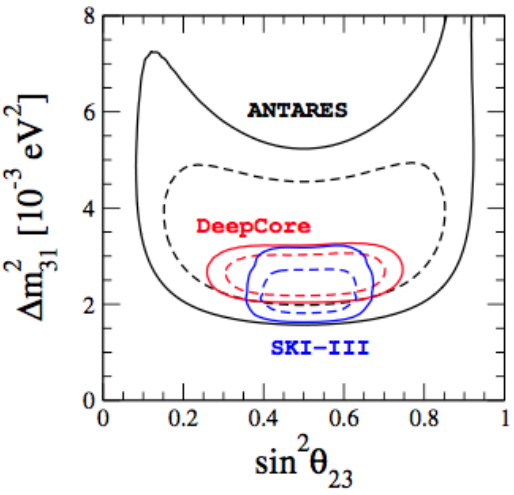

Figure 1.2: Allowed region for the atmospheric oscillation parameters, according to the most recent experiments. From (1).

Double Chooz, they were crucial in the determination of θ_{13}, whose best fit value is

$$\begin{aligned} \sin^2\theta_{13} &= 2.155^{+0.075}_{-0.090} \quad \text{Normal Ordering} \\ \sin^2\theta_{13} &= 2.155^{+0.092}_{-0.092} \quad \text{Inverted Ordering} \end{aligned} \tag{1.24}$$

Despite the great sensitivity achieved in constraining most of the oscillation parameters, three of them are still unknown: the octant of θ_{23}, the value of the phase δ and the mass ordering, i.e. the sign of Δm^2_{23}.
As already stressed, the possibility of non-standard neutrino interactions have been strongly suggested after the introduction of a mass term for neutrinos. In fact, NSI could strengthen the theoretical knowledge of the oscillation parameters, giving corrections that might give hints on the value of the yet unknown parameters. Moreover, NSI accounts for new interactions that breakingly change the way neutrinos oscillates. If those interactions are described in an Effective Field Theory approach, then solar, atmospheric and reactor experiments can provide important bounds on the energy scale of the theory and on the strength of the couplings. Some of the phenomenological implications will be treated in Chapter 3 where two among the most promising experiment will be analyzed.

1.4 THE EFFECTIVE FIELD THEORY APPROACH

One of the most embraceable theoretical tool that actually allows to build an *UV completion* of the SM is the EFT approach. In this scenario, the SM is considered as a low energy approximation of a more fundamental theory, in which the arising heavier mediators have been integrated out.

Before starting to build the EFT Lagrangian, a more naive but explicative way to understand such an important tool is necessary.
One of the main reasons behind the validity of introducing the EFT approach lies

in the concept that all physical processes are characterized by different energy scales. The quantum field theories describing those processes are valid under some defined scale, over which a more general theory becomes significant. The classic, and historical, example of Fermi Theory is quite explicative.

As it is known, QED describes very well the properties of electrons and photons at energies of the order of 1 MeV, without being affected by more massive particles or more energetic interactions. QED is *renormalizable* and *predictive* in this range of energy, but it's not the full and complete theory of nature. EFT can give insights of that complete theory, involving more massive mediators, without losing predictivity and remaining *approximately* renormalizable under the energy scale dictated by the mediators.
Coming back to the example, beyond the 1 MeV scale, at higher energy, where more massive particles start to play a role, weak interaction processes need to be implemented in the Lagrangian. The typical energy scale of weak interactions is dictated by the vector boson masses, the mediator of that interaction, $m_{EW} \simeq 80$ GeV. Many processes involving weak interactions, however, such as the muon decay, take place at energies much smaller than m_{EW}. When this condition is fulfilled, the EFT, in this framework the Fermi Theory, defined by the Lagrangian

$$\mathcal{L}_{\text{Fermi}} = \frac{G_F}{\sqrt{2}} J^+_\mu J^{\mu -} = \frac{G_F}{\sqrt{2}} (\bar{e}_{Li} \gamma_\mu \nu_{Li})(\bar{\nu}_{Lj} \gamma^\mu e_{Lj}) \,, \tag{1.25}$$

is fully predictive and can be seen like a *contact interaction*. This might look like a *non-renormalizable* interaction, since it involves massive couplings, but since it's defined only under a certain mass scale we can safely use it in processes whose energy is under that mass scale. Moreover, you can safely assume that the complete theory, at m_{EW} scale, shall involve only renormalizable terms.
In fact, that's exactly the case in exam. When considering processes whose energy scale is of the order of m_{EW}, the complete Lagrangian must be recovered so that, when integrating out the massive degrees of freedom from it, the Fermi Theory Lagrangian emerges. This means that the complete renormalizable theory and the effective one have the same power of predictivity for processes whose energy scale is much smaller than the mass of the heaviest mediator.
Taking that in mind, it is clear why, starting with (21), many authors began to interpret the SM as an incomplete theory, an effective theory where heavier fields where integrated out, that was only valid under the unknown scale Λ, determined by some new mediator. That assumption allows to introduce new interaction in order to take into account, and possibly solve, SM incompletenesses.

For what concerns this work, NSI will be parametrized in an EFT approach, which allows, after referring to the experimental results, to put boundaries on the effective energy scale and coupling coefficients in order to obtain some hints of the complete, renormalizable theory beyond the SM. The procedure followed in order to build the Effective Lagrangian will be exemplified in chapter 2, while the bounds on the coefficients will be analyzed in chapter 3.

BUILDING THE EFT LAGRANGIAN The procedure to find this effective Lagrangian is quite general, since it's independent of the supermassive particles which are not dynamical degrees of freedom at energies below Λ.
The effective field theory valid below that energy scale should satisfy some fundamental requirements:

- its gauge group must be $G_{SM} = SU(3)_C \times SU(2)_L \times U(1)_Y$,
- all the SM degrees of freedom have to be incorporated as fundamental fields,
- the low energy limit is the SM, ruling out the possibility of new particles below Λ scale.

Fulfilling these requirements inevitably implies that the effective Lagrangian can be written as an expansion in the Λ scale power

$$\mathcal{L}_{\text{eff}} = \sum_{d>4} \frac{1}{\Lambda^{d-4}} C_i^{(d)} Q_i^{(d)} \,, \tag{1.26}$$

where Q_i^d are all the possible operators of dimension d which are G_{SM} invariant and are built with the SM fields, while C_i^d, called *Wilson coefficients*, are the dimensionless couplings that contain information about the couplings of the complete, higher energy, theory.

This work will deal only with the $d = 6$ operators, which is quite a non restrictive assumption, since higher dimensional operator effects would be suppressed by the inverse power of the scale. The complete set of those operators, derived by (22), consists of 59 operators. They introduce new and flavour changing interactions among the SM particles, induce SM coupling modifications and W and Z masses corrections. The extent of these corrections, in comparison with the experimental results, may give hints on the value of the C_i.
The complete list of operators can be found in the Appendix A.

RENORMALIZATION GROUP EQUATION Starting with a theory defined at the Λ scale, in order to recollect the theory at a lower energy scale μ described by $\mathcal{L}(\mu)$, the powerful tool of Renormalization Group Equation (RGE) is required. The C_i can be determined by a general procedure called *matching*.

The RGE procedure starts when, going to one loop in the perturbation theory, a fictitious scale μ appears in the dimensional regularization of divergent integrals, in the form of a large logarithm

$$\alpha \ln \frac{M}{\mu} \sim \mathcal{O}(1) \,, \tag{1.27}$$

that spoils the perturbative expansion of the parameter α. This scale must evidently cancel in the calculation of physical quantities. The cancellation is possible when the theory is correctly renormalized, so that the scale μ appearing in the one loop integral, will cancel with the *renormalization scale* arising in the RG evolution, while calculating physical quantities.

The *renormalization procedure* is more delicate since the operators Q_i have in general two kinds of divergences: the *standard* one, that can be fixed renormalizing *couplings* and *wave functions*; and another type originating from the highest dimension of these *composite* operators with respect to the one of the SM.

Composite Operators Renormalization

Composite operators involve products of fields in the same space-time point. An example is the simple bare mass operator

$$M^0 = \bar{\psi}^0 \psi^0(x)\,. \tag{1.28}$$

In order to make Green's function containing M^0 finite, an additional operator counterterm is required. The renormalized M reads

$$M = \frac{1}{Z_M} M^0 = \frac{Z_\psi}{Z_M} \bar{\psi}\psi\,, \tag{1.29}$$

where Z_M is the operator counterterm. In a more general case, like the one in exam, where there are several composite operators Q_i, a renormalization matrix is required, causing an operator mixing, such as

$$Q_i^0 = (Z_Q^{-1})_{ij} Q_j\,. \tag{1.30}$$

Taking into account the coupling and the wave function renormalization as well, one obtains the cancellation of all the divergencies along with the cancellation of the μ scale. An explicit demonstration of the validity of that procedure will be given in 2.2.
It is straightforward to see, following (23) that this counterterm can be absorbed in the renormalization of the Wilson coefficients as well, so that

$$C_i^0 = Z_{ij}^C C_j = \frac{1}{Z_{ij}^C} C_i\,. \tag{1.31}$$

This particular feature will produce, in general, a non diagonal anomalous dimension matrix γ_{ij}. Knowing so, it is possible to write the renormalization group equation for the Wilson coefficients

$$\dot{C}_i \equiv \mu \frac{\mathrm{d}}{\mathrm{d}\mu} C_i(\mu) = \gamma_{ij} C_j(\mu)\,, \tag{1.32}$$

where

$$\gamma_{ij} = \left(Z^{-1} \mu \frac{\mathrm{d}}{\mathrm{d}\mu} Z \right)_{ij}\,. \tag{1.33}$$

Using ordinary perturbation theory the differential equation 1.32 can be formally solved, using as initial condition $C_i(M)$, computed by matching the full theory into the effective one, obtaining

$$C_i(\mu) = P \exp\left[\int_{g=M}^{g=\mu} \mathrm{d}g \frac{\gamma(g)}{\beta(g)} \right]_{ij} C_j(M)\,, \tag{1.34}$$

where P denotes the *coupling constant ordering* of the anomalous dimension matrix.
Choosing as initial condition $C_i(M)$ is extremely important, since it allows to solve the large logarithm problem. Considering the leading logarithmic approximation (LLA) of that general solution, in fact, one is able to sum up all the terms like 1.27 end restore the perturbative approach, eliminating all divergencies.

In that procedure, what is important to stress is that the operator renormalization produces an *operator mixing* thanks to the anomalous dimension matrix γ_{ij}. This means that operators that weren't present at the scale Λ can, in general, arise at different scales, thanks to the evolution of their coefficients. In fact, the running of their coefficient may contain coefficients of other operators, that were present at Λ scale. This particular feature will be exhaustively described in **??**.

MATCHING PROCEDURE As stated in (24), in order to obtain the theory at a lower energy a procedure called *matching* must be followed.
To determine the values of the coefficients C_i one must compute the amplitudes $\mathcal{M}$ at a given order in perturbation theory both using the theory modified by the integration of heavy degrees of freedom and the EFT as follows

$$\mathcal{M} = \langle f_n | \mathcal{L}^* | i_n \rangle = \sum_i C_i \langle f_n | Q_i | i_n \rangle + \text{h.c.} \tag{1.35}$$

In general, in order to obtain $\mathcal{L}_{\text{eff}}$ at the generic scale μ, one have to solve 1.32 in the LLA limit obtaining

$$C_i(\mu) = C_i(\Lambda) + \dot{C}_i(\Lambda) \ln \frac{\Lambda}{\mu} . \tag{1.36}$$

where the matching condition must be fulfilled.
Doing so, the Lagrangian is obtained summing over all the possible coefficients and flavor structures, obtaining

$$\mathcal{L}_{\text{eff}} = \frac{1}{\Lambda^2} \sum_i \sum_{prst} C^i_{prst}(\mu) Q^i_{prst} . \tag{1.37}$$

Concluding, the employment of the RG improved perturbation theory allows to consistently implement a perturbative procedure that leads to an effective low-energy Lagrangian. This provides an easier framework for phenomenological computations in substitution to the SM one.

In 2, the general procedure treated in the above presentation, will be specified in the case of the Lagrangian chosen to take into account NSI effects. Starting from a $\mathcal{L}_{\text{eff}}(\Lambda)$, integrating out heavy degrees of freedom, performing matching conditions and using RGE, the low energy scale $\mathcal{L}_{\text{eff}}(0.1\ \text{GeV})$ is obtained.
In 3 such Lagrangian will be used to obtain bounds on the couplings, referring to present and future experimental data.

2

AN EFT APPROACH TO NEUTRINO PHYSICS

As previously stated, under the scale $\Lambda \sim 1$ TeV the effective Lagrangian that describes NP effects would be of the form

$$\mathcal{L}_{\text{eff}} = \sum_i \frac{1}{\Lambda^2} [C_i]_{prst} [Q_i]_{prst} \,, \tag{2.1}$$

where the $[Q_i]_{prst}$ are dimension-six operators invariant under G_{SM} and the $[C_i]_{prst}$ their coefficients. The p, r, s, t are flavor indices, which will be omitted if not necessary. It's straightforward to notice that the flavor structure is completely not determined a priori and flavor changing is always possible.

Such general Lagrangian, will be specialized by suitably choosing only the operators contributing to NSI processes. As a consequence, the $\mathcal{L}_{\text{eff}}(\Lambda)$ in the mass basis will be obtained in 2.1. In 2.2, by making use of the RGE, the Wilson coefficients are evolved in order to obtain the Lagrangian at a generic scale $\mu < \Lambda$. In particular, the phenomenological implication arising at m_{EW}, studying $\mathcal{L}_{\text{eff}}(m_{\text{EW}})$, are discussed. Finally, in 2.4 we derived the low energy effective Lagrangian $\mathcal{L}_{\text{low}}$ at the scale relevant to neutrino interactions.

2.1 THE EFFECTIVE LAGRANGIAN AT THE SCALE Λ

This work will not tackle the study of the complete $\mathcal{L}_{\text{eff}}$, containing all the 59 operators. For the purpose of taking into account Non Standard neutrino Interactions, in fact, it would be suitable enough to restrict the analysis to operators which give a direct contribution to the observables of interest, like neutrino oscillation probability or neutrino production and detection cross sections. As will be treated in chapter 3, in fact, NSI can occur both at the source and at the detector due to the non-orthogonality of flavor states. Therefore, the flavor conversion $\nu_\mu^{s/d} \to \nu_\tau^{s/d}$ can be induced without oscillation.

Neutrinos are produced in the Sun in a series of processes under the name of *pp chain*. The main contribution to their production (around 95%) is given by the reactions

$$\begin{aligned} p \,+\, p &\to d \,+\, e^+ \,+ \nu_e \\ p \,+ e^- \,+\, p &\to d \,+ \nu_e \,, \end{aligned} \tag{2.2}$$

but, due to the small energy of the neutrinos produced this way ($E_\nu < 0.42$ MeV), they can hardly be detected. Most of the detected neutrinos are produced in the Sun via *electron capture* processes or *β-decays*, which are more rare processes but

the energy of the neutrinos produced is higher ($E_\nu > 1 \div 10$ MeV).

As seen in 1.3, also atmospheric neutrinos must be considered. They are more energetic ($E_\nu \gtrsim 1$GeV) and the main channel of production are *semileptonic* and *leptonic decay*

$$\begin{aligned} \pi^+ &\to \mu^+ + \nu_\mu \\ \mu^+ &\to e^+ + \nu_e + \bar{\nu}_\mu \,. \end{aligned} \tag{2.3}$$

No matter how they are produced, the detection depends on the experiment and usually involves *electron scattering* and *charged* and *neutral semi-leptonic* processes as outlined in (25).

In most of NSI analysis only the operator $Q_{\ell\ell}$, which describes neutral and charged leptonic currents, is considered. In this work, the analysis will be broadened to a more general basis of operators. In particular, we will include the following four fermions operators:

$$\begin{aligned} &\text{Purely Leptonic Operators} \\ &[Q_{\ell\ell}] \equiv (\bar{\ell}\gamma_\mu \ell)(\bar{\ell}\gamma^\mu \ell) \\ &[Q_{\ell e}] \equiv (\bar{\ell}\gamma_\mu \ell)(\bar{e}\gamma^\mu e)\,, \\ &\\ &\text{Semi-Leptonic Operators} \\ &[Q^{(1)}_{\ell q}] \equiv (\bar{\ell}\gamma_\mu \ell)(\bar{q}\gamma^\mu q) \\ &[Q^{(3)}_{\ell q}] \equiv (\bar{\ell}\gamma_\mu \tau^I \ell)(\bar{q}\gamma^\mu \tau^I q) \\ &[Q_{\ell e d q}] \equiv (\bar{\ell}^j e)(\bar{d} q^j) \\ &[Q^{(1)}_{\ell e q u}] \equiv (\bar{\ell}^j e)\epsilon_{jk}(\bar{q}^k u) \\ &[Q^{(3)}_{\ell e q u}] \equiv (\bar{\ell}^j \sigma_{\mu\nu} e)\epsilon_{jk}(\bar{q}^k \sigma^{\mu\nu} u)\,. \end{aligned} \tag{2.4}$$

Interactions involving the Higgs Bosons ($\psi^2\phi^3$ and $\psi^2\phi^2 D$) were not included because they would have modified Z and W couplings, which are instead precisely known from measurements.

Moreover, a further assumption is to assume that NP couples only to third generations, but not to the first two, as the latter are strongly constrained experimentally. NP couplings to lighter generations shall emerge when rotating to the mass basis. This assumption is realized in many concrete flavour models (such as $U(1)$ and $U(2)$ flavour models) and in models where minimal flavour violation or partial compositeness paradigms are assumed, according to (26).

A few comment on the structure and nature of the chosen operators is needed.

- All the operators are $SU(3)_C \times SU(2) \times U(1)_Y$ invariant. Whereas for operators with a vector structure and for the scalar $Q_{\ell e d q}$ this feature is almost

self-evident, for the scalar and tensor operators $Q^{(1),(3)}_{\ell equ}$ instead, it gets really explicative to prove it. Those operators, in fact, have a $(\bar{L}R)(\bar{L}R)$ structure, which at first sight does not seem $SU(2)$ invariant. We then furnish a proof for $Q^{(1)}_{\ell equ}$ since the one for $Q^{(3)}_{\ell equ}$ is completely analogous.

$$\begin{aligned} Q^{(1)}_{\ell equ} &= (\bar{\ell}^j e)\epsilon_{jk}(\bar{q}^k u) = (\bar{\ell}(i\tau_2)\bar{q}^T)(e\,u) \\ &\xrightarrow{\text{under } SU(2)} (e^{-ig\theta_i\tau_i}\bar{\ell}(i\tau_2)e^{-ig\theta_i\tau_i^T}\bar{q}^T)(e\,u) \\ &\xrightarrow{\tau_2\tau_i^T=-\tau_i\tau_2} \underbrace{e^{-ig\theta_i\tau_i}e^{+ig\theta_i\tau_i}}_{\mathbb{1}}(\bar{\ell}(i\tau_2)\bar{q}^T)(e\,u) \\ &= (\bar{\ell}(i\tau_2)\bar{q}^T)(e\,u)\,. \end{aligned} \tag{2.5}$$

- The proposed set of operators provides a complete basis of four-fermions operators producing $(V-A)$ lepton currents. Although, it stands out quite clearly an apparent asymmetry between leptonic and semi-leptonic operators.
  The first difference is that, thanks to a Fierz transformation, one can produce both neutral and charged current from the fully leptonic $Q_{\ell\ell}$, while one need to introduce $Q^{(3)}_{\ell q}$ to produce semi-leptonic charged currents. Moreover, it is easy to show that a leptonic operator like it would even be redundant, in fact

$$(\bar{\ell}_p\gamma_\mu\tau^I\ell_r)(\bar{\ell}_s\tau_I\gamma^\mu\ell_t) \overset{\tau^I_{jk}\tau^I_{mn}=2\delta_{jn}\delta_{mk}-\delta_{jk}\delta_{mn}}{=} 2Q^{ptsr}_{\ell\ell} - Q^{prst}_{\ell\ell}\,. \tag{2.6}$$

  The same feature is not possible for the semi-leptonic case because of the color structure.
  The second difference is the absence of purely leptonic scalar and tensor operators. A purely leptonic operator with a $Q_{\ell edq}$ structure would be redundant, since it can be obtained from Q_{le} via a Fierz transformation. In fact

$$(\bar{\ell}_p\gamma_\mu\ell_r)(\bar{e}_s\gamma^\mu e_t) = 2(\bar{\ell}_p\,e_t)(\bar{e}_s\,\ell_r)\,, \tag{2.7}$$

  where, again, the same feature is not possible for the semi-leptonic case because of the color structure.
  For what concerns the possibility of purely leptonic operators with a $Q^{(1),(3)}_{\ell equ}$ like structure, that is ruled out by the conservation of the hypercharge, that would be violated in a fully leptonic case

$$\begin{aligned} &(\bar{\ell}^j e)\epsilon_{jk}(\bar{\ell}^k e) \qquad Y_{\text{tot}} = 1 \\ &(\bar{\ell}^j\sigma_{\mu\nu}e)\epsilon_{jk}(\bar{\ell}^k\sigma^{\mu\nu}e) \qquad Y_{\text{tot}} = 1\,. \end{aligned} \tag{2.8}$$

  where we used the conventions on hypercharge already summarized in 1.1, $Y = T_3 - Q$. Note that using an analogous convention one would have obtained $Y_{tot} = -1$ which, obviously, in any case represent a violation of the conservation of hypercharge.

Having considered those operators, the NP Lagrangian at the Λ scale becomes

$$\begin{aligned}\mathcal{L}^0_{\text{eff}}(\Lambda) =& \frac{1}{\Lambda^2}\big(C_\ell[Q_{\ell\ell}]_{3333} + C_1[Q^{(1)}_{\ell q}]_{3333} + C_3[Q^{(3)}_{\ell q}]_{3333} + C_e[Q_{\ell e}]_{3333} \\ &+ C_s[Q_{\ell edq}]_{3333} + C_{s1}[Q^{(1)}_{\ell equ}]_{3333} + C_{s3}[Q^{(3)}_{\ell equ}]_{3333}\big)\end{aligned} \tag{2.9}$$

The operators in 2.9 are in the interaction basis. In order to switch to the mass basis the transformations in 1.10 must be performed, obtaining diagonalized Yukawa matrices but eventually producing mixing in the other sectors, as previously described.
It could be useful to define some suitable matrices, in order to lighten the notation

$$\begin{gathered}\lambda^u_{ij} = V^{*u}_{3i}V^u_{3j} \quad \lambda^d_{ij} = V^{*d}_{3i}V^d_{3j} \quad \lambda^e_{ij} = V^{*e}_{3i}V^e_{3j} \quad \lambda^{ud}_{ij} = V^{*u}_{3i}V^d_{3j} \\ \Gamma^d_{ij} = R^{*d}_{3i}R^d_{3j} \quad \Gamma^u_{ij} = R^{*u}_{3i}R^u_{3j} \quad \Gamma^e_{ij} = R^{*e}_{3i}R^e_{3j}\,.\end{gathered} \tag{2.10}$$

Finally, the Effective Lagrangian at scale Λ, in the mass basis, reads

$$\begin{aligned}\mathcal{L}^0_{\text{eff}}(\Lambda) =& \frac{C_l}{\Lambda^2}(\bar e_L\gamma^\mu\lambda_e e_L)(\bar e_L\gamma_\mu\lambda_e e_L) + \frac{C_l}{\Lambda^2}(\bar\nu_L\gamma^\mu\lambda_e\nu_L)(\bar\nu_L\gamma_\mu\lambda_e\nu_L) \\ &+ \frac{2C_l}{\Lambda^2}(\bar e_L\gamma^\mu\lambda_e e_L)(\bar\nu_L\gamma_\mu\lambda_e\nu_L) + \frac{2C_3}{\Lambda^2}(\bar e_L\gamma^\mu\lambda_e\nu_L)(\bar u_L\gamma_\mu\lambda_{ud}d_L) + \text{h.c.} \\ &+ \frac{C_1-C_3}{\Lambda^2}(\bar e_L\gamma^\mu\lambda_e e_L)(\bar u_L\gamma_\mu\lambda_u u_L) + \frac{C_1+C_3}{\Lambda^2}(\bar e_L\gamma^\mu\lambda_e e_L)(\bar d_L\gamma_\mu\lambda_d d_L) \\ &+ \frac{C_1+C_3}{\Lambda^2}(\bar\nu_L\gamma^\mu\lambda_e\nu_L)(\bar u_L\gamma_\mu\lambda_u u_L) + \frac{C_1-C_3}{\Lambda^2}(\bar\nu_L\gamma^\mu\lambda_e\nu_L)(\bar d_L\gamma_\mu\lambda_d d_L) \\ &+ \frac{C_e}{\Lambda^2}(\bar e_L\gamma^\mu\lambda_e e_L)(\bar e_R\gamma_\mu\Gamma_e e_R) + \frac{C_e}{\Lambda^2}(\bar\nu_L\gamma^\mu\lambda_e\nu_L)(\bar e_R\gamma_\mu\Gamma_e e_R) \\ &+ \frac{C_s}{\Lambda^2}(\bar\nu_L V^*_e R_e e_R)(\bar d_R R^*_d V_u u_L) + \frac{C_s}{\Lambda^2}(\bar e_L V^*_e R_e e_R)(\bar d_R R^*_d V_d d_L) \\ &+ \frac{C_{s1}}{\Lambda^2}[(\bar\nu_L V^*_e R_e e_R)(\bar d_L V^*_d R_u u_R) - (\bar e_L V^*_e R_e e_R)(\bar u_L V^*_u R_u u_R)] \\ &+ \frac{C_{s3}}{\Lambda^2}[(\bar\nu_L V^*_e\sigma^{\mu\nu} R_e e_R)(\bar d_L V^*_d\sigma_{\mu\nu} R_u u_R) \\ &- (\bar e_L V^*_e\sigma^{\mu\nu} R_e e_R)(\bar u_L V^*_u\sigma_{\mu\nu} R_u u_R)]\end{aligned} \tag{2.11}$$

2.2 THE EFFECTIVE LAGRANGIAN AT THE SCALE m_{EW}

In order to obtain $\mathcal{L}_{\text{eff}}(m_{\text{EW}})$, the procedure exposed in 1.4 will be followed. This means that the Renormalization Group Equations (RGE) for the C_i will be employed, in order to obtain an expression for the *Wilson coefficients* at the generic scale μ. Notice that, because of the peculiarity of *composite operators renormalization*, it will be possible to obtain a Lagrangian containing many new operators that were not present at scale Λ. For this reason, many peculiar characteristics will be carefully analyzed.
After doing so, the Effective Lagrangian at scale μ is obtained specifying the

generic scale $\mu = m_{EW}$ and integrating out the heavy degrees of freedom, namely the Z and W bosons.

RENORMALIZATION GROUP EVOLUTION Following the procedure exposed in 1.4 deals, first of all, with finding the solution to 1.32 using a suitable initial condition, the equation reads

$$\frac{d}{d\mu} C_i \equiv \dot{C}_i = \gamma_{ij} C_j \,, \tag{2.12}$$

and the solution, in the leading logarithm approximation, reads

$$C_i(\mu) = C_i(\Lambda) + \gamma_{ij} C_j \ln \frac{\Lambda}{\mu} \,, \tag{2.13}$$

where $\mathcal{L}^0_{eff}(\Lambda)$ has been used as initial condition, which means that the only non-zero coefficients at the Λ scale are the ones in 2.4.

The general and explicit solution for all 59 operators can be found in (27), (28) and (29), in which the anomalous dimension matrix has been calculated for every Wilson coefficient. Such solution has been used in the present work, being careful to specialize the general case taking into account only the non zero-coefficients and the possible flavor structures.
That procedure should be repeated for all the operators involved in the RGE flow, but for our purposes we can consider only the operators of the form $\psi^2\phi^3$, $\psi^2\phi^2 D$ and the leptonic and semileptonic four fermions operators. Doing so, it is possible to obtain $\mathcal{L}_{eff}$ at the generic scale μ simply performing

$$\mathcal{L}_{eff} = \frac{1}{\Lambda^2} \sum_i \sum_{prst} C^i_{prst}(\mu) Q^i_{prst} \,, \tag{2.14}$$

which will contain operators that were not present at the Λ scale.
It is important to stress that, without the presence of the matrix γ_{ij} in 2.12 it would be impossible to produce any *operator mixing*.

Let's see explicitly how this procedure works by applying it to the leptonic operator $Q_{\ell\ell}$.
First, the general expression of the equation must be evaluated at the Λ scale. Doing so, all the operators that did not appear in 2.4 will vanish.
Then, the equation obtained must be solved for the different flavor structures, which are: (3333), $(33ss)$, $(ss33)$, $(3ss3)$ and $(33st)$. It is interesting to notice that this procedure not only produces the appearance of new operators but also of new flavor structures, since at the Λ scale only the (3333) was allowed.
In the end, summing over the different flavor structures, being careful to consider possible symmetries that may simplify the flavor structure, the complete solution can be found.
The equation respected by C_{ll}, having performed some simplifications, namely

$N_C = 3$, $y_l = \frac{1}{2}$, $y_q = \frac{1}{6}$ and $\gamma^{(Y)}_{l\ ab} = \frac{1}{2}[Y_e^\dagger Y_e]_{ab}$ and noticing that only the up component of Y are non negligible, reads

$$\begin{aligned}
\dot{C}_{\substack{\ell\ell\\prst}}\Big|_\Lambda &= \frac{1}{3}g_1^2 C_{\substack{\ell\ell\\prww}}\delta_{st} + \frac{1}{3}g_1^2 C_{\substack{\ell\ell\\stww}}\delta_{pr} + \frac{1}{3}g_1^2 C_{\substack{\ell\ell\\wwst}}\delta_{pr} + \frac{1}{3}g_1^2 C_{\substack{\ell\ell\\wwpr}}\delta_{st} \\
&+ \frac{1}{6}g_1^2 C_{\substack{\ell\ell\\swwt}}\delta_{pr} + \frac{1}{6}g_1^2 C_{\substack{\ell\ell\\pwwr}}\delta_{st} + \frac{1}{6}g_1^2 C_{\substack{\ell\ell\\wrpw}}\delta_{st} + \frac{1}{6}g_1^2 C_{\substack{\ell\ell\\wtsw}}\delta_{pr} \\
&- \frac{1}{6}g_2^2 C_{\substack{\ell\ell\\pwwr}}\delta_{st} - \frac{1}{6}g_2^2 C_{\substack{\ell\ell\\swwt}}\delta_{pr} - \frac{1}{6}g_2^2 C_{\substack{\ell\ell\\wrpw}}\delta_{st} - \frac{1}{6}g_2^2 C_{\substack{\ell\ell\\wtsw}}\delta_{pr} \\
&+ \frac{1}{3}g_2^2 C_{\substack{\ell\ell\\swwr}}\delta_{pt} + \frac{1}{3}g_2^2 C_{\substack{\ell\ell\\pwwt}}\delta_{rs} + \frac{1}{3}g_2^2 C_{\substack{\ell\ell\\wrsw}}\delta_{pt} + \frac{1}{3}g_2^2 C_{\substack{\ell\ell\\wtpw}}\delta_{rs} \\
&+ 6g_2^2 C_{\substack{\ell\ell\\ptsr}} - 3(g_2^2 - g_1^2) C_{\substack{\ell\ell\\prst}} + \frac{1}{3}g_1^2 C^{(1)}_{\substack{\ell q\\prww}}\delta_{st} + \frac{1}{3}g_1^2 C^{(1)}_{\substack{\ell q\\stww}}\delta_{pr} \\
&- g_2^2 C^{(3)}_{\substack{\ell q\\prww}}\delta_{st} - g_2^2 C^{(3)}_{\substack{\ell q\\stww}}\delta_{pr} + 2g_2^2 C^{(3)}_{\substack{\ell q\\srww}}\delta_{pt} + 2g_2^2 C^{(3)}_{\substack{\ell q\\ptww}}\delta_{sr} \\
&+ \frac{1}{3}g_1^2 C_{\substack{e\\prww}}\delta_{st} + \frac{1}{3}g_1^2 C_{\substack{e\\stww}}\delta_{pr}\,.
\end{aligned} \tag{2.15}$$

That differential equation must be solved for the different flavour structure. In this case, having studied a purely leptonic operator, one need to be aware of the peculiar relation typical of this operators.
They are Fierz Identity, which implies $(\bar{L}_a L_b)(\bar{L}_c L_d) = (\bar{L}_a L_d)(\bar{L}_c L_b)$ and the fact that we're dealing only with left leptons, which implies $(\bar{L}_a L_b)(\bar{L}_c L_d) = (\bar{L}_c L_d)(\bar{L}_a L_b)$.

Taking that in mind, the following solutions are obtained

$$\begin{cases}
C_{\substack{\ell\ell\\3333}}(\mu) = C_{\ell\ell} - \dfrac{L}{(4\pi)^2} 3\left(g_2^2 + g_1^2\right) C_{\ell\ell} \\
C_{\substack{\ell\ell\\3ss3}}(\mu) = C_{\substack{\ell\ell\\s33s}}(\mu) = -\dfrac{L}{(4\pi)^2} 2\left(g_2^2 C_{\ell\ell} + 2g_2^2 C_3\right) \\
C_{\substack{\ell\ell\\33ss}}(\mu) = C_{\substack{\ell\ell\\ss33}}(\mu) = -\dfrac{L}{(4\pi)^2}\left[\left(2g_1^2 - \dfrac{2}{3}g_2^2\right) C_{\ell\ell} + \dfrac{2}{3}g_1^2 C_1 - 2g_2^2 C_3 - \dfrac{2}{3}g_1^2 C_e\right],
\end{cases} \tag{2.16}$$

where, for the sake of lightening the notation, we defined $L = \ln \frac{\Lambda}{\mu}$.

Hence, after repeating this procedure for all the operators of interest, carefully considering the peculiar properties of each one, summing them all, following 2.14, one finally gets the full Lagrangian at the generic scale μ. Such general Lagrangian can be specified at the wanted scale, being careful to integrate degrees of freedom that are not dynamical.

In general we can split the Lagrangian in three sector, each one of which accounting for a different group of operators, as following

$$\mathcal{L}_{\text{eff}}(\mu) = \delta\mathcal{L}_L + \delta\mathcal{L}_{SL} + \delta\mathcal{L}_V. \tag{2.17}$$

Explicitly the *Leptonic*, *Semi-leptonic* and *Vector Lagrangian* read

$$\begin{aligned}\delta\mathcal{L}_L =& \frac{L}{(4\pi)^2\Lambda^2}\Bigg[Q_{\substack{\ell\ell\\3333}}(3g_1^2-3g_2^2)C_{\ell\ell}+Q_{\substack{\ell\ell\\3ss3}}\left(-\frac{4}{3}g_2^2C_{\ell\ell}-4g_2^2C_3\right)\\&+Q_{\substack{\ell\ell\\33ss}}\left(\left(\frac{2}{3}g_2^2-2g_1^2\right)C_{\ell\ell}+\frac{2}{3}g_1^2C_1-\frac{2}{3}g_1^2C_e+2g_2^2C_3\right)\\&+Q_{\substack{e\\3333}}(6g_1^2C_e)+Q_{\substack{e\\33ss}}\left(-4g_1^2C_{\ell\ell}+\frac{4}{3}g_1^2C_1-\frac{4}{3}g_1^2C_e\right)\\&+Q_{\substack{e\\ss33}}\left(-\frac{2}{3}g_1^2C_e\right)+Q_{\substack{ee\\33ss}}\left(-\frac{4}{3}g_1^2C_e\right)\Bigg]\end{aligned} \tag{2.18}$$

$$\begin{aligned}\delta\mathcal{L}_{SL} =& \frac{L}{(4\pi)^2\Lambda^2}\Bigg[Q^{(1)}_{\substack{\ell q\\3333}}(g_1^2C_1-9g_2^2C_3)+Q^{(1)}_{\substack{\ell q\\33ss}}\left(\frac{2}{3}g_1^2C_{\ell\ell}-\frac{2}{9}g_1^2C_1+\frac{2}{9}g_1^1C_e\right)\\&+Q^{(1)}_{\substack{\ell q\\ss33}}\left(-\frac{2}{3}g_1^2C_1\right)+Q^{(1)}_{\substack{\ell q\\33st}}\left(-\frac{1}{2}[Y_u^\dagger Y_u]_{s3}\delta_{3t}-\frac{1}{2}\delta_{s3}[Y_u^\dagger Y_u]_{3t}\right)C_1\\&+Q^{(3)}_{\substack{\ell q\\3333}}\left(\left(6g_2^2+g_1^2\right)C_3-3g_2^2C_1\right)+Q^{(3)}_{\substack{\ell q\\33ss}}\left(-2g_2^2C_3-\frac{2}{3}g_2^2C_{\ell\ell}\right)\\&+Q^{(3)}_{\substack{\ell q\\ss33}}\left(-\frac{2}{3}g_2^2C_3\right)+Q^{(3)}_{\substack{\ell q\\33st}}\left(-\frac{1}{2}[Y_u^\dagger Y_u]_{s3}\delta_{3t}-\frac{1}{2}\delta_{s3}[Y_u^\dagger Y_u]_{3t}\right)C_3\\&+Q_{\substack{\ell u\\33ss}}\left(\frac{8}{3}g_1^2C_{\ell\ell}-\frac{8}{9}g_1^2C_1+\frac{8}{9}g_1^2C_e\right)+Q_{\substack{\ell u\\33st}}\left(2[Y_u]_{s3}[Y_u^\dagger]_{3t}C_1\right)\\&+Q_{\substack{\ell d\\33ss}}\left(-\frac{4}{3}g_1^2C_{\ell\ell}+\frac{4}{9}g_1^2C_1-\frac{4}{9}g_1^2C_e\right)+Q_{\substack{qe\\33ss}}\left(-\frac{4}{3}g_1^2C_1\right)\\&+Q_{\substack{qe\\ss33}}\left(\frac{2}{9}g_1^2C_e\right)+Q_{\substack{ed\\33ss}}\left(-\frac{4}{9}g_1^2C_e\right)+Q_{\substack{eu\\33ss}}\left(\frac{8}{9}g_1^2C_e\right)\\&+Q_{\substack{ee\\33ss}}\left(-\frac{2}{3}g_1^2C_e\right)+Q_{\substack{ee\\ss33}}\left(-\frac{2}{3}g_1^2C_e\right)+Q_{\substack{\ell edq\\3333}}\left(\frac{8}{3}g_1^2+8g_3^2\right)C_s\\&+Q_{\substack{\ell edq\\33st}}\left(-\frac{1}{2}[Y_u^\dagger Y_u]_{s3}\delta_{3t}C_s\right)\\&+Q^{(1)}_{\substack{\ell equ\\3333}}\left(\left(-\frac{11}{3}g_1^2+8g_3^2\right)C_s^{(1)}-\left(30g_1^2+18g_2^2\right)C_s^{(3)}\right)\\&+Q^{(3)}_{\substack{\ell equ\\3333}}\left(\left(-\frac{2}{9}g_1^2+3g_2^2-\frac{8}{3}g_3^2\right)C_s^{(3)}+\left(-\frac{5}{8}g_1^2-\frac{3}{8}g_2^2\right)C_s^{(1)}\right)\\&+Q^{(1)}_{\substack{\ell equ\\33st}}\left(-\frac{1}{2}[Y_u^\dagger Y_u]_{s3}\delta_{3t}-\delta_{s3}[Y_uY_u^\dagger]_{3t}\right)C_s^{(1)}\\&+Q^{(3)}_{\substack{\ell equ\\33st}}\left(-\frac{1}{2}[Y_u^\dagger Y_u]_{s3}\delta_{3t}-\delta_{s3}[Y_uY_u^\dagger]_{3t}\right)C_s^{(3)}\Bigg]\end{aligned} \tag{2.19}$$

$$\begin{aligned}\delta\mathcal{L}_{V,H} =& \frac{L}{(4\pi)^2\Lambda^2}\left[Q^{(1)}_{\substack{H\ell\\33}}\left(+2g_1^2C_{\ell\ell}-\frac{2}{3}g_1^2C_1+\frac{2}{3}g_1^2C_e-6\lambda^u_{33}y_t^2C_1\right)\right.\\&+Q^{(3)}_{\substack{H\ell\\33}}\left(-\frac{2}{3}g_2^2C_{\ell\ell}-2g_2^2C_3+6\lambda^u_{33}y_t^2C_3\right)+Q_{\substack{He\\33}}\left(-\frac{2}{3}g_2^2C_e\right)\\&+Q^{(1)}_{\substack{Hq\\33}}\left(+\frac{2}{3}g_1^2C_1\right)+Q^{(3)}_{\substack{Hq\\33}}\left(-\frac{2}{3}g_2^2C_3\right)+Q_{\substack{eH\\33}}(-12[Y_uY_u^\dagger Y_u]_{st}\delta_{st}C^{(1)}_{\ell equ})\\&\left.+\ Q_{\substack{eHW\\33}}(-6g_2[Y_u]_{st}\delta_{st}C^{(3)}_{\ell equ})+Q_{\substack{eHB\\33}}(-10g_1[Y_u]_{st}\delta_{st}C^{(3)}_{\ell equ})\right]\ .\end{aligned} \tag{2.20}$$

Some comments are needed: first of all, it is important to notice that in the evolution of $Q_{\ell edq}$, $Q^{(1)}_{\ell equ}$ and $Q^{(3)}_{\ell equ}$, the strong coupling g_3 is involved. As it is known, the strong force is asymptotically free and at low scales can become highly non perturbative.
Most importantly it is important to stress that many new operators, even with different chiral structure with respect to the Λ scale basis chosen emerge. They account both for operators with an SM structure, that can linearly modify some SM parameters, like G_F, g_1, g_2, $\sin\theta_W$ and y_f and operators with a new structure that produce new interactions.
For this reason, a closer look on $\delta\mathcal{L}_V$ should be given, since it contains terms that can produce new interactions, namely *magnetic moment type interactions* and give contribution to modification of Z, W boson and Yukawa couplings at one loop.

$\delta\mathcal{L}_{V,H}$ ANALYSIS In order to analyse the extent of the eventual modification to SM parameters the operators in $\delta\mathcal{L}_V$ must be rewritten in the mass basis, taking $\phi = \frac{1}{\sqrt{2}}(0, v+h)^{\mathrm{T}}$ and rotating the field following the convention

$$\begin{aligned}W^3_\mu &= sin\theta_W A_\mu + cos\theta_W Z_\mu\\ B_\mu &= cos\theta_W A_\mu - sin\theta_W Z_\mu\end{aligned} \tag{2.21}$$

Magnetic-type couplings

Operators that produce new magnetic moment-type interaction are in the form $\psi^2 X\phi$ and, according to (21) produce a Lagrangian containing

$$\begin{aligned}O_{eHB} =& e\frac{v}{\Lambda^2}(\bar e_L\sigma^{\mu\nu}e_R)(-A_{\mu\nu}+2\tan(\theta)_W\partial_\mu Z_\nu)\\ O_{eHW} =& e\frac{v}{\Lambda^2}(\bar e_L\sigma^{\mu\nu}e_R)(A_{\mu\nu}-2\tan(\theta)_W\partial_\mu Z_\nu)\\&-2\frac{g}{\cos\theta_W}\frac{v}{\Lambda^2}(\bar e_L\sigma^{\mu\nu}e_R)(\partial_\mu Z_\nu - ig\cos\theta_W W^+_\mu W^-_\nu)\\&+2\sqrt{2}g\frac{v}{\Lambda^2}(\bar\nu\sigma^{\mu\nu}e_R)(D_\mu - ig\cos(\theta)_W Z_\mu)W^+_\nu + \text{h.c.}\,,\end{aligned} \tag{2.22}$$

where $D_\mu = \partial_\mu - ieA_\mu$ and $A_{\mu\nu} = \partial_\mu A_\nu - \partial_\nu A_\mu$ and where we didn't show the terms depending on the Higgs field.

Yukawa coupling modification

Operators that produce a modification in the Yukawa couplings are in the

form $\psi^2\phi^3$. In our case only the leptonic operator is produced in the RGE flow and, taking $\phi = \frac{1}{\sqrt{2}}(0, v+h)^{\rm T}$ reads

$$H_{e\phi} = \frac{v^3}{\Lambda^2}\bar{e}_L e_R + 3\frac{v^2}{\Lambda^2}(\bar{e}_L e_R)h + \text{h.c.} \tag{2.23}$$

In particular the Yukawa coupling to leptons becomes

$$y_e = y_e^{\rm SM} + 2\frac{v^2}{\Lambda^2}(-12[Y_u Y_u^\dagger Y_u]_{st}\delta_{st}C^{(1)}_{\ell equ})\,. \tag{2.24}$$

We listed for completeness those operators but, since they won't give contribution to observable interesting for the study of NSI we will neglect them for now on, for the sake of simplicity.

EW couplings modifications

In the end, we analyze the part of the Lagrangian that produces modification to Z and W couplings, the only one that is actually relevant in the following. In order to explicitly evaluate the extent of the corrections to Z and W couplings, we list the involved operator

$$\begin{aligned}
Q^{(1)}_{\substack{H\ell\\33}} &= \frac{v^2}{2}\frac{g_2}{c_w}[(\bar{\nu}_L\gamma^\mu\lambda_e\nu_L) + (\bar{e}_L\gamma^\mu\lambda_e e_L)]Z_\mu + \delta\mathcal{L}_H \\
Q^{(3)}_{\substack{H\ell\\33}} &= -v^2\frac{g_2}{\sqrt{2}}[(\bar{\nu}_L\gamma^\mu\lambda_e e_L)W^+_\mu + \text{h.c.}] - \frac{v^2}{2}\frac{g_2}{c_W}[(\bar{\nu}\gamma^\mu\lambda_e\nu_L) - (\bar{e}_L\gamma^\mu\lambda_e e_L)]Z_\mu + \delta\mathcal{L}_H \\
Q_{\substack{He\\33}} &= \frac{v^2}{2}\frac{g_2}{c_W}[\bar{e}_R\gamma^\mu\Gamma_e e_R]Z_\mu + \delta\mathcal{L}_H \\
Q^{(1)}_{\substack{Hq\\33}} &= \frac{v^2}{2}\frac{g_2}{c_w}[(\bar{u}_L\gamma^\mu\lambda_u u_L) + (\bar{d}_L\gamma^\mu\lambda_d d_L)]Z_\mu + \delta\mathcal{L}_H \\
Q^{(3)}_{\substack{Hq\\33}} &= -v^2\frac{g_2}{\sqrt{2}}[(\bar{u}_L\gamma^\mu\lambda_{ud} d_L)W^+_\mu + \text{h.c.}] - \frac{v^2}{2}\frac{g_2}{c_W}[(\bar{u}\gamma^\mu\lambda_u u_L) - (\bar{d}_L\gamma^\mu\lambda_d d_L)]Z_\mu + \delta\mathcal{L}_H\,,
\end{aligned}$$

where $c_W = \cos\theta_W$.

It is clear that it is possible to express $\delta\mathcal{L}_V$ through three terms, accounting for Z, W and H sector separately

$$\delta\mathcal{L}_V = \delta\mathcal{L}_Z + \delta\mathcal{L}_W + \delta\mathcal{L}_H\,. \tag{2.25}$$

While $\delta\mathcal{L}_H$ contains terms producing new interactions not present in the SM, $\delta\mathcal{L}_Z$ and $\delta\mathcal{L}_W$ have the same structure of the Electro-Weak couplings, hence they contains corrections to named couplings.

The total Lagrangian describing Electro-Weak sector can be rewritten in order to take into account those corrections in a more explicit way, as a linear correction to the EW couplings

$$\begin{aligned}\mathcal{L}^{\text{tot}}_{Z,W} &= \mathcal{L}_{SM} + \delta\mathcal{L}_Z + \delta\mathcal{L}_W \\ &= -\frac{g_2}{c_W}\sum_f((g_f^L + \Delta g_f^L)_{ij}\bar{f}_L^i\gamma^\mu f_L^j + (g_f^R + \Delta g_f^R)_{ij}\bar{f}_R^i\gamma^\mu f_R^j)Z_\mu \\ &\quad -\frac{g_2}{\sqrt{2}}((g_l + \Delta g_l)_{ij}\bar{\nu}^i\gamma^\mu e_L^j + (g_q + \Delta g_q)_{ij}\bar{u}_L^i\gamma^\mu d_L^j + \text{h.c.})W_\mu^+ ,\end{aligned} \tag{2.26}$$

where $g_f^{L,R}$, $g_{l,q}$ express the SM couplings, while $\Delta g^{L,R}$ and $\Delta g_{\ell,q}$ contain the NP corrections.

The SM couplings read

$$\begin{cases}(g_f^L)_{ij} = (T_3 - q_f s_W^2)\delta_{ij} \\ (g_f^R)_{ij} = (-q_f s_W^2)\delta_{ij} \\ (g_\ell)_{ij} = \delta_{ij} \\ (g_q)_{ij} = (V_{\text{CKM}})_{ij}\end{cases} \tag{2.27}$$

The modified Z couplings read

$$\begin{cases}(\Delta g_e^L)_{ij} = \frac{L}{(4\pi)^2}\frac{v^2}{\Lambda^2}\left[+\frac{g_2^2}{3}(C_{\ell\ell} + 3g_2^2) + \frac{g_1^2}{3}(C_1 - C_e - 3C_{\ell\ell}) + 3\lambda_{33}^u y_t^2(C_1 - C_3)\right]\lambda_{ij}^e \\ (\Delta g_\nu^L)_{ij} = \frac{L}{(4\pi)^2}\frac{v^2}{\Lambda^2}\left[-\frac{g_2^2}{3}(C_{\ell\ell} + 3g_2^2) + \frac{g_1^2}{3}(C_1 - C_e - 3C_{\ell\ell}) + 3\lambda_{33}^u y_t^2(C_1 + C_3)\right]\lambda_{ij}^e \\ (\Delta g_d^L)_{ij} = \frac{L}{(4\pi)^2}\frac{v^2}{\Lambda^2}\left[-\frac{1}{3}(g_1^2 C_1 - g_2^2 C_3)\right]\lambda_{ij}^d \\ (\Delta g_u^L)_{ij} = \frac{L}{(4\pi)^2}\frac{v^2}{\Lambda^2}\left[-\frac{1}{3}(g_1^2 C_1 + g_2^2 C_3)\right]\lambda_{ij}^u \\ (\Delta g_e^R)_{ij} = \frac{L}{(4\pi)^2}\frac{v^2}{\Lambda^2}\left[-\frac{g_1^2}{3}C_e\right]\Gamma_{ij}^e\end{cases} \tag{2.28}$$

And the modified W couplings read

$$\begin{cases}(\Delta g_l)_{ij} = \frac{L}{(4\pi)^2}\frac{v^2}{\Lambda^2}\left[-\frac{2}{3}g_2^2(C_{\ell\ell} + 3C_3) + 6\lambda_{33}^u y_t^2 C_3\right]\lambda_{ij} \\ (\Delta g_q)_{ij} = \frac{L}{(4\pi)^2}\frac{v^2}{\Lambda^2}\left[-\frac{2}{3}g_2^2 C_3\right]\lambda_{ij}^{ud}\end{cases} \tag{2.29}$$

It is straightforward to notice that corrections to Z and W couplings provide a non diagonal flavor structure, encoded in λ_{ij}^f and Γ_{ij}^f matrices.
That provides two breaking difference with respect to the SM:

- A source of lepton flavor violation in the charged current, directly at tree level, is introduced,
- A source of flavor violation in neutral current both for leptons (L and R current) and quarks (only L current) emerge.

Moreover, it is important to notice also the introduction of a dependence on the fictitious scale μ in the couplings, inside $L = \ln(\Lambda \setminus \mu)$. The cancellation of named scale will be proved in section 2.3.

INTEGRATING OUT HEAVY DEGREES OF FREEDOM After having found, thanks to Renormalization Group Evolution of the couplings, $\mathcal{L}_{\text{eff}}(\mu)$, the next step is to integrate out heavy degrees of freedom, such as Z and W boson fields, since they don't represent dynamical quantities when running μ to m_{EW} scale.
To do so, some suitable substitutions have to be done, just like in the Fermi theory. In that context the vector ($V = W, Z$) propagator, under the *Fermi approximation* became

$$iD_F^{\alpha\beta}(k, m_V) = i\frac{-g^{\alpha\beta} + \frac{k^\alpha k^\beta}{m_V}}{k^2 - m_V^2 + i\epsilon} \to i\frac{g^{\alpha\beta}}{m_V^2}\,, \tag{2.30}$$

which corresponds to a *contact interaction*.
The fields in the Lagrangian, as a consequence, are modified as follows

$$W_\mu^{+,-} \to \frac{g_{\nu\mu}}{m_W^2}\frac{J^{\nu\,+,-}}{\sqrt{2}} \quad Z_\mu \to \frac{g_{\nu\mu}}{m_Z^2}\frac{J^{\nu\,0}}{2\cos\theta_W}\,, \tag{2.31}$$

where symmetry factors have been taken into account. Finally, 2.26 becomes

$$\mathcal{L}_{Z,W}^{tot} \approx -\frac{2}{v^2}(J_{\text{SM}}^{\mu\,0}J_{\mu\,\text{SM}}^0 + J_{\text{SM}}^{\mu\,+}J_{\mu\,\text{SM}}^- + 2J_{\text{SM}}^{\mu\,0}J_{\mu\,\text{NP}}^0 + J_{\text{SM}}^{\mu\,+}J_{\mu\,\text{NP}}^- + \text{h.c.})\,, \tag{2.32}$$

where only linear terms in Δg, have been taken into account.
It is clear that the Lagrangian contains now terms in the form of four fermions operator, and the ones containing NP corrections might give contributions to terms in $\delta\mathcal{L}_L$ and $\delta\mathcal{L}_{SL}$.

Having done so, it is possible to write the effective Lagrangian at $\mu = m_{EW}$, being sure that all the heavy degrees of freedom have been integrated out, at tree level

$$\mathcal{L}_{\text{eff}}(m_{EW}) = \frac{1}{\Lambda^2}\sum_i C_i(m_{EW})Q_i\,. \tag{2.33}$$

Given Lagrangian must be expressed in the mass basis using 1.10 relations. Moreover some additional and useful relations for operators of flavor structure 3333, 33ss, ss33 and 3ss3 can be used in order to shorten the calculation such as

$$\begin{cases} \bar{f}_{3L}^i\gamma_\mu f_{3L}^i = \bar{f}_L^m\gamma_\mu\lambda_f f_L^m \\ \bar{f}_{3R}^i\gamma_\mu f_{3R}^i = \bar{f}_R^m\gamma_\mu\Gamma_f f_R^m \\ \sum_s \bar{f}_s^i\gamma_\mu f_s^i = \bar{f}^m\gamma_\mu f^m \end{cases} \tag{2.34}$$

For operators whose flavor structure is 33st, instead, some more attention must be employed, obtaining the following relations

$$\begin{cases} \sum_{st} \left([Y_u^\dagger Y_u]_{s3}\delta_{3t} + \delta_{s3}[Y_u^\dagger Y_u]_{3t} \right) V_{u,ti} V_{u,sj}^* = y_t^2 (P_3 \lambda_u + \lambda_u P_3)_{ij} \\ \sum_{st} [Y_u]_{s3} [Y_u^\dagger]_{3t} R_{u,sj}^* R_{u,ti} = y_t^2 \lambda_3 3^u \delta_{3j} \delta_{i3} \end{cases} \tag{2.35}$$

Having used all this relations, and adding the contributions coming from 2.32 to the corresponding four fermions operators, the effective Lagrangian at the m_{EW} scale is obtained

$$\mathcal{L}_{\text{eff}}(m_{\text{EW}}) = \frac{1}{(4\pi)^2 \Lambda^2} \ln \frac{\Lambda}{m_{\text{EW}}} \sum_i \xi_i Q_i. \tag{2.36}$$

The correct, modified, couplings ξ_i along with their corresponding operators Q_i are listed in the table 2.1.

Table 2.1: Operators in $\mathcal{L}_{\rm eff}(m_{\rm EW})$ and their coefficients ξ_i

Leptonic operators in $\mathcal{L}_{\rm eff}(m_{\rm SM})$

Q_i	ξ_i
$(\bar{e}^i_L\gamma_\mu e^j_L)(\bar{e}^k_L\gamma^\mu e^\ell_L)$	$\lambda_e^{kl\ell}\delta^{ij}[\frac{4}{3}e^2(C_1 - C_e - 3C_3 - 4C_{\ell\ell}) - 12\lambda_{33}y_t^2(C_1 - C_3)(-\frac{1}{2} + s_W^2)] + \lambda_e^{ij}\lambda_e^{k\ell}(-3(g_1^2+g_2^2)C_{\ell\ell})$
$(\bar{e}^i_L\gamma_\mu e^j_L)(\bar{\nu}^k_L\gamma^\mu \nu^\ell_L)$	$\lambda_e^{k\ell}\delta^{ij}[\frac{4}{3}e^2(C_1 - C_e + 3C_3 - 2C_{\ell\ell}) - 12\lambda_{33}y_t^2(C_1 + C_3)(-\frac{1}{2} + s_W^2)] + \lambda_e^{ij}\lambda_e^{k\ell}(-6(g_1^2+g_2^2)C_{\ell\ell}) + \lambda_e^{ij}\delta^{k\ell}(-6\lambda_{33}^u y_t^2(C_1 - C_3))$
$(\bar{e}^i_L\gamma_\mu e^j_L)(\bar{e}^k_R\gamma^\mu e^\ell_R)$	$\delta^{ij}\Gamma_e^{k\ell}(-\frac{4}{3}e^2C_e) + \lambda_e^{ij}\delta^{k\ell}[\frac{4}{3}e^2(C_1 - 3C_3 - C_e - 4C_{\ell\ell}) - 12\lambda_{33}y_t^2(C_1 - C_3)s_W^2] + \lambda_e^{ij}\Gamma_e^{k\ell}(6g_1^2C_e)$
$(\bar{\nu}^i_L\gamma_\mu \nu^j_L)(\bar{\nu}^k_L\gamma^\mu \nu^\ell_L)$	$\delta^{ij}\lambda_e^{k\ell}(-6\lambda_{33}^u y_t^2(C_1+C_3)) + \lambda_e^{ij}\lambda_e^{k\ell}(-3(g_1^2+g_2^2)C_{\ell\ell})$
$(\bar{\nu}^i_L\gamma^\mu \nu^j_L)(\bar{e}^k_R\gamma_\mu e^\ell_R)$	$\lambda_e^{ij}\delta^{k\ell}[\frac{4}{3}e^2(C_1+3C_3-C_e-2C_{\ell\ell}) - 12\lambda_{33}y_t^2(C_1+C_3)s_W^2] + \lambda_e^{ij}\Gamma_e^{ij}(6g_1^2C_e)$
$(\bar{e}^i_R\gamma_\mu e^j_R)(\bar{e}^k_R\gamma^\mu e^\ell_R)$	$\Gamma_e^{ij}\delta_{k\ell}(\frac{4}{3}g_1^2C_e) + \Gamma_e^{ij}\Gamma_e^{k\ell}(\frac{4}{3}g_1^2s_W^2C_e)$
$(\bar{\nu}^i_L\gamma_\mu e^j_L)(\bar{e}^k_L\gamma^\mu \nu^\ell_L)$	$(\lambda_e^{ij}\delta^{k\ell} + \delta^{ij}\lambda_e^{k\ell})(-12\lambda_{33}y_t^2C_3)$

Semi-leptonic operators in $\mathcal{L}_{\rm eff}(m_{\rm EW})$

Q_i	ξ_i
$(\bar{\nu}^i_L\gamma^\mu \nu^j_L)(\bar{u}^k_L\gamma_\mu u^\ell_L)$	$\lambda_e^{ij}\delta^{k\ell}[\frac{8}{9}e^2(C_e - 3C_3 + 2C_{\ell\ell} - C_1) - 12\lambda_{33}y_t^2(C_1+C_3)(\frac{1}{2} - \frac{2}{3}\sin^2_W)] + \lambda_e^{ij}\lambda_u^{k\ell}(g_1^2 - 3g_2^2)(C_1+C_3) + \lambda_e^{ij}(\lambda_u^{k3}\delta^{3\ell} + \delta^{k3}\lambda_u^{3\ell})(-\frac{1}{2}y_t^2(C_1+C_3))$
$(\bar{\nu}^i_L\gamma^\mu \nu^j_L)(\bar{d}^k_L\gamma_\mu d^\ell_L)$	$\lambda_e^{ij}\delta^{k\ell}[\frac{4}{9}e^2(C_1 - C_e + 3C_3 - 2C_{\ell\ell}) - 12\lambda_{33}y_t^2(C_1 + C_3)(-\frac{1}{2} + \frac{1}{3}\sin^2_W)] + \lambda_e^{ij}\lambda_d^{k\ell}(g_1^2 + 3g_2^2)C_1 - (g_1^2 + 15g_2^2)C_3 + \lambda_e^{ij}((\lambda_{ud}^\dagger)^{k3}V_{\rm CKM}^{3\ell} + (V_{\rm CKM}^\dagger)^{k3}\lambda_{ud}^{3\ell})(-\frac{1}{2}y_t^2(C_1 - C_3))$
$(\bar{\nu}^i_L\gamma^\mu \nu^j_L)(\bar{u}^k_R\gamma_\mu u^\ell_R)$	$\lambda_e^{ij}\delta^{k\ell}[\frac{8}{9}e^2(C_e - 3C_3 + 2C_{\ell\ell} - C_1) + 8\lambda_{33}y_t^2(C_1 + C_3)\sin^2_W] + \lambda_e^{ij}\delta^{k3}\delta^{3\ell}(2y_t^2\lambda_{33}C_1)$
$(\bar{\nu}^i_L\gamma^\mu \nu^j_L)(\bar{d}^k_R\gamma_\mu d^\ell_R)$	$\lambda_e^{ij}\delta^{k\ell}[\frac{4}{9}e^2(C_1+3C_3-2C_{\ell\ell}-C_e) - 4\lambda_{33}y_t^2(C_1+C_3)\sin^2_W]$
$(\bar{e}^i_L\gamma_\mu e^j_L)(\bar{u}^k_L\gamma^\mu u^\ell_L)$	$\delta^{ij}\lambda_e^{k\ell}(-\frac{4}{3}e^2(C_1 - C_3)) + \lambda_e^{ij}\delta^{k\ell}[\frac{8}{9}e^2(C_e + 3C_3 + 4C_{\ell\ell} - C_1) - 12\lambda_{33}y_t^2(C_1 - C_3)(\frac{1}{2} - \frac{2}{3}\sin^2_W)] + \lambda_e^{ij}\lambda_u^{k\ell}((g_1^2+3g_2^2)C_1 - (g_1^2+15g_2^2)C_3) + \lambda_e^{ij}(-\frac{1}{2}y_t^2(C_1 - C_3))$
$(\bar{e}^i_L\gamma^\mu e^j_L)(\bar{u}^k_R\gamma_\mu u^\ell_R)$	$\lambda_e^{ij}\delta^{k\ell}[\frac{8}{9}e^2(C_e + 3C_3 + 4C_{\ell\ell} - C_1) + 8\lambda_{33}y_t^2(C_1 - C_3)\sin^2_W] + \lambda_e^{ij}\delta^{k3}\delta^{3\ell}(2y_t^2\lambda_{33}C_1)$
$(\bar{e}^i_L\gamma_\mu e^j_L)(\bar{d}^k_L\gamma^\mu d^\ell_L)$	$\delta^{ij}\lambda_d^{k\ell}(-\frac{4}{3}e^2(C_1 + C_3)) + \lambda_e^{ij}\delta^{k\ell}[\frac{4}{9}e^2(C_1 - C_e - 3C_3 - 4C_{\ell\ell}) - 12\lambda_{33}y_t^2(C_1 - C_3)(-\frac{1}{2} + \frac{1}{3}\sin^2_W)] + \lambda_e^{ij}\lambda_d^{k\ell}(g_1^2 - g_2^2)(C_1 + C_3) + \lambda_e^{ij}((\lambda_{ud}^\dagger)^{k3}V_{\rm CKM}^{3\ell} + (V_{\rm CKM}^\dagger)^{k3}\lambda_{ud}^{3\ell}))(-\frac{1}{2}y_t^2(C_1+C_3))$
$(\bar{e}^i_L\gamma_\mu e^j_L)(\bar{d}^k_R\gamma^\mu d^\ell_R)$	$\lambda_e^{ij}\delta^{k\ell}[\frac{4}{9}e^2(C_1 - C_e - 3C_3 + 4C_{\ell\ell}) - 4\lambda_{33}y_t^2\sin^2_W(C_1 - C_3)]$
$(\bar{e}^i_R\gamma_\mu e^j_R)(\bar{u}^k_L\gamma^\mu u^\ell_L)$	$\delta^{ij}\lambda_u^{k\ell}(-\frac{4}{3}e^2(C_1 - C_3)) + \Gamma_e^{ij}\delta^{k\ell}(\frac{8}{9}e^2C_e)$
$(\bar{e}^i_R\gamma_\mu e^j_R)(\bar{d}^k_L\gamma^\mu d^\ell_L)$	$\delta^{ij}\lambda_d^{k\ell}(-\frac{4}{3}e^2(C_1 + C_3)) + \Gamma_e^{ij}\delta^{k\ell}(\frac{4}{9}e^2C_e)$
$((\bar{e}^i_R\gamma^\mu e^j_R)\bar{u}^k_R\gamma_\mu u^\ell_R)$	$\Gamma_e^{ij}\delta^{k\ell}(\frac{8}{9}e^2C_e)$
$(\bar{e}^i_R\gamma^\mu e^j_R)(\bar{d}^k_R\gamma_\mu d^\ell_R)$	$\Gamma_e^{ij}\delta^{k\ell}(-\frac{4}{9}e^2C_e)$
$(\bar{\nu}^i_L e^j_R)(\bar{d}^k_R u^\ell_L)$	$(V_e^*R_e)^{ij}((R_d^*V_u)^{k\ell}(\frac{8}{3}g_1^2 + 8g_3^2)C_s + ((\lambda_u)^{k3}\delta^{3\ell})(-\frac{1}{2}y_t^2C_s))$
$(\bar{e}^i_L e^j_R)(\bar{d}^k_R d^\ell_L)$	$(V_e^*R_e)^{ij}((R_d^*V_d)^{k\ell}(\frac{8}{3}g_1^2 + 8g_3^2)C_s + ((\lambda_u)^{k3}\delta^{3\ell})(-\frac{1}{2}y_t^2C_s))$
$(\bar{\nu}^i_L e^j_R)(\bar{d}^k_L u^\ell_R)$	$(V_e^*R_e)^{ij}((V_d^*R_d)^{k\ell}((-\frac{11}{3}g_1^2 + 8g_3^2)C_s^1 - (30g_1^2 + 18g_2^2)C_s^3) + ((\lambda_u)^{k3}\delta^{3\ell})(-\frac{1}{2}y_t^2C_s^1))$
$(\bar{e}_Le_R)(\bar{u}_Lu_R)$	$(V_e^*R_e)((V_u^*R_d)((\frac{11}{3}g_1^2 - 8g_3^2)C_s^1 + (30g_1^2 + 18g_2^2)C_s^3) + (\lambda_u^{3k}\delta^{3\ell} + \delta^{k3}\lambda_u^{3\ell})(\frac{1}{2}y_t^2C_s^1))$
$(\bar{\nu}^i_L\sigma_{\mu\nu}e^j_R)(\bar{d}^k_L\sigma^{\mu\nu}u^\ell_R)$	$(V_e^*R_e)^{ij}((V_d^*R_d)^{k\ell}(-\frac{2}{9}g_1^2 + 6g_2^2 - \frac{8}{3}g_3^2)C_s^3 + (\frac{5}{8}g_1^2 - \frac{3}{8}g_2^2)C_s^1 + (\lambda_u^{3k}\delta^{3\ell} + \delta^{k3}\lambda_u^{3\ell})(-\frac{1}{2}y_t^2C_s^3))$
$(\bar{e}^i_L\sigma_{\mu\nu}e^j_R)(\bar{u}^k_L\sigma^{\mu\nu}u^\ell_R)$	$(V_e^*R_e)^{ij}((V_d^*R_d)^{k\ell}(\frac{2}{9}g_1^2 - 6g_2^2 + \frac{8}{3}g_3^2)C_s^3 - (\frac{5}{8}g_1^2 - \frac{3}{8}g_2^2)C_s^1 + (\lambda_u^{3k}\delta^{3\ell} + \delta^{k3}\lambda_u^{3\ell})(\frac{1}{2}y_t^2C_s^3))$
$(\bar{\nu}^i_L\gamma_\mu e^j_L)(\bar{d}^k_L\gamma^\mu u^\ell_L)$	$\lambda_e^{ij}\lambda_{ud}^{k\ell}(-12g_2^2C_1 + 4(6g_2^2 + g_1^2)C_3) + \lambda_e^{ij}\delta^{k\ell}V_{\rm CKM}(-12\lambda_{33}y_t^2C_3) + \lambda_e^{ij}(\lambda_{ud}^\dagger)^{k3}V_{\rm CKM}^{3\ell} + (V_{\rm CKM}^\dagger)^{k3}\lambda_{ud}^{3\ell})(-y_t^2C_3)$

2.3 CANCELLATION OF THE μ SCALE

As exposed in previous sections, the RG evolution of couplings introduces a dependence on the fictitious scale μ. On the other hand, cross sections, and in general all observable quantities, must be independent on any arbitrary scale. Thanks to renormalization procedure, in fact, that μ dependence is just the one needed to cancel μ scale emerging in regularized integrals in one loop diagrams. That cancellation is checked explicitly in the following example, calculating the W boson decay in leptons, $W^+ \to e_L^+ \nu_L$.

The involved diagrams are

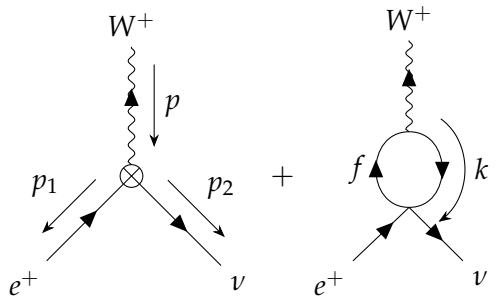

(2.37)

The amplitude for the formal tree level diagram, with a "one-loop" vertex, reads

$$\mathcal{M}_a = \mathcal{M}_{\text{SM}} + \Delta\mathcal{M}_\ell = -i\frac{g_2}{\sqrt{2}}\bar{u}_i \not{\epsilon}(g_l + \Delta g^l)_{ij} P_L v_j \tag{2.38}$$

where

$$\Delta\mathcal{M}_\ell = -i\frac{g_2}{\sqrt{2}} v^2 \frac{L}{(4\pi)^2\Lambda^2}\left[-\frac{2}{3}g_2^2 C_{\ell\ell} - 2g_2^2 C_3 + 6\lambda_{33}^u y_t^2 C_3\right](\bar{u}_i \not{\epsilon} P_L \lambda_{ij}^e v_j). \tag{2.39}$$

is the sector of the amplitude containing the μ dependence, through L.

The four fermions operators contributing to the total one loop diagram amplitude are

$$\begin{aligned} &(1) \quad \frac{2C_{\ell\ell}}{\Lambda^2}(\bar{e}_L\gamma_\mu\lambda_e\nu_L)(\bar{\nu}_L\gamma^\mu\lambda_e e_L) \\ &(2) \quad \frac{2C_3}{\Lambda^2}(\bar{e}_L\gamma_\mu\lambda_e\nu_L)(\bar{u}_L\gamma^\mu\lambda_{ud} d_L) \end{aligned} \tag{2.40}$$

and corresponds to two different one loop diagrams, with "tree level" vertices and different fermions running in the loop.
Hence, the total one loop amplitude should be composed of two parts

$$\mathcal{M}_{\text{loop}} = \mathcal{M}_{\text{loop}}^{(1)} + \mathcal{M}_{\text{loop}}^{(2)} \tag{2.41}$$

The result of the computation of $\mathcal{M}_{\text{loop}} + \Delta\mathcal{M}_\ell$ should not depend on the renormalization scale μ, as will be proven in the following. For the detailed cal-

culation of the one loop amplitude we refer to the Appendix C.

The one loop amplitude with operator (1) inserted, i.e. with leptons in the loop, reads

$$\mathcal{M}^{(1)}_{\text{loop}} = \frac{4i}{(4\pi)^2\Lambda^2} C_{\ell\ell} \frac{g_2}{\sqrt{2}} (\bar{u}_i \not{\epsilon} P_L \lambda^e_{ij} v_j) \int_0^1 \mathrm{d}x\, m_W^2 x(1-x) \ln \frac{\mu^2}{\Delta} \tag{2.42}$$

An analogous calculation must be followed in order to obtain $\mathcal{M}^{(2)}_{\text{loop}}$, the one loop amplitude with operator (2) inserted. In the assumption that the only non negligible quark mass is that of the top, m_t, this amplitude reads

$$\begin{aligned}\mathcal{M}^{(2)}_{\text{loop}} =& \frac{12i}{(4\pi)^2\Lambda^2} C_3 \frac{g_2}{\sqrt{2}} \int_0^1 \mathrm{d}x \left[\lambda^u_{33} \left(m_t^2(x-1) + 2m_W^2 x(1-x) \right) \ln \frac{\mu^2}{\Delta'} \right. \\ &\left. + (1-\lambda^u_{33})(2m_W^2 x(1-x)) \ln \frac{\mu^2}{\Delta} \right] (\bar{u}_i \not{\epsilon} P_L \lambda^e_{ij} v_j)\,.\end{aligned} \tag{2.43}$$

In conclusion, summing 2.42 and 2.43 one obtains

$$\begin{aligned}\mathcal{M}_{\text{loop}} =& \frac{4i}{(4\pi)^2\Lambda^2} \frac{g_2}{\sqrt{2}} (\bar{u}_i \not{\epsilon} P_L \lambda^e_{ij} v_j) [(2C_{\ell\ell} + 6C_3) m_W^2 \mathcal{I}_2^\mu - 3m_t^2 \lambda_3 3 C_3 \mathcal{I}_1^\mu + \\ &+ 6m_t^2 C_3 \lambda_{33} \mathcal{I}_3]\,,\end{aligned} \tag{2.44}$$

where

$$\begin{aligned}\mathcal{I}_1^\mu &= \int_0^1 \mathrm{d}x\, (1-x) \ln \frac{\mu^2}{\Delta'} \\ \mathcal{I}_2^\mu &= \int_0^1 \mathrm{d}x\, x(1-x) \ln \frac{\mu^2}{\Delta} \\ \mathcal{I}_3 &= \int_0^1 \mathrm{d}x\, x(1-x) \ln \frac{\Delta}{\Delta'}\,.\end{aligned} \tag{2.45}$$

In the end, conveniently rewriting 2.38, the sum of the one loop and the RGE Feynman Amplitudes reads

$$\mathcal{M}_a + \mathcal{M}_{\text{loop}} = \frac{i}{(4\pi)^2\Lambda^2} v^2 \frac{g_2}{\sqrt{2}} (\bar{u}_i \not{\epsilon} P_L \lambda^e_{ij} v_j) [(2g_2^2 C_{\ell\ell} + 6g_2^2 C_3)\mathcal{I}_2 - 6\lambda_{33} y_t^2 C_3 \mathcal{I}_1 + 6g_2^2 C_3 \lambda_{33} \mathcal{I}_3]$$

where

$$\begin{aligned}\mathcal{I}_1 &= \int_0^1 \mathrm{d}x\, (1-x) \ln \frac{\Lambda^2}{\Delta'} \\ \mathcal{I}_2 &= \int_0^1 \mathrm{d}x\, x(1-x) \ln \frac{\Lambda^2}{\Delta}\end{aligned} \tag{2.46}$$

which does not depend on the fictitious scale μ, concluding the demonstration. Similar procedures can be followed to prove the cancellation of the μ scale in any other process.

2.4 THE EFFECTIVE LOW ENERGY SCALE LAGRANGIAN

As outlined in the previous discussion, every physical process is characterized by a specific energy scale. When introducing the EFT approach, the energy scales of the processes define also the EFT valid in the considered range.
This peculiar characteristic was already sketched in paragraph 2.2 where, considering energy scales $\mu \leq m_{\text{EW}}$, 2.17 was modified because W_μ and Z_μ didn't stand for dynamical degrees of freedom anymore, at such energies.
In this sense, every energy threshold defined by the mass of a particle represents a boundary between EFT Lagrangians where different degrees of freedom are dynamical.

As seen in the previous sections, many interactions involving neutrinos are characterized by really small energies, typically of the order of m_μ and m_π, i.e. $E_\nu \sim 0.1$ GeV . For practical reasons, one can safely assume to put the low energy boundary at a slightly higher energy, i.e. 2 GeV.
In order to correctly describe those processes within an EFT approach, it is crucial to obtain a Lagrangian defined at such scale. Again, by means of RGE and matching procedures, this low energy scale Lagrangian can be obtained by carefully integrate the heavy d.o.f. that are not dynamical anymore.
When running under the m_{EW} scale, there are just one energy scale defined by the masses of the bottom m_b and that have to be crossed, in order to get to 2 GeV. When going across those scales all the degrees of freedom that are not dynamical anymore have to be integrated out, reducing the number of d.o.f..

One can define the effective Lagrangian at scale 2 GeV $< \mu < m_b$ as

$$\mathcal{L}_{\text{eff}} = \frac{1}{\Lambda^2} \sum_i \hat{C}_i(\mu) Q_i \,. \tag{2.47}$$

In order to obtain $\hat{C}_i(\mu)$ the matching between the Wilson coefficients at every threshold must be fulfilled.
In table 2.2 the different effective field theories, characterized by different dynamical d.o.f, for the different energetic ranges, are listed.

Table 2.2: Energy thresholds in the range $m_{\text{EW}} \div 2$ GeV

energy range	EFT Lagrangian	d.o.f
$\Lambda > \mu > m_{\text{EW}}$	$\mathcal{L}_{\text{eff}} = \frac{1}{\Lambda^2} \sum_i C_i(\mu) Q_i$	$W, Z, u, d, c, s, b, t, e, \mu, \tau$
$m_{\text{EW}} > \mu > m_b$	$\mathcal{L}_{\text{eff}} = \frac{1}{\Lambda^2} \sum_i \bar{C}_i(\mu) Q_i$	$u, d, c, s, b, e, \mu, \tau$
$m_b > \mu > 2$ GeV	$\mathcal{L}_{\text{eff}} = \frac{1}{\Lambda^2} \sum_i \hat{C}_i(\mu) Q_i$	u, d, c, s, e, μ, τ

The matching condition reads

$$\bar{C}_i(m_b) = \hat{C}_i(m_b) \,, \tag{2.48}$$

while the RGE flow for the Wilson coefficients in the different energy ranges reads

$$\begin{aligned}\bar{C}_i(\mu) &= \bar{C}_i(m_{\text{EW}}) - \frac{a_i}{(4\pi)^2}\ln\frac{m_{\text{EW}}}{\mu} \qquad m_b < \mu < m_{\text{EW}} \\ \hat{C}_i(\mu) &= \hat{C}_i(m_b) - \frac{b_i}{(4\pi)^2}\ln\frac{m_b}{\mu} \qquad 2\,\text{GeV} < \mu < m_b\end{aligned} \tag{2.49}$$

where the coefficients a_i and b_i must be determined using the matching procedure.
Using 2.48 in 2.49, one obtains the expression for $\hat{C}_i(\mu)$

$$\hat{C}_i(\mu) = C_i(m_{\text{EW}}) - \underbrace{\frac{1}{(4\pi)^2}\left(a_i \ln\frac{m_{\text{EW}}}{m_b} + b_i \ln\frac{m_b}{\mu}\right)}_{\delta C_i(\mu)}, \tag{2.50}$$

rewriting $\delta C_i(\mu)$ making explicit the μ dependence, one obtains

$$\delta C_i(\mu) = \frac{1}{(4\pi)^2}\ln\frac{m_{\text{EW}}}{\mu}\delta\xi_i\,, \tag{2.51}$$

with

$$\delta\xi_i = -\frac{1}{\ln\frac{\mu}{m_{\text{EW}}}}\left(a_i \ln\frac{m_{\text{EW}}}{m_b} + b_i \ln\frac{m_b}{\mu}\right). \tag{2.52}$$

Putting 2.51 in 2.47, remembering the expression for $C_i(m_{\text{EW}})$ used in 2.36, one obtains

$$\mathcal{L}_{\text{eff}} = \frac{1}{16\pi^2\Lambda^2}\ln\frac{\Lambda}{m_{\text{EW}}}\Sigma_i\xi_i Q_i + \frac{1}{16\pi^2\Lambda^2}\ln\frac{m_{\text{EW}}}{\mu}\sum_i \delta\xi_i Q_i \tag{2.53}$$

that is the effective Lagrangian at scale 2 GeV $< \mu < m_c$, once the coefficients a_i, b_i are determined.
In order to identify the coefficients two main procedure can be followed.

The first one basically deals with exploiting the matching condition, imposing the cancelation of the fictitious scale μ. The first step is to identify four fermion processes that receive contribution only from a single Q_i.
Then, the diagrams contributing to the process must be depicted. In general, one expect the process to receive three contributions: (i) a truly tree-level contribution, that will be irrelevant for our purposes, (ii) a formal tree-level contribution where the vertices are proportional to the unknown coefficients and are "at one loop" i.e. there is an RGE modification of the vertex and (iii) a one-loop contribution with the insertion of Λ scale operators in 2.4, i.e. "tree level" vertices.
Wanting to calculate the one loop corrections, it is important to stress that under the m_{EW} scale the two vector bosons that are still dynamical degrees of freedom are the photon and the gluon. This means that the one-loop diagrams (with tree-level vertices) can involve only the exchange of virtual photon or gluon and of the fermions that are dynamical in the considered energy range. Evidently, all the processes that cannot receive one-loop contributions, will have $\delta\xi = 0$.
In the end, imposing

$$\mathcal{M}_{\text{RGE}} + \mathcal{M}_{\text{loop}} = \text{independent from } \mu\,, \tag{2.54}$$

it is possible to obtain conditions on the coefficients and completely determine a_i, b_i and c_i.

Diagrammatically, the matching condition reduces to the following pictorial relation:

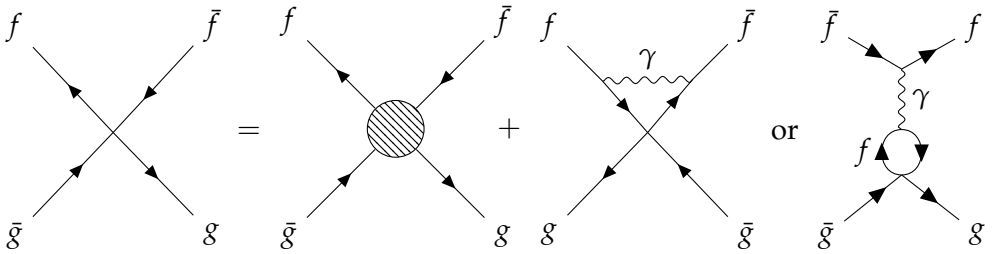

(2.55)

The other path deals directly with finding a solution to the RGE and is outlined by (30). This solution can be achieved by computing the anomalous dimension matrix for the Q_i accounting for both QED and QCD corrections. Once again, one chooses a process and calculates the one loop corrections emerging after inserting gluon and photon propagators. Calculating QED (and QCD) corrections to a process essentially stands for the calculation of the anomalous dimension matrix γ arising between the operators participating to such process.

In fact, as already stated in 1.4, the anomalous dimension matrix γ is defined as

$$\gamma_{ij} = \frac{1}{Z_{ik}} \left(\frac{dZ}{d \ln \mu} \right)_{kj} , \tag{2.56}$$

where Z is a renormalization factor that allows to eliminate divergencies ($Q_i^0 = (Z^{-1})_{ij} Q_j$) and μ is the renormalization scale.
Then, one can transfer the divergency of the operator Q_i to its coefficient C_i so that

$$\mu \frac{d}{d\mu} C_i(\mu) = \gamma_{ij} C_j(\mu) . \tag{2.57}$$

Since such Z can be expanded perturbatively, at one loop one gets

$$Z_{ij} = 1 + Z_{ij}^{(2)} + \mathcal{O}(\alpha^2) . \tag{2.58}$$

A simple consequence, directly from 2.56 and 2.58, is that

$$\gamma_{ij} = \epsilon Z_{ij}^{(2)} + \mathcal{O}(\alpha^2). \tag{2.59}$$

Concluding, in order to obtain the anomalous dimension matrix at one loop, all one need to do is to calculate $Z_{ij}^{(2)}$, simply evaluating the one loop $\frac{1}{\epsilon}$ pole terms.

Various examples of both procedures will be provided: it was chosen to follow the first procedure for what concerns operators involving neutral current because in that case, as we will see, only two types of one-loop corrections can

arise in the calculations: *electromagnetic current-current* and *electromagnetic penguins* both leptonic and hadronic. The second procedure outlined, instead, will be applied to a charged current process, i.e. QED and QCD corrections to pion decay.

CURRENT-CURRENT OPERATORS Current-current neutral operators can have Vector or Scalar (and Tensor) vertices.
In order to solve 2.55, one needs to list all the one loop diagrams that produces a correction to those kind of operators:

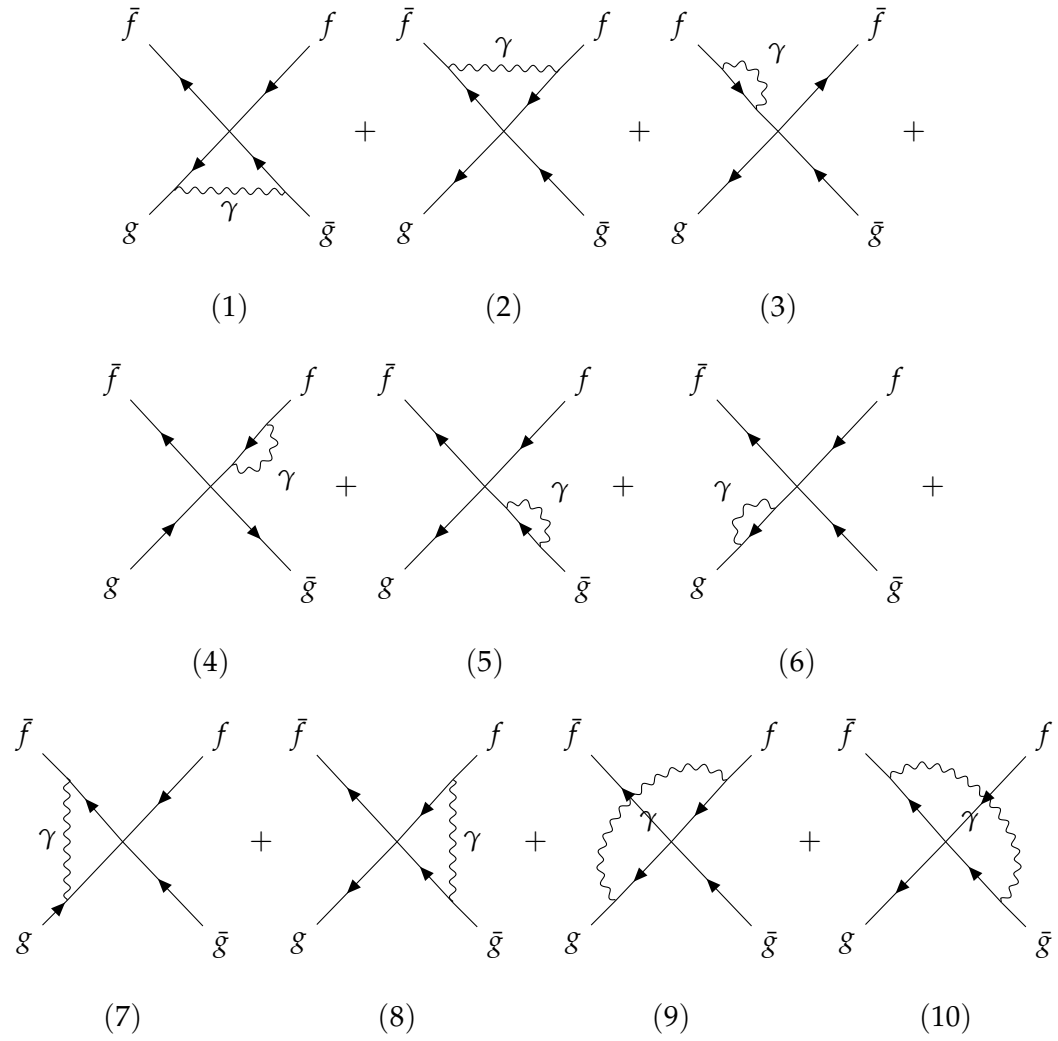

Vector operators are given by the product of two $V - A$ currents and have the form $Q_{CC} = (\bar{f}\gamma^\mu M^f P_{L/R} f)(\bar{g}\gamma_\mu M^g P_{L/R} g)$, where f and g are fermions, $P_{L/R}$ is a projector and $M^{f,g}$ is either $\lambda^{f,g}$ or $\Gamma^{f,g}$. *Vector vertices*

Let's consider the generic process $\bar{f}_i f \to \bar{g}g$, which receives contribution at one loop with the insertion of Q itself and produces the diagrams from (1) to (10).

Diagrams (1) and (2) concern vertex corrections, while diagrams from (3) to (6) correspond to wave function renormalization for every external leg. Because QED is a renormalizable theory, using Ward Identity it is straightforward to check that those diagrams give no contribution to the divergent part at all. Moreover, for that same reason, QCD corrections will not be treated.

Hence, only diagrams from (7) to (10) give a non zero contribution to the one loop amplitude[1].

Being $\mathcal{M}_{(7)} = \mathcal{M}_{(8)}$ and $\mathcal{M}_{(9)} = \mathcal{M}_{(10)}$ the total one loop amplitude reads

$$\mathcal{M}_{\text{loop}} = 2\mathcal{M}_{(7)} + 2\mathcal{M}_{(9)} \,. \tag{2.60}$$

The complete calculations of such amplitudes can be found in Appendix C.

The expression for the $\mathcal{M}_{(7)}$ amplitude, having isolated only the dependence on μ, reads

$$\mathcal{M}^{\mu}_{(7)} = \frac{i}{16\pi^2\Lambda^2}(\pm 4e^2 q_f q_g C_i) \ln \mu^2 M^f_{ij} M^g_{ij} (\bar{v}\gamma_\mu P u)(\bar{u}\gamma^\mu P v) \tag{2.61}$$

Since the only difference in the calculation of $\mathcal{M}_{(9)}$ lies in the Dirac structure of the numerator, it is easy to find its expression and isolate the μ dependence, obtaining

$$\mathcal{M}^{\mu}_{(9)} = \frac{i}{16\pi^2\Lambda^2}(\mp e^2 q_f q_g C_i) \ln \mu^2 M^f_{ij} M^g_{ij} (\bar{v}\gamma_\mu P u)(\bar{u}\gamma^\mu P v) \,. \tag{2.62}$$

Then, inserting 2.61 and 2.62 in 2.60, one obtains the sector of the one loop amplitude with μ dependence

$$\mathcal{M}^{\mu}_{\text{loop}} = \frac{i}{16\pi^2\Lambda^2}(\pm 6e^2 q_f q_g C_i) \ln \mu^2 M^f_{ij} M^g_{ij} (\bar{v}\,\gamma_\mu P u)(\bar{u}\gamma^\mu P v) \,. \tag{2.63}$$

This represents the right part of the pictoric equation 2.55.
The left part takes into account the RGE modifications and must be evaluated in the different energy ranges.
Using 2.49 in the range $m_b < \mu < m_{\text{EW}}$ one gets

$$\mathcal{M}^{\mu}_{(\text{RGE})} = \frac{i}{16\pi^2\Lambda^2}\,\frac{a}{2}\,\ln \mu^2 M^f_{ij} M^g_{ij} (\bar{v}\gamma_\mu P u)(\bar{u}\gamma^\mu P v) \,. \tag{2.64}$$

Equating 2.63 and 2.64, in order to obtain the cancellation of the μ dependence, one gets

$$a = \pm 12 e^2 q_f q_g C_i \,. \tag{2.65}$$

1 Notice again that if one of the external leg is a neutrino, or in presence of a charged current, the discussion above changes. For this reason the special case of the operator $Q^3_{\ell q} = (\bar{v}\gamma_\mu P_L \ell)(\bar{u}\gamma_\mu P_L d)$ will be treated in a different section.

In the other energy ranges 2.63 is not modified, so that $a = b$.
This implies that 2.52 becomes

$$\delta\xi_i = -a = \mp 12 e^2 q_f q_g C_i \,, \tag{2.66}$$

which allows us to compute the coefficients for every Q_{CC} operator.

Scalar vertices

Scalar operators need to be analyzed separately since the different vertex Dirac structure modifies the calculations with respect to the vector operators.
Scalar operators of the form $Q_S = (\bar{f} A^i P_{L/R} f)(\bar{g} A_i P_{R/L} g)$ are modified at one loop by the insertion of Q_S itself, with vertex corrections, where the mediator is the photon. It is not possible to construct Penguin operators since those Q_S involve chiral currents, that don't couple with the photon.
The main difference with respect to the Vector case is that the different Dirac structures of the vertex do not assure the validity of the Ward identity. In this case then, one needs to calculate the contributions from all (1) to (10) diagrams [2]. This calculation can be found in the Appendix C.

Considering a generic process $\bar{f'}_i f_j \to \bar{g'}_k g_l$, that receives contribution only by the insertion of Q_{S_i} itself the involved diagrams are just the same that the one of the vector case.
The sum of the part of all the amplitudes that depend on μ, for the different vertex structures, reads

$$\mathcal{M}_{Q_S} = \left[\frac{q_f^2 + q_{f'}^2 + q_g^2 + q_{g'}^2}{2} \mathrm{I}_1 - 4(q_f q'_f + q_g q'_g) + (q_f q_g - q_f q_{g'} + q_{f'} q_g - q_{f'} q_{g'}) \right] \times$$
$$\times \frac{i C_S}{16\pi\Lambda^2} \ln \mu^2 (\bar{v} P_L u)(\bar{u} P_R v)$$

$$\mathcal{M}_{Q_S^1} = \left[\frac{q_f^2 + q_{f'}^2 + q_g^2 + q_{g'}^2}{2} \mathrm{I}_1 - 4(q_f q'_f + q_g q'_g)) C_S^1 + (q_f q_g + q_{f'} q_{g'}) i (C_S^1 - 12 C_S^3) \right.$$
$$\left. - (q_f q_{g'} + q_{f'} q_g) i (C_S^1 + 12 C_S^3) \right] \frac{1}{16\pi^2\Lambda^2} \ln \mu^2 (\bar{v} P_L u)(\bar{u} P_L v)$$

$$\mathcal{M}_{Q_S^3} = \left[\frac{q_f^2 + q_{f'}^2 + q_g^2 + q_{g'}^2}{2} \mathrm{I}_1 C_S^3 + (q_f q_g + q_{f'} q_{g'}) i (3 C_S^3 - \frac{1}{4} C_S^1) - (q_f q_{g'} + q_{f'} q_g) i (3 C_S^3 + \frac{1}{4} C_S^1) \right] \times$$
$$\times \frac{1}{16\pi^2\Lambda^2} \ln \mu^2 (\bar{v} \sigma^{\mu\nu} P_L u)(\bar{u} \sigma_{\mu\nu} P_L v) \,.$$

2 Once again, the case where one of the legs is a neutrino will be treated with particular carefulness in the following.

Comparing the result with 2.64 in order to obtain the cancellation of the μ dependence, since the result does not change in the different energy ranges, one gets

$$\begin{aligned}\delta\xi(Q_S) = -a(Q_S) = -2\Bigg[&\frac{q_f^2+q_{f'}^2+q_g^2+q_{g'}^2}{2}\,\mathrm{I}_1 - 4(q_f q'_f + q_g q'_g)\\ &+ (q_f q_g - q_f q_{g'} + q_{f'} q_g - q_{f'} q_{g'})\Bigg] C_S\end{aligned}$$

$$\begin{aligned}\delta\xi(Q_S^1) = -a(Q_S^1) = -2\Bigg[&\frac{q_f^2+q_{f'}^2+q_g^2+q_{g'}^2}{2}\,\mathrm{I}_1 - 4(q_f q'_f + q_g q'_g))C_S^1\\ &+ (q_f q_g + q_{f'} q_{g'})i(C_S^1 - 12C_S^3) - (q_f q_{g'} + q_{f'} q_g)i(C_S^1 + 12C_S^3)\Bigg]\end{aligned} \tag{2.67}$$

$$\begin{aligned}\delta\xi(Q_S^3) = -a(Q_S^3) = -2\Bigg[&\frac{q_f^2+q_{f'}^2+q_g^2+q_{g'}^2}{2}\,\mathrm{I}_1 C_S^3 +\\ &(q_f q_g + q_{f'} q_{g'})i(3C_S^3 - \frac{1}{4}C_S^1) - (q_f q_{g'} + q_{f'} q_g)i(3C_S^3 + \frac{1}{4}C_S^1)\Bigg]\end{aligned}$$

thanks to which one can calculate all the modifications to the couplings of scalar operators.

PENGUIN OPERATORS Penguin operators can have both hadrons or leptons running in the loop.

Hadronic penguins Hadronic penguins operators are given by the product of a $(V-A)$ hadronic current and a vector lepton current and have the form $Q_P^H = (\bar{q}\gamma_\mu M^q P q)(\bar{\ell}\gamma^\mu \ell)$ where q are quarks and ℓ are leptons. Notice that they can involve only neutral currents because of the photon coupling.

In that case, let's consider the generic semi-leptonic process $\bar{q}_i q_j \to \bar{\ell}_k \ell_k$. The contributing one loop diagram is

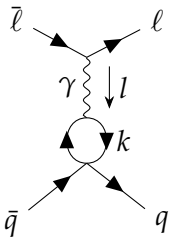

(2.68)

where, given the chosen operators at the Λ scale 2.4 and the necessity of the leptons to couple with the photon, only charged leptons runs in the loop.

The complete calculation of the one loop amplitude can be found in the Appendix C, and the final expression reads

$$\mathcal{M}_P^{\mu,H} = \frac{i}{16\pi^2\Lambda^2}\left(-\frac{2}{3}e^2 q_l q_e C_P\right)\sum_i \lambda_{ii}^e \ln\mu^2 M_{ij}^q (\bar{v}\gamma_\rho P u)(\bar{u}\gamma_\mu v)\,, \tag{2.69}$$

where only the part with a μ dependence was outlined.

This amplitude is not modified in the different energy ranges. In fact, in the ranges $m_b < \mu < m_{\text{EW}}$, and 2 GeV $< \mu < m_b$ all the leptons are dynamical d.o.f and $\sum_i \lambda_{ii}^e = 1$.

Taking that in mind, comparing the result with 2.64 one obtains

$$a = b = -\frac{4}{3}e^2 q_g C_P\,. \tag{2.70}$$

Using 2.70, 2.52 becomes

$$\delta\xi_i = \frac{4}{3}e^2 q_g\,. \tag{2.71}$$

This result allows us to compute the coefficients for every semi leptonic Q_P^H operator.

Leptonic penguins

Leptonic penguins operators are given by the product of a $(V-A)$ leptonic current and a vector current. They have the form $Q_P^L = (\bar{\ell}\gamma_\mu M^\ell P\ell)(\bar{f}\gamma^\mu f)$.
The same considerations made in the hadronic case hold.

In that case, let's consider the generic process $\bar{\ell}_i\ell_j \to \bar{f}_k f_k$.
The contributing one loop diagram is

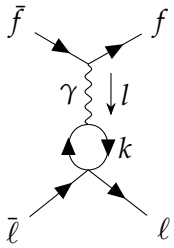

(2.72)

where both quark and charged leptons run in the loop.

Let's consider, for example, the case of charged leptons running in the loop.
While the complete calculation of the one loop amplitude can be found in the Appendix C, the final expression, isolating the μ dependence reads

$$\mathcal{M}_P^L = -\frac{2ie^2}{16\pi^2\Lambda^2}\left[\frac{2}{3}q_e(C_L^e\sum_i\lambda_{ii}^e + C_R^e\sum_i\Gamma_{ii}^e) + q_uC_L^u\sum_j\lambda_{jj}^u + q_dC_L^d\sum_k\lambda_{kk}^d\right]\times$$
$$\times\ln\mu^2 M_{ij}^e(\bar{v}\gamma_\mu Pu)(\bar{u}\gamma^\mu v)\,. \tag{2.73}$$

This amplitude is modified in the different energy ranges.
In the energy range $m_b < \mu < m_{EW}$ in fact, all fermions except the top are dynamical. Hence, summing over $i = 1,2,3$; $j = 1,2$ and $k = 1,2,3$, and equating the result with 2.64 one gets

$$a = -4e^2q_g\left[\frac{2}{3}q_l(C_L^e + C_R^e) + q_uC_L^u(1-\lambda_{33}^u) + q_dC_L^d\right]. \tag{2.74}$$

Analogously, in the energy range 2 GeV $< \mu < m_b$ one has to sum over $i = 1,2,3$; $j = 1,2$ and $k = 1,2$ obtaining

$$b = -4e^2q_g\left[\frac{2}{3}q_l(C_L^e + C_R^e) + q_uC_L^u(1-\lambda_{33}^u) + q_dC_L^d(1-\lambda_{33}^d)\right]. \tag{2.75}$$

Using 2.74 and 2.75, then 2.52 becomes

$$\delta\xi_i = -\frac{4}{3}e^2q_g\left[-2(C_L^e + C_R^e) + 2C_L^u - C_L^d - 2C_L^u(\lambda_{33}^u) + C_L^d\hat{\lambda}_{33}^d\ln\frac{m_b}{\mu}\right], \tag{2.76}$$

which allows to compute the coefficients for every leptonic and semi leptonic Q_P^L operator.

Thanks to 2.66, 2.67, 2.71 and 2.76 one can calculate the coefficients for all operators containing neutral currents. The results are listed in the table 2.3.

Table 2.3: Neutral-Current operators in $\mathcal{L}_{\text{eff}}$ and their coefficients $\delta\xi_i$

Leptonic operators in $\mathcal{L}_{\text{eff}}(m_{\text{EW}})$

Q_i	$\delta\xi_i$
$(\bar{\nu}_L^i\gamma^\mu\nu_L^j)(\bar{e}^k\gamma_\mu e^\ell)$	$\lambda_e^{ij}\delta^{k\ell}(\frac{4}{3}e^2q_g)[-2(C_{\ell\ell}+C_e)+C_1+3C_3+2q_\ell(C_e\hat{\Gamma}_{33}^e)\ln\frac{m_c}{\mu}-2(C_1+C_3)(\lambda_{33}^u+\hat{\lambda}_{22}^u\ln\frac{m_c}{\mu})+(C_1-C_3)\lambda_{33}^{\hat{d}}\ln\frac{m_b}{\mu}]$
$(\bar{e}_L^i\gamma^\mu e_L^j)(\bar{e}_R^k\gamma_\mu e_R^\ell)$	$\lambda_e^{ij}\Gamma_e^{\ell k}(-12e^2C_e)+\lambda_e^{ij}\delta^{k\ell}(\frac{4}{3}e^2q_g[-2(C_{\ell\ell}+C_e)+C_1-3C_3+2q_\ell(C_e\hat{\Gamma}_{33}^e)\ln\frac{m_c}{\mu}-2(C_1-C_3)(\lambda_{33}^u+\hat{\lambda}_{22}^u\ln\frac{m_c}{\mu})+(C_1+C_3)\lambda_{33}^{\hat{d}}\ln\frac{m_b}{\mu}])-\delta^{ij}\Gamma^{k\ell}(\frac{4}{3}e^2C_e)$
$(\bar{e}_L^i\gamma^\mu e_L^j)(\bar{e}_L^k\gamma_\mu e_L^\ell)$	$\lambda_e^{ij}\lambda_e^{k\ell}(+12e^2C_e)+\lambda_e^{ij}\delta^{k\ell}(\frac{4}{3}e^2q_g[-2(C_{\ell\ell}+C_e)+C_1-3C_3+2q_\ell(C_e\hat{\Gamma}_{33}^e)\ln\frac{m_c}{\mu}-2(C_1-C_3)(\lambda_{33}^u+\hat{\lambda}_{22}^u\ln\frac{m_c}{\mu})+(C_1+C_3)\lambda_{33}^{\hat{d}}\ln\frac{m_b}{\mu}])$
$(\bar{e}_R^i\gamma^\mu e_R^j)(\bar{e}_R^k\gamma_\mu e_R^\ell)$	$\Gamma^{ij}\delta^{k\ell}(-\frac{4}{3}e^2C_e)$

Semi-leptonic operators in $\mathcal{L}_{\text{eff}}(m_{\text{EW}})$

Q_i	$\delta\xi_i$
$(\bar{\nu}_L^i\gamma^\mu\nu_L^j)(\bar{u}^k\gamma_\mu u^\ell)$	$\lambda_e^{ij}\delta^{k\ell}(-\frac{4}{3}e^2q_g)[-2(C_{\ell\ell}+C_e)+C_1+3C_3+2q_\ell(C_e\hat{\Gamma}_{33}^e)\ln\frac{m_c}{\mu}-2(C_1+C_3)(\lambda_{33}^u+\hat{\lambda}_{22}^u\ln\frac{m_c}{\mu})+(C_1-C_3)\lambda_{33}^{\hat{d}}\ln\frac{m_b}{\mu}]$
$(\bar{\nu}_L^i\gamma^\mu\nu_L^j)(\bar{d}^k\gamma_\mu d^\ell)$	$\lambda_e^{ij}\delta^{k\ell}(\frac{4}{9}e^2q_g)[-2(C_{\ell\ell}+C_e)+C_1+3C_3+2q_\ell(C_e\hat{\Gamma}_{33}^e)\ln\frac{m_c}{\mu}-2(C_1+C_3)(\lambda_{33}^u+\hat{\lambda}_{22}^u\ln\frac{m_c}{\mu})+(C_1-C_3)\lambda_{33}^{\hat{d}}\ln\frac{m_b}{\mu}]$
$(\bar{e}_L^i\gamma^\mu e_L^j)(\bar{u}_L^k\gamma_\mu u_L^\ell)$	$\lambda_e^{ij}\lambda_u^{k\ell}(+8e^2(C_1-C_3))+\delta^{ij}\lambda_u^{k\ell}(-\frac{4}{3}e^2)(C_1-C_3)+\lambda_e^{ij}\delta^{k\ell}(-\frac{4}{3}e^2q_g)[-2(C_{\ell\ell}+C_e)+C_1-3C_3+2q_\ell(C_e\hat{\Gamma}_{33}^e)\ln\frac{m_c}{\mu}-2(C_1-C_3)(\lambda_{33}^u+\hat{\lambda}_{22}^u\ln\frac{m_c}{\mu})+(C_1+C_3)\lambda_{33}^{\hat{d}}\ln\frac{m_b}{\mu}]$
$(\bar{e}_L^i\gamma^\mu e_L^j)(\bar{d}_L^k\gamma_\mu d_L^\ell)$	$\lambda_e^{ij}\lambda_d^{k\ell}(-8e^2(C_1-C_3))+\delta^{ij}\lambda_d^{k\ell}(-\frac{4}{3}e^2(C_1+C_3))+\lambda_e^{ij}\delta^{k\ell}(\frac{4}{9}e^2q_g)[-2(C_{\ell\ell}+C_e)+C_1-3C_3+2q_\ell(C_e\hat{\Gamma}_{33}^e)\ln\frac{m_c}{\mu}-2(C_1-C_3)(\lambda_{33}^u+\hat{\lambda}_{22}^u\ln\frac{m_c}{\mu})+(C_1+C_3)\lambda_{33}^{\hat{d}}\ln\frac{m_b}{\mu}]$
$(\bar{e}_L^i\gamma^\mu e_L^j)(\bar{u}_R^k\gamma_\mu u_R^\ell)$	$\lambda_e^{ij}\delta^{k\ell}(-\frac{4}{3}e^2q_g)[-2(C_{\ell\ell}+C_e)+C_1-3C_3+2q_\ell(C_e\hat{\Gamma}_{33}^e)\ln\frac{m_c}{\mu}-2(C_1-C_3)(\lambda_{33}^u+\hat{\lambda}_{22}^u\ln\frac{m_c}{\mu})+(C_1+C_3)\lambda_{33}^{\hat{d}}\ln\frac{m_b}{\mu}]$
$(\bar{e}_L^i\gamma^\mu e_L^j)(\bar{d}_R^k\gamma_\mu d_R^\ell)$	$\lambda_e^{ij}\delta^{k\ell}(\frac{4}{9}e^2q_g)[-2(C_{\ell\ell}+C_e)+C_1-3C_3+2q_\ell(C_e\hat{\Gamma}_{33}^e)\ln\frac{m_c}{\mu}-2(C_1-C_3)(\lambda_{33}^u+\hat{\lambda}_{22}^u\ln\frac{m_c}{\mu})+(C_1+C_3)\lambda_{33}^{\hat{d}}\ln\frac{m_b}{\mu}]$
$(\bar{e}_R^i\gamma^\mu e_R^j)(\bar{u}_R^k\gamma_\mu u_R^\ell)$	$\Gamma_e^{ij}\delta^{k\ell}(\frac{8}{9}e^2C_e)$
$(\bar{e}_R^i\gamma^\mu e_R^j)(\bar{d}_R^k\gamma_\mu d_R^\ell)$	$\Gamma_e^{ij}\delta^{k\ell}(-\frac{4}{9}e^2C_e)$
$(\bar{e}_R^i\gamma^\mu e_R^j)(\bar{u}_L^k\gamma_\mu u_L^\ell)$	$\Gamma_e^{ij}\delta^{k\ell}(\frac{8}{9}^2C_e)+\delta^{ij}\lambda_u^{k\ell}(\frac{4}{3}e^2(C_1-C_3))(1-\hat{\lambda}_{33}^e\ln\frac{m_c}{\mu})$
$(\bar{e}_R^i\gamma^\mu e_R^j)(\bar{d}_L^k\gamma_\mu d_L^\ell)$	$\Gamma_e^{ij}\delta^{k\ell}(-\frac{4}{9}e^2C_e)+\delta^{ij}\lambda_d^{k\ell}(\frac{4}{3}e^2(C_1+C_3))(1-\hat{\lambda}_{33}^e\ln\frac{m_c}{\mu})$
$(\bar{e}_L^ie_R^j)(\bar{d}_R^kd_L^\ell)$	$-2(V_e^*R_e)^{ij}(R_d^*V_d)[\frac{13}{9}I_1+4\cdot\frac{13}{9}]C_S$
$(\bar{e}_L^ie_R^j)(\bar{u}_L^ku_R^\ell)$	$-2(V_e^*R_e)^{ij}(R_d^*V_d)[(\frac{13}{9}I_1+4\cdot\frac{13}{9})C_S^1+\frac{4}{3}(C_S^1-12C_S^3)]$
$(\bar{e}_L^i\sigma_{\mu\nu}e_R^j)(\bar{u}_L^k\sigma^{\mu\nu}u_R^\ell)$	$-2(V_e^*R_e)^{ij}(R_d^*V_d)[(\frac{13}{9}I_1+4\cdot\frac{13}{9})C_S^3+\frac{4}{3}(3C_S^3-\frac{1}{4}C_S^1)]$

QED AND QCD CORRECTIONS TO PION DECAY The case of charged currents operators differs from the one of neutral currents operators because different diagrams need to be considered. In that section the general calculation will not be performed, but we will specify the treatise by means of one explicative and useful examples: the pion decay. This processes is of main interest in neutrino physics since it represents one of the main channel of production of atmospheric neutrinos.

In the case of the semi-leptonic pion decay the operators, and the related coefficients, that contribute to the process $u\bar{d} \to \mu^- \bar{\nu}$ at the Λ scale are:

$$\begin{aligned}
&\frac{C_3}{\Lambda^2} Q^3_{\ell q} \to -\frac{C_3}{\Lambda^2}(\bar{\mu}\gamma_\mu P_L \nu)(\bar{u}\gamma^\mu P_L d) \\
&\frac{C_s}{\Lambda^2} Q_{\ell e d q} \to \frac{C_s}{\Lambda^2}(\nu P_L \bar{\mu})(d P_R \bar{u}) \\
&\frac{C^1_s}{\Lambda^2} Q^1_{\ell e q u} \to \frac{C^1_s}{\Lambda^2}(\nu P_L \bar{\mu})(d P_L \bar{u}) \\
&\frac{C^3_s}{\Lambda^2} Q^3_{\ell e q u} \to \frac{C^3_s}{\Lambda^2}(\nu \sigma^{\mu\nu} P_L \bar{\mu})(d \sigma_{\mu\nu} P_L \bar{u})
\end{aligned} \tag{2.77}$$

and the sum of QED and QCD correction reads, factorizing the one loop factor $\frac{\alpha}{2\pi}$ out of $Z^{(2)}$, one gets

$$\frac{\mathrm{d}\vec{C}(\mu)}{\mathrm{d}\log\mu} = \left(\frac{\alpha_{\mathrm{em}}(\mu)}{2\pi}\gamma_{\mathrm{em}} + \frac{\alpha_{\mathrm{s}}(\mu)}{2\pi}\gamma_{\mathrm{s}}\right)\vec{C}(\mu)\,, \tag{2.78}$$

where $\vec{C} = \{C_3, C_s, C^1_s, C^3_s\}$.

QED corrections

QED corrections to the semi-leptonic pion decay arise from one loop diagrams having tree level vertices where the loop is generated from wave-function and vertex corrections via the exchange of a virtual photon.

The involved diagram, for every vertex, are listed below:

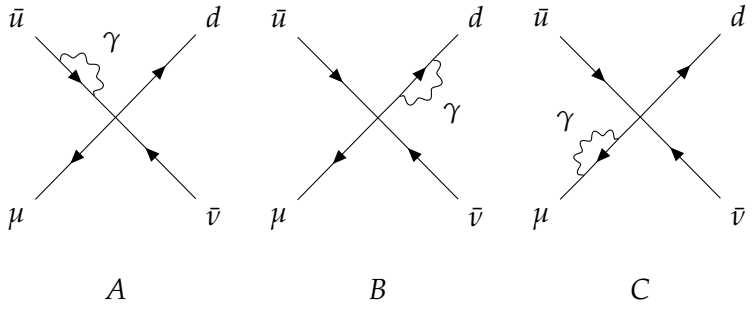

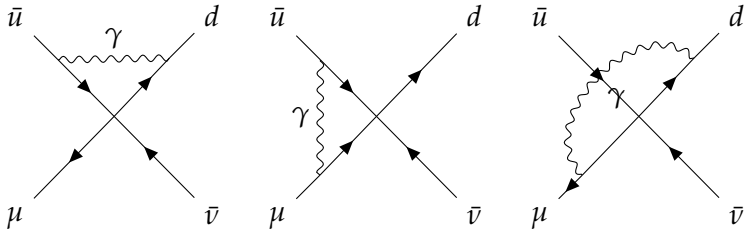

D E F

Diagrams A, B, C

The wave-function corrections, i.e. diagrams with self energy in one of their external legs, give the same contributions no matter what the vertex structure is. Such diagrams are composite and the correction they bring with them is linearly proportional to Z_2 the wave-function counterterm of QED (*31*).

$$\mathcal{M}^{\text{div}}_{A,B,C} = i\frac{q_f^2}{2}\frac{\alpha_{\text{em}}}{2\pi}\frac{C_i Q_i}{\Lambda^2}\frac{1}{\epsilon} \tag{2.79}$$

where an additional $\frac{1}{2}$ term is due as a symmetry factor.

Diagram D

For what concerns diagram D the contributions is modified by the Dirac structure of the different vertexes. The amplitude reads

$$\mathcal{M}_D = e^2 q_u q_d \frac{C_i}{\Lambda^2}(\bar{u}A_i v)\int \frac{\mathrm{d}^D k}{(2\pi)^D}\mu^{4-D}\frac{(\bar{v}\gamma^\rho(-\not{k}-\not{p}+m_u)B^i(\not{p}'+\not{k}+m_d)\gamma_\rho u)}{(k^2-\lambda^2)[(k+p)^2-m_u^2][(k+p')^2-m_d^2]},$$

where k_μ is the loop momentum, λ is the mass regulator of the photon, p_μ and p'_μ are the external momentum and A_i and B_i stands for the different Dirac structure of the vertex, associated to the $C_i = \{C_3, C_s, C_s^1, C_s^3\}$, as follows:

$$(A_i)(B^i) = \{(\gamma_\mu P_L)(\gamma^\mu P_L), (P_L)(P_R), (P_L)(P_L), (\sigma^{\mu\nu}P_L)(\sigma_{\mu\nu}P_L)\}\,. \tag{2.80}$$

Considering only the terms with a squared power of k, since the k^0 are non divergent and the k^1 are zero when the integral is performed, one gets the results listed in table 2.4.

Table 2.4: Matrix element for different vertex structures in diagram D

$(A_i)(B^i)$	$\mathcal{M}_D^{\text{div}}$
$(\gamma_\mu P_L)(\gamma^\mu P_L)$	$-q_u q_d \frac{\alpha_{\text{em}}}{2\pi}\frac{C_3 Q^3_{\ell q}}{\Lambda^2}\frac{1}{\epsilon}$
$(P_L)(P_R)$	$-4q_u q_d \frac{\alpha_{\text{em}}}{2\pi}\frac{C_s Q_{\ell edq}}{\Lambda^2}\frac{1}{\epsilon}$
$(P_L)(P_L)$	$-4q_u q_d \frac{\alpha_{\text{em}}}{2\pi}\frac{C_s^1 Q^3_{\ell equ}}{\Lambda^2}\frac{1}{\epsilon}$
$(\sigma^{\mu\nu}P_L)(\sigma_{\mu\nu}P_L)$	0

Diagram E

For what concerns the diagram E, there is a dependence on the Dirac structure

of the vertex as well.
The amplitude reads

$$\mathcal{M}_E = e^2 q_u q_\mu \frac{C_i}{\Lambda^2} \int \frac{\mathrm{d}^D k}{(2\pi)^D} \mu^{4-D} \frac{(\bar{v}\gamma^\rho(-\not{k}+\not{p}+m_u)A_i u)(\bar{u}\gamma_\rho(\not{k}-\not{p}'+m_\mu)B^i v)}{(k^2-\lambda^2)[(k-p)^2-m_u^2][(k-p')^2-m_d^2]} \,.$$

Considering only the terms with a squared power of k, since the k^0 are not divergent and the k^1 are zero when the integral is performed, one gets the results listed in table 2.5.

Table 2.5: Matrix element for different vertex structures in diagram E.

$(A_i)(B^i)$	$\mathcal{M}_E^{\mathrm{div}}$
$(\gamma_\mu P_L)(\gamma^\mu P_L)$	$-4 q_u q_\mu \frac{\alpha_{\mathrm{em}}}{2\pi} \frac{C_3 Q^3_{\ell q}}{\Lambda^2} \frac{1}{\epsilon}$
$(P_L)(P_R)$	$q_u q_\mu \frac{\alpha_{\mathrm{em}}}{2\pi} \frac{C_s Q_{\ell e d q}}{\Lambda^2} \frac{1}{\epsilon}$
$(P_L)(P_L)$	$q_u q_\mu \frac{\alpha_{\mathrm{em}}}{2\pi} \left(\frac{C_s^1 Q^1_{\ell e q u} - \frac{1}{4} C_s^1 Q^3_{\ell e d q}}{\Lambda^2} \right) \frac{1}{\epsilon}$
$(\sigma^{\mu\nu} P_L)(\sigma_{\mu\nu} P_L)$	$q_u q_\mu \frac{\alpha_{\mathrm{em}}}{2\pi} \left(\frac{3 C_s^3 Q^3_{\ell e q u} - 12 C_s^3 Q^1_{\ell e d q}}{\Lambda^2} \right) \frac{1}{\epsilon}$

Diagram F The structure of diagram F is quite analogous to the one of diagram E, for every vertex.
The amplitude reads

$$\mathcal{M}_F = e^2 q_u q_\mu \frac{C_i}{\Lambda^2} \int \frac{\mathrm{d}^D k}{(2\pi)^D} \mu^{4-D} \frac{(\bar{v}\gamma^\rho(-\not{k}+\not{p}+m_d)A_i u)(\bar{u}B_i(\not{k}-\not{p}'+m_\mu)\gamma_\rho v)}{(k^2-\lambda^2)[(k-p)^2-m_u^2][(k-p')^2-m_d^2]} \,.$$

Again, considering only the terms with a squared power of k, since the k^0 are non divergent and the k^1 are zero when the integral is performed, one gets the results listed in table 2.6.

Table 2.6: Matrix element for different vertex structures in diagram F.

$(A_i)(B^i)$	$\mathcal{M}_F^{\mathrm{div}}$
$(\gamma_\mu P_L)(\gamma^\mu P_L)$	$-q_d q_\mu \frac{\alpha_{\mathrm{em}}}{2\pi} \frac{C_3 Q^3_{\ell q}}{\Lambda^2} \frac{1}{\epsilon}$
$(P_L)(P_R)$	$-q_d q_\mu \frac{\alpha_{\mathrm{em}}}{2\pi} \frac{C_s Q_{\ell e d q}}{\Lambda^2} \frac{1}{\epsilon}$
$(P_L)(P_L)$	$-q_d q_\mu \frac{\alpha_{\mathrm{em}}}{2\pi} \left(\frac{C_s^1 Q^1_{\ell e q u} + \frac{1}{4} C_s^1 Q^3_{\ell e d q}}{\Lambda^2} \right) \frac{1}{\epsilon}$
$(\sigma^{\mu\nu} P_L)(\sigma_{\mu\nu} P_L)$	$-q_d q_\mu \frac{\alpha_{\mathrm{em}}}{2\pi} \left(\frac{3 C_s^3 Q^3_{\ell e q u} + 12 C_s^3 Q^1_{\ell e d q}}{\Lambda^2} \right) \frac{1}{\epsilon}$

Then, from 2.59 one gets for the anomalous dimension matrix γ_{em}

$$\gamma_{\text{em}} = \begin{pmatrix} Q - q_{ud} - 4q_{u\mu} - q_{\mu d} & 0 & 0 & 0 \\ 0 & Q - 4q_{ud} + q_{u\mu} - q_{\mu d} & 0 & 0 \\ 0 & 0 & Q - 4q_{ud} + q_{u\mu} - q_{\mu d} & -12q_{\mu d} - 12q_{\mu u} \\ 0 & 0 & -\frac{1}{4}q_{\mu d} - \frac{1}{4}q_{\mu u} & Q + 3q_{u\mu} - 3q_{\mu d} \end{pmatrix}$$

with $Q = \sum_{i=\mu,u,d} \frac{q_i^2}{2}$ and $q_{ij} = q_i q_j$.

Notice that such matrix is not diagonal, producing a mixing between the scalar and tensor operators $Q^1_{\ell edq}$ and $Q^3_{\ell edq}$.

QCD Corrections

QCD corrections to the semi-leptonic pion decay arise from one loop diagrams built via the exchange of virtual gluons coupled with the quark legs. Since the structure of the gluon vertex is completely analogous to the one of the photon, since both of them are neutral vector bosons, there will be only minor modification with respect to the result found in the QED case.
In particular, the structure will be the same, and the only modification would refer to charge coefficients, namely

$$e^2 q_i q_j \to g_S^2 C_F \,, \tag{2.81}$$

where C_F is the Casimir in the fundamental representation, which reads

$$C_F = (t^a)^i_j (t^b)^\ell_m \delta^j_\ell \delta^{ab} = T_F \left(N_C - \frac{1}{N_C} \right) , \tag{2.82}$$

where $T_F = \frac{1}{2}$ is the Dynkin in the fundamental representation and $N_C = 3$ the number of colors so that $C_F = \frac{4}{3}$.

The involved diagram, for every vertex, are listed below:

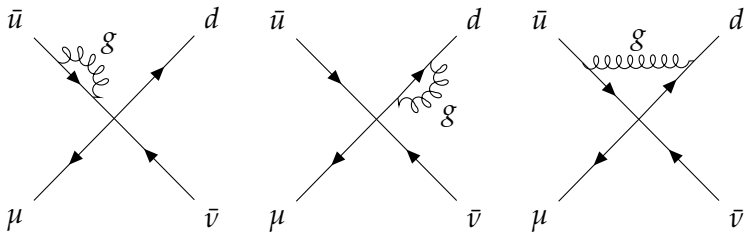

G *H* *I*

Diagrams G and H

Analogously to the case of A, B and C diagrams, the contribution will be independent on the vertex structure. But, differently from the case of QED, as we will see, in this case the sum of the contribution from A, B and C will be zero when the vertex has a vertex structure.

Let's see it explicitly by calculating the contribution for the different diagrams for the different vertex structures.

Using 2.81 in 2.79 the divergent amplitude, for every vertex reads

$$\mathcal{M}^{\text{div}}_{G,H} = i\frac{C_F}{2}\frac{C_i Q_i}{\Lambda^2}\frac{\alpha_S}{2\pi}\frac{1}{\epsilon}\,. \tag{2.83}$$

Diagram I Applying the same reasoning to diagram I, using 2.81 in $\mathcal{M}_D$ the divergent amplitude, modified by the different Dirac structure, reads

$$\mathcal{M}_I = g_S^2 C_F \frac{C_i}{\Lambda^2}(\bar{u}A_i v)\int \frac{\mathrm{d}^D k}{(2\pi)^D}\mu^{4-D}\frac{(\bar{v}\gamma^\rho(-\not{k}-\not{p}+m_u)B^i(\not{p}'+\not{k}+m_d)\gamma_\rho u}{(k^2-\lambda^2)[(k+p)^2-m_u^2][(k+p')^2-m_d^2]} \tag{2.84}$$

and the results for the different vertex structures are listed in table 2.7.

Table 2.7: Matrix element for different vertex structures in diagram I.

$(A_i)(B^i)$	$\mathcal{M}_I^{\text{div}}$
$(\gamma_\mu P_L)(\gamma^\mu P_L)$	$-C_F\frac{\alpha_S}{2\pi}\frac{C_3 Q^3_{\ell q}}{\Lambda^2}\frac{1}{\epsilon}$
$(P_L)(P_R)$	$-4C_F\frac{\alpha_S}{2\pi}\frac{C_s Q_{\ell edq}}{\Lambda^2}\frac{1}{\epsilon}$
$(P_L)(P_L)$	$-4C_F\frac{\alpha_S}{2\pi}\frac{C^1_s Q^3_{\ell equ}}{\Lambda^2}\frac{1}{\epsilon}$
$(\sigma^{\mu\nu}P_L)(\sigma_{\mu\nu}P_L)$	0

Then, from 2.59 one gets the anomalous dimension matrix γ_S, which reads

$$\gamma_S = \begin{pmatrix} 0 & 0 & 0 & 0 \\ 0 & -3C_F & 0 & 0 \\ 0 & 0 & -3C_F & 0 \\ 0 & 0 & 0 & C_F \end{pmatrix}$$

where, as anticipated, the contribution to the vector vertex is zero. Moreover, differently to γ_{em}, this anomalous dimension matrix is diagonal, so there is no mixing between the different operators.

3

NON STANDARD NEUTRINO INTERACTIONS

As outlined in the previous sections, various experimental results confirmed that neutrino have masses and oscillate between different flavors.
In the beginning, such peculiar properties were identified as the only source of lepton flavor violation (LFV) in the SM. It became clear, however, that it is possible to introduce extra LFV sources when introducing new and dimension six operators in the EW Lagrangian. Such interactions, called Non-Standard Neutrino Interactions (NSIs) can affect neutrino oscillation experiments, modifying the propagation of neutrinos in matter.
Moreover, NSIs can also affect the production and the detection processes, directly at the source and at the detector, producing *wrong flavor* neutrinos, without oscillation. Those peculiar properties will be treated in 3.1 where an instructive example of a modification provided by NSIs is explicitly calculated.

On the experimental side, current oscillation data from solar and atmospheric neutrino experiments leave room for the existence of sub-leading effects, induced by NSIs. Future, high precision, experiments may shed further light on the strength of such interactions.
For these reasons, we treat in 3.2 one of the most important neutrino observatory at work nowadays, IceCube, in order to understand how the experimental data are gathered and what are the challenges in getting the best out of the existing data in order to parametrize NSIs.
However, it is also important to discuss what progress can be achieved in the future, since that kind of studies helps planning new experiments and analyses. For this reason, in 3.4 a clear overview of one of the most promising future experiment, DUNE, will be held, in order to understand whether and when it would be possible to detect NSIs.

Subsequently, the most important observables at stake in the named experiments will be analyzed, first in the general parametrization found in literature, involving ϵ_i parameters, then specifying the parameters with C_i, thanks to the low energy Lagrangian obtained in Chapter 2.

3.1 MODIFIED PION AND MUON DECAY

In order to give an example of how one can obtain an observable from which important hints on the coefficients of the various operators emerging at the Λ

scale may be deduced, we calculate the decay rate of the $\pi^- \to \mu^- \bar{\nu}_\mu$ and $\mu \to e\bar{\nu}_e\nu_\mu$, which represent two of the main channels of production of neutrinos in the atmosphere.
By the comparison between the modified and SM decay width, as long as with the experimental results, one can put boundaries on the allowed values of the ϵ_i and consequently of the C_i.

SEMI LEPTONIC PION DECAY One of the main channel of production of atmospheric neutrinos is the pion decay: $\bar{u}d \to \mu^- \bar{\nu}$. The energies involved are of the order of $m_\pi \sim 0.1$ GeV.
At those energies g_S has grown so big that a perturbative approach is no longer possible. For this reason, in order to calculate the decay width, it is no longer possible to draw Feynman diagrams and writing down a Feynman amplitude.
One needs to follow an approach based on symmetries and Quantum Mechanical tools.
First of all, in order to calculate the amplitude, one needs to specify the interaction Lagrangian, and how the elements of the Hilbert space have been built up. In fact, in general the amplitude reads

$$\mathcal{M} = \langle \mu\nu_\mu | \, \mathcal{L}_{\text{int}} \, | \pi^- \rangle \ , \tag{3.1}$$

where $\mathcal{L}_{\text{int}}$ is the interaction Lagrangian and $|\pi^-\rangle$, $|\mu\nu_\mu\rangle$ are respectively the initial and the final state.

The interaction Lagrangian must contain the low energy dimension six operators contributing to the process, whose coefficients have been extracted in 2.4. Here, we will make use of another parametrization for those coefficients, but the relation among the two will be given subsequently. The interaction Lagrangian reads

$$\begin{aligned} \mathcal{L}_{\text{int}} = \frac{G_F}{\sqrt{2}} V_{ud} \Big[&(1+\epsilon_L)(\nu\gamma^\mu P_L \bar{\mu})(\bar{u}\gamma_\mu P_L d) + \epsilon_S^R (\nu P_L \bar{\mu})(\bar{u} P_R d) \\ &+ \epsilon_S^L (\nu P_L \bar{\mu})(\bar{u} P_L d) + \epsilon_T (\nu \sigma^{\mu\nu} P_L \bar{\mu})(\bar{u}\sigma_{\mu\nu} P_L d) \Big] \ , \end{aligned} \tag{3.2}$$

where the ϵ_i coefficients are related to the C_i, conveniently rescaling the G_F dependence, once one specifies the Λ scale Lagrangian.

The complete Lagrangian, a priori, should contain also a $(\nu\gamma^\mu P_L \bar{\mu})(\bar{u}\gamma_\mu P_R d)$ term (32). This operator originates from the operator $Q_{\phi ud}$ at the Λ scale, after the running under the EW scale and the integration of the heavy degrees of freedom.
In the present work we chose to select only four fermion operators containing $(V-A)$ lepton currents: for this reason $Q_{\phi ud}$ was not included in the Λ scale. The choice of the operator basis at the Λ scale is arbitrary but well motivated. In fact, the insertion of $Q_{\phi ud}$ would have implied that all the $\psi^2\phi^2 D$ operators should have been included, producing a large basis to work with. Such a large basis was far beyond the scope of the present work, but could be definitely considered in the future. Moreover, since the renormalization of those kind of

operators is moltiplicative and does not involve mixing, its exclusion does not affect too much the final result and can be easily added, if necessary.
In addition, such contribution does not represent a new source of LFV, being Lepton Flavor Universal. Then, it clearly represents quite a less interesting scenario, with respect to the aim of the present work.

The complete calculation is performed in C, where we made use of PCAC relations. In the end, the total decay width, integrated over the solid angle, reads

$$\Gamma = \Gamma_{\text{SM}} \left| 1 + \epsilon_L - (\epsilon_S^L - \epsilon_S^R) \frac{m_\pi^2}{m_\mu (m_d + m_u)} \right|^2 , \tag{3.3}$$

where Γ_{SM} has been factorized in order to compare the result to the one without effective interactions and reads

$$\Gamma_{\text{SM}} = \frac{1}{8\pi} (G_F^2 f_\pi^2 V_{ud}^2 m_\mu^2) \left(1 - \frac{m_\mu^2}{m_\pi^2} \right) m_\pi \, . \tag{3.4}$$

MUON DECAY Another important channel of production of neutrinos in the atmosphere is the muon decay $\mu^- \to e^- \bar{\nu}_e \nu_\mu$ which occurs at energies of the order of $m_\mu \sim 0.1$ GeV.

Since only leptons are involved, the calculation of that amplitude can proceed without the carefulness of the previous case. The perturbative approach is allowed and one can follow the standard procedure, quoted in appendix C.

The interaction Lagrangian contains all the low energy dimension six operators contributing to the process, whose coefficients have been extracted in 2.4. The interaction Lagrangian reads

$$\mathcal{L}_{\text{int}} = \frac{G_F}{\sqrt{2}} \left[(1 + \epsilon_{\ell\ell}) (\nu_\mu \gamma^\mu P_L \bar{\mu}) (\bar{\nu}_e \gamma_\mu P_L e) + \epsilon_{\ell e} (\bar{\nu}_e \gamma^\mu P_L \nu_\mu) (\bar{\mu} \gamma_\mu P_R e) \right] , \tag{3.5}$$

where the ϵ_i can be related to the C_i once the Λ scale Lagrangian is provided.

Using Feynman rules one obtains a Feynman amplitude that reads

$$\begin{aligned} \mathcal{M} = -i \frac{G_F}{\sqrt{2}} [& (1 + \epsilon_{\ell\ell}) (\bar{u}(p_e) \gamma^\mu (1 - \gamma_5) u(p_\mu)) (\bar{u}(p_{\nu_\mu}) \gamma_\mu (1 - \gamma_5) v(p_{\nu_e})) \\ & + \epsilon_{\ell e} (\bar{u}(p_e) \gamma^\mu (1 + \gamma_5) u(p_\mu)) (\bar{u}(p_{\nu_\mu}) \gamma_\mu (1 - \gamma_5) v(p_{\nu_e}))] \, . \end{aligned} \tag{3.6}$$

By using Gammology relations, one gets the modulo-squared amplitude, averaged over the spins of the initial state, which reads

$$\frac{1}{4} |\mathcal{M}|^2 = 4 G_F^2 (p_\mu \cdot p_{\nu_\mu}) (p_e \cdot p_{\nu_\mu}) \left[|1 + \epsilon_{\ell\ell}|^2 + 4 |\epsilon_{\ell e}|^2 \right] . \tag{3.7}$$

The total decay width reads

$$\Gamma = \Gamma_{\text{SM}} \left[|1 + \epsilon_{ll}|^2 + 4 |\epsilon_{le}|^2 \right] \tag{3.8}$$

where Γ_{SM} has been factorized in order to compare the standard expression with the modified one and reads

$$\Gamma_{SM} = \frac{G_F^2}{192\pi^3} m_\mu^5 \,. \tag{3.9}$$

We can see that the term ϵ_{le} does not sum coherently with the SM, for this reason we can neglect it.

The Fermi constant

Before directly analyzing the different observables of interest, it is instructive to make a brief comment on the modification of the Fermi constant, in order to have a more complete overview on the case in exam.
It is clear that all the observable processes in neutrino experiments,, are mediated by weak interactions. For this reason, when modifying the cross sections in order to introduce NSI effects, one should be aware that also the Fermi constant G_F itself receives a modification. This modification is directly related with the modification to the muon decay amplitude and must be absorbed in the redefinition of G_F^0, the value of the SM, for this reason, given the Λ scale basis we chose, it reads

$$G_F^0 = G_F - \delta G_F = G_F \left(1 - \frac{v^2}{16\pi^2\Lambda^2}\left(3C_3 y_t^2 \lambda_e^{22} \lambda_{33}^u \log\left(\frac{\Lambda}{m_{EW}}\right)^2\right)\right) , \tag{3.10}$$

where G_F is the experimental value extracted from muon decay rate measurements.
Numerically, this correction is below the 0.1% level and it is usually negligible. Given the sensitivity that will be reached at DUNE though, a priori one should include these modifications. In order to do so, a simple redefinition of G_F^0 should be performed.
Actually, as we will see in the following, this modification gives no effect on the observable R_N at stake at DUNE. This, in fact, is usually defined through ratios of NSI cross sections of weak processes so, since the numerator and the denominator undergo the same redefinition, in the end the correction simply cancels.
Only the observable R_t and R_e undergoes a modification, since they involve a ratio between NSI and SM quantities. For this reason, the redefinition of G_F will be implemented only in these quantities.

The CKM matrix

It is also interesting to analyze how other input parameters, such as the entries of the CKM matrix, undergo NSI modifications after the introduction of the Λ scale of dimension-six operators. In particular, we will focus on the quantity V_{ud} which is involved in one of the processes at stake at DUNE, the neutrino scattering off nuclei.
Since V_{ud} is usually extracted from beta-decays rate measurements, one should study the NSI modifications to this amplitude, as already seen in the case of G_F and the modified muon decay rate. Nevertheless, in this case there is a huge difference: in our set up, in fact, Λ scale NP does not couples with first generations, hence the neutron decay rate does not receive a direct modification.

But, since beta-decays are mediated by weak interaction, Γ_β actually receives a modification through the redefinition of the input parameter G_F

$$\begin{aligned}\Gamma^0_\beta &\propto (G^0_F)^2 |V^0_{ud}|^2 \xrightarrow{3.10} (G_F - \delta G_F)^2 |V^0_{ud}|^2 \\ &\propto G_F^2 |V^0_{ud}|^2 \left(1 - 2\frac{\delta G_F}{G_F}\right)\end{aligned} \tag{3.11}$$

then, one can redefine V_{ud} in order to absorb this modification, obtaining

$$\begin{aligned}V^0_{ud} &\simeq V_{ud}\left(1 + \frac{\delta G_F}{G_F}\right) \\ &\simeq V_{ud}\left(1 + \frac{v^2}{16\pi^2\Lambda^2}\left(3C_3 y_t^2 \lambda_e^{22} \lambda^u_{33} \log\left(\frac{\Lambda}{m_{EW}}\right)^2\right)\right).\end{aligned} \tag{3.12}$$

The only DUNE observable that will be affected by this redefinition will be R_N since it involves a ration between neutral and charged semi-leptonic weak currents.

3.2 THE ICECUBE NEUTRINO OBSERVATORY

The IceCube Neutrino Observatory is nowadays the largest neutrino telescope in the world. It is located near the Amundsen-Scott South Pole Station, and consists of a cubic-kilometer detector made of instrumented ice, buried at a depth of 2.5 km.
It contains two sub-detectors: (i) DeepCore, a denser portion in the center of the main detector, which lowers the neutrino energy threshold in order to make possible the study of neutrino oscillations; (ii) IceTop, which is located above IceCube (IC). It is used as a calibration detector and to measure the flux and composition of cosmic rays.

The main fields of interest that are studied at IC are: the measure of Cosmic Rays and in particular of the anisotropy in the arrival directions of muons, using IceTop; the search for sterile neutrinos and the measure of the atmospheric oscillation parameters, using DeepCore; the indirect search for Dark Matter, posing the most stringent upper limits yet for spin-dependent interactions of dark matter particles with ordinary matter.

In addition, many next generation experiments are scheduled to be held in the next years at IC such as PINGU, the Precision IceCube Next Generation Upgrade, which will allow to study neutrino oscillations at an energy threshold of a few GeV, hopefully enabling the determination of many neutrino properties, such as mass hierarchy (20).

THE ICECUBE DETECTOR IC is a Čerenkov detector: neutrinos are not electrically charged but when they interact with the ice in the detector they produce

charged secondary particles that emit Čerenkov light, traveling through the ice[1]. The detector consists of 86 strings containing various photomultiplier tubes, called Digital Optical Modules (DOMs) that can detect the Čerenkov radiation produced by secondary particles. Of those strings, only 8 form DeepCore.

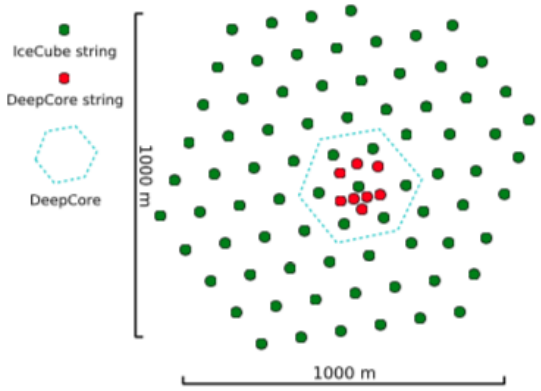

Figure 3.1: Detector geometry: the relative position of the strings is highlighted. From (33).

Thanks to this topology it is possible to reconstruct the direction of the muon with a resolution of 12° at 10 GeV. Moreover, from the the track length of the muon, it is possible to measure its energy allowing to reconstruct the energy of the neutrino. The energetic range DeepCore is allowed to measure spans from 5 GeV to the order of a TeV.

Nevertheless, many systematic uncertainties affect the collected data, among them:

- *Ice column scattering coefficients*: scattering of light in the ice which could spoil the determination of the incoming angle of neutrinos.
- *Overall normalization*: a parameter that scales the event rate expectation freely. This absorbs overall normalization uncertainties due to total cosmic ray flux.
- *Oscillation parameter*: the simultaneous fit for the standard oscillation parameters $\sin^2\theta_{23}$ and Δm_{23}.

NEUTRINO PHYSICS AT ICECUBE One of the main field of research at IC is neutrino physics. In the energy range DeepCore is sensitive, it is possible to observe atmospheric neutrino oscillations and even try to perform searches for sterile neutrinos.
Moreover, since the effect of the NSIs is expected to grow with the distance traveled through matter, the flux of atmospheric neutrinos detected by IC at the

1 The Čerenkov effect takes place when a charged particle travels through a medium with a greater speed than the one of light in that medium. Electromagnetic radiation is emitted at particular angle θ. For this reason this effect is widely exploited to detect high-energy charged particles.

South Pole is ideal for such a study.

The measure of neutrino oscillation parameters at IC is based on the search for a deficit among neutrinos traveling through Earth, thus with a Zenith angle of 90°. In that set up, the disappearence probability for ν_μ peaks at $\sim$ 25 GeV, but the oscillation signal is measurable up to energies of 100 GeV.

Table 3.1: Oscillation parameters measured at IceCube

	Δm^2_{23}	$\sin^2\theta_{23}$
NH	2.310×10^{-3} eV^2	0.514
IH	-2.321×10^{-3} eV^2	0.508

The measures of atmospheric oscillation parameters are comparable with those obtained by MINOS, T2K and Super-Kamiokande.

Having observed in long lasting researches that the survival probability for atmospheric muon neutrinos depends on the energy of the incoming neutrino, one can use the data in Table 3.1 in order to obtain boundaries on the strength of NSIs that might eventually modify this probability, taking into account all the systematic uncertainties and the construction set up that are peculiar of this experiment.
At the energies and oscillation lenghts taken in exam at IC, as will be fully exposed in 3.3, the so called *source and detector NSIs*, are too subdominant so that only *matter NSI* strength was analysed.

Moreover, in the case of atmospheric neutrinos, the presence of large NSI couplings could spoil the excellent description given by classic neutrino oscillation. For this reason there exist quite strong bounds on the magnitude of matter NSI, from atmospheric neutrino data. The results obtained from IC data are depicted in Figure 3.2.

IC data produce some of the most stringent bounds ever obtained for flavor-changing matter NSIs, in full agreement with longer lasting experiment like Super Kamiokande, such as

$$-0.0067 < \epsilon^m_{\mu\tau} < 0.0081 \qquad (90\%\text{C.L.})\,, \tag{3.13}$$

which shall probably be improved by one order of magnitude by PINGU.

Having said so, it is important to review how NSIs are parametrized in an EFT approach. Then, it would be possible to calculate the modified survival and oscillation probabilities and compare the result with the standard predictions.
A number of remarks on the detection prospects at Čerenkov detectors like IceCube will also be provided, specifying the overview with the experimental characteristics of the DeepCore detector.

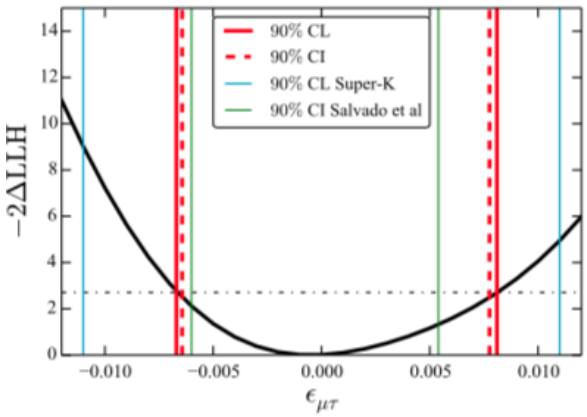

Figure 3.2: Confidence limits from the analysis performed in (33), on the NSI parameter $\epsilon^m_{\mu\tau}$. Dashed vertical red lines show the 90% credibility interval using a flat prior on $\epsilon_{\mu\tau}$. The light blue vertical lines show the Super-Kamiokande 90% confidence limit. The light green lines show the 90% credibility region from (34).

3.3 NSIS AT ICECUBE

Let us consider neutrino NSIs as generated by NP at a Λ scale and described in a model independent way by an EFT approach. In the case in exam, we will take into account only dimension-six four-fermion operators, both purely leptonic and semileptonic.
These can be neutral current (NC) operators, which are usually called *matter NSIs* since they modify neutrino propagation in matter, or charged current (CC) operators which are referred to as *production and detection NSIs* since they modify the flavor eigenstate at the source and at the detector, adding coherently to the SM term.

MODIFIED OSCILLATION PROBABILITY In order to understand the mechanism behind the production of *wrong flavor* neutrinos at the source and the detector, and to parametrize the extent of matter NSI corrections, let us consider the following example of an experiment, where a neutrino is produced in association with a lepton ℓ and another lepton ℓ' is detected.

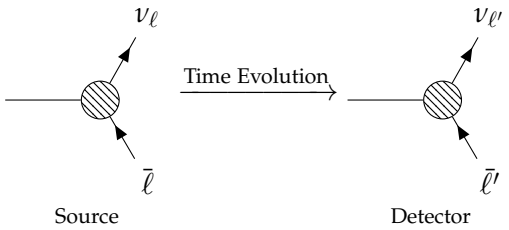

(3.14)

The generally accepted interpretation was to assume $\nu_\ell \to \nu_{\ell'}$ oscillation. However, when introducing NSIs, which violate flavor symmetry directly at the source and detector, there could be sources of flavor violation different from

the oscillation.
For the sake of simplicity, let us consider the effective Lagrangian encoding all NSIs, containing both CC and NC operators

$$\begin{aligned}\mathcal{L}_{\text{NSI}} = &-2\sqrt{2}G_F[(\delta_{\alpha\beta}+\epsilon_{\alpha\beta})(\bar{\ell}\gamma^\mu P_L\nu)(J^+_\mu) + \epsilon^{fL}_{\alpha\beta}(\bar{\nu}_\alpha\gamma_\mu P_L\nu_\beta)(\bar{f}\gamma^\mu P_L f)\\ &+\epsilon^{fR}_{\alpha\beta}(\bar{\nu}_\alpha\gamma_\mu P_L\nu_\beta)(\bar{f}\gamma^\mu P_R f) + \text{h.c.}\,,\end{aligned} \tag{3.15}$$

where J^+_μ denotes the SM charged current, both leptonic and quarkonic, and the sum over f runs over $f = u, d, \ell$.
The parameters $\epsilon^f_{\alpha\beta}$, $\epsilon^{fL}_{\alpha\beta}$ and $\epsilon^{fR}_{\alpha\beta}$ parametrize the strength of NSIs. We will relate them to Wilson coefficients, since we specified the operators that are present in the low-energy effective Lagrangian.

In order to understand the effect of production and detection NSIs, let us consider a Quantum Mechanic approach, denoting by $|\nu^s_\alpha\rangle$ the state of the neutrino produced at the source and by $|\nu^d_\alpha\rangle$ the neutrino detected. One can parametrize these states, with respect to the flavor eigenstate, as

$$\left|\nu^{p=s,d}_\alpha\right\rangle = \frac{\sum_\beta(\delta_{\alpha\beta}+\epsilon^p_{\alpha\beta})\left|\nu_\beta\right\rangle}{\sqrt{\sum_\beta|\delta_{\alpha\beta}+\epsilon^p_{\alpha\beta}|^2}}\,, \tag{3.16}$$

where $\epsilon^s_{\alpha\beta} = \epsilon_{\alpha\beta}$ and $\epsilon^d_{\alpha\beta} = \epsilon^*_{\alpha\beta}$ are the strength of the CC term.

In order to further simplify the discussion, it is requested to make some assumption.

- NSIs affect only generations $2 \leftrightarrow 3$, which is clearly a non-restrictive assumption when dealing with atmospheric neutrinos;
- The expansion at first order in $\epsilon^p_{\alpha\beta}$ is a good approximation, since the ϵ's are small quantities, surely less then 1;
- $\epsilon^p_{\alpha\beta}$ is real.

In order to obtain a more manageable expressions, the following relations must be employed

$$\begin{aligned} u_p &= \frac{(1+\epsilon^p_{\mu\mu})}{\sqrt{|1+\epsilon^p_{\mu\mu}|^2+|\epsilon^p_{\mu\tau}|^2}}\,, \qquad t_p = \frac{\epsilon^p_{\tau\mu}}{\sqrt{|1+\epsilon^p_{\mu\mu}|^2+|\epsilon^p_{\mu\tau}|^2}}\,,\\ z_d &= \frac{(1+\epsilon^d_{\tau\tau})}{\sqrt{|1+\epsilon^d_{\tau\tau}|^2+|\epsilon^d_{\mu\tau}|^2}}\,, \qquad w_d = \frac{\epsilon^d_{\tau\mu}}{\sqrt{|1+\epsilon^d_{\tau\tau}|^2+|\epsilon^d_{\mu\tau}|^2}}\,. \end{aligned} \tag{3.17}$$

Following these requirements one gets

$$\begin{aligned} \left|\nu^p_\mu\right\rangle &\equiv u_p\left|\nu^p_\mu\right\rangle + t_p\left|\nu^p_\tau\right\rangle \approx \left|\nu_\mu\right\rangle + \epsilon^p_{\mu\tau}\left|\nu_\tau\right\rangle\,,\\ \left|\nu^p_\tau\right\rangle &\equiv w_p\left|\nu^p_\mu\right\rangle + z_p\left|\nu^p_\tau\right\rangle \approx \epsilon^p_{\mu\tau}\left|\nu_\mu\right\rangle + \left|\nu_\tau\right\rangle\,, \end{aligned} \tag{3.18}$$

which are clearly non orthogonal states.
In fact

$$\left\langle \nu_\alpha^s \middle| \nu_\beta^d \right\rangle = \epsilon_{\alpha\beta} = \begin{cases} 1 + \mathcal{O}(\epsilon^2) & \alpha = \beta \\ \epsilon^s_{\alpha\beta} + \epsilon^d_{\alpha\beta} + \mathcal{O}(\epsilon^2) & \alpha \neq \beta \end{cases} \tag{3.19}$$

where the standard case is recovered imposing $\epsilon \to 0$.

In order to check how NSIs (both CC and NC) affect the oscillation probability, let us follow the procedure outlined in 1.3.

The expression for the modified Hamiltonian in the flavor basis is modified by matter NSIs and is parametrized as follows:

$$H = \frac{1}{2E} U \begin{pmatrix} m_2^2 & 0 \\ 0 & m_3^2 \end{pmatrix} U^\dagger + \begin{pmatrix} V_{\mu\mu} & V_{\mu\tau} \\ V^*_{\mu\tau} & V_{\tau\tau} \end{pmatrix}, \tag{3.20}$$

where U is the well known PMNS matrix, the elements of the matrix that modifies the Hamiltonian are

$$V_{\alpha\beta} = V_d \epsilon^m_{\alpha\beta} \quad \text{where} \quad \begin{cases} V_d \equiv \sqrt{2} G_F n_d(x) \\ \epsilon^m_{\alpha\beta} \equiv \frac{n_(x)}{n_d(x)} (\epsilon^R_{\alpha\beta} + \epsilon^L_{\alpha\beta}) \,, \end{cases} \tag{3.21}$$

$n_d(x)$ is the density at the detector and $n(x)$ the density of the medium, which one can assume to be approximately constant.

Since IceCube is sensible to atmospheric neutrinos only, the NSIs predicted in our framework would affect only the second and the third generation. Moreover, for long baselines as the ones taken into account at IceCube (the Earth diameter), CC NSIs are actually negligible, but we incorporate them anyway in the general expression of the modified probability. Being said so, since the relation between the flavor and the mass eigenstates is the well known 1.16, it is possible to calculate the ν_μ survival probability. $P_{\mu\mu}(L)$ is given by

$$\begin{aligned} P_{\mu\mu}(L) =& |u_s u_d^* + t_s t_d^*|^2 \cos^2\left(\frac{\Delta E L}{2}\right) \\ &+ |(u_s u_d^* - t_s t_d^*)\cos 2\theta - (u_s t_d^* e^{i\phi} + t_s u_d^* e^{-i\phi}) \sin 2\theta|^2 \sin^2\left(\frac{\Delta E L}{2}\right) \\ &- \mathrm{Im}[(u_s u_d^* + t_s t_d^*)((u_s u_d^* - t_s t_d^*)\cos 2\theta - (u_s t_d^* e^{i\phi} + t_s u_d^* e^{-i\phi}) \sin 2\theta)] \sin(\Delta E L) \,. \end{aligned} \tag{3.22}$$

Analogously, the ν_μ transition probability can directly be obtained from $P_{\mu\mu}$ via some simple substitutions. It reads

$$P_{\mu\tau}(L) = P_{\mu\mu}(L)_{u_d \to w_d, t_d \to z_d} \,, \tag{3.23}$$

where

$$\Delta E = \sqrt{\left(\frac{\Delta m^2_{23}}{2E}\cos 2\theta_0 + V_{\mu\mu} - V_{\tau\tau}\right)^2 + 4\left|-\frac{\Delta m^2_{23}}{4E}\sin 2\theta_0 + V_{\mu\tau}\right|^2} \tag{3.24}$$

$$\sin 2\theta = \frac{2\left|-\frac{\Delta m^2_{23}}{4E}\sin 2\theta_0 + V_{\mu\tau}\right|}{\Delta E} \tag{3.25}$$

$$\cos 2\theta = \frac{\frac{\Delta m^2_{23}}{4E}\sin 2\theta_0 + V_{\mu\mu} - V_{\tau\tau}}{\Delta E} \tag{3.26}$$

$$\phi = \arg\left(-\frac{\Delta m^2_{23}}{4E}\sin 2\theta_0 + V^*_{\mu\tau}\right) \tag{3.27}$$

It is instructive to expand those expressions at first order in the ϵ parameter, since it gives a much simpler and immediate expression. Conservation probability reads

$$\begin{aligned} P_{\mu\mu}(L) &= \left|\left\langle \nu^s_\mu(0)\middle|\nu^d_\mu(t)\right\rangle\right|^2 \\ &= 1 - \sin^2(2\theta_0)\sin^2 x \\ &- \frac{1}{2}\sin^2(2\theta_0)\sin(2x)[(\epsilon^m_{\mu\mu} - \epsilon^m_{\tau\tau})\cos(2\theta_0) - 2\,\mathrm{Re}(\epsilon^m_{\mu\tau})\sin(2\theta_0)]V_d L \\ &+ \frac{1}{2}\sin(4\theta_0)\frac{\sin^2 x}{x}[2\,\mathrm{Re}(\epsilon^m_{\mu\tau})\cos(2\theta_0) + (\epsilon^m_{\mu\mu} - \epsilon^m_{\tau\tau})\sin(2\theta_0)]V_d L \\ &- \sin(4\theta_0)\sin^2 x\,\mathrm{Re}(\epsilon^s_{\mu\tau} + \epsilon^d_{\mu\tau}) - \sin(2\theta_0)\sin(2x)\,\mathrm{Im}(\epsilon^s_{\mu\tau} - \epsilon^d_{\mu\tau})\,, \end{aligned} \tag{3.28}$$

while transition probability

$$\begin{aligned} P_{\mu\tau}(L) &= \left|\left\langle \nu^s_\mu(0)\middle|\nu^d_\tau(t)\right\rangle\right|^2 \\ &= \sin^2(2\theta_0)\sin^2 x \\ &+ \frac{1}{2}\sin^2(2\theta_0)\sin(2x)[(\epsilon^m_{\mu\mu} - \epsilon^m_{\tau\tau})\cos(2\theta_0) - 2\,\mathrm{Re}(\epsilon^m_{\mu\tau})\sin(2\theta_0)]V_d L \\ &- \frac{1}{2}\sin(4\theta_0)\frac{\sin^2 x}{x}[2\,\mathrm{Re}(\epsilon^m_{\mu\tau})\cos(2\theta_0) + (\epsilon^m_{\mu\mu} - \epsilon^m_{\tau\tau})\sin(2\theta_0)]V_d L \\ &- \sin(4\theta_0)\sin^2 x\,\mathrm{Re}(\epsilon^s_{\mu\tau} + \epsilon^d_{\mu\tau}) - \sin(2\theta_0)\sin(2x)\,\mathrm{Im}(\epsilon^s_{\mu\tau} - \epsilon^d_{\mu\tau})\,, \end{aligned} \tag{3.29}$$

where

$$x = \frac{\Delta m^2 L}{4E}\,. \tag{3.30}$$

Via simple algebra it is straightforward to see now that, due to the non orthogonality of the source and detector states, the total probability is not unitary. In fact

$$P_{\mu\mu}(L) + P_{\mu\tau}(L) = 1 - \sin(4\theta_0)\sin^2 x\,\mathrm{Re}(\epsilon^d_{\tau\mu} + \epsilon^d_{\mu\tau}) - \sin(2\theta_0)\sin(2x)\,\mathrm{Im}(\epsilon^d_{\tau\mu} - \epsilon^d_{\mu\tau}) \neq 1 \tag{3.31}$$

where

$$x = \frac{\Delta m^2 L}{2E}\,. \tag{3.32}$$

Few more points need to be stressed:

- When neutrino interactions are described only by the SM, $\epsilon_i \to 0$, one recovers the usual expressions of survival and oscillation probability, as well as orthogonality and unitarity of probability:

$$P_{\mu\mu}(L) = 1 - \sin^2(2\theta_0)\sin^2 x\,, \quad P_{\mu\tau}(L) = \sin^2(2\theta_0)\sin^2 x\,.$$

- Model-dependent bounds in several new physics scenarios indicate that constraints on CC NSIs are typically much more stringent.

- In the limits $\Delta m^2 \gg E/L$ and $\Delta m^2 \sim 0$, the oscillation and survival probabilities become x-independent. In the case of NSIs, $P_{\mu\tau}(L) \neq 0$, even for massless neutrinos, but it is constant in distance, hence it does not show an oscillation pattern.

Having made this important premise, in order to produce bounds on the parameters of the Λ scale Lagrangian, we need to specify the expressions of the ϵ_i parameters as they emerge in our setup. They read

- Source/Detector parameters

$$\begin{aligned}\epsilon^{\ell\ell}_{\alpha\beta} &= \frac{v^2}{16\pi^2\Lambda^2}(-12\lambda^e_{\alpha\beta}y_t^2\lambda^u_{33}C_3)\log\frac{\Lambda}{m_{\mathrm{EW}}}\,,\\ \epsilon^{s\ell}_{\alpha\beta} &= \frac{v^2}{16\pi^2\Lambda^2}(-12\lambda^e_{\alpha\beta}y_t^2V_{\mathrm{CKM}}C_3)\log\frac{\Lambda}{m_{\mathrm{EW}}}\,.\end{aligned} \tag{3.33}$$

- Matter parameters

$$\begin{aligned}\epsilon^{m\,u}_{\alpha\beta} &= \frac{v^2}{16\pi^2\Lambda^2}\lambda^e_{\alpha\beta}\log\frac{\Lambda}{m_{\rm EW}}\left[\frac{16}{9}e^2(C_e - 3C_3 + 2C_{\ell\ell} - C_1)\right.\\ &\left.-12\lambda_3 3^u y_t^2\left(\frac{1}{2} - \frac{4}{3}\sin^2\theta_W\right)\right],\\ \epsilon^{m\,d}_{\alpha\beta} &= \frac{v^2}{16\pi^2\Lambda^2}\lambda^e_{\alpha\beta}\log\frac{\Lambda}{m_{\rm EW}}\left[\frac{8}{9}e^2(C_1 - C_e + 3C_3 - 2C_{\ell\ell})\right.\\ &\left.-12\lambda^u_{33}y_t^2(C_1 + C_3)\left(-\frac{1}{2} + \frac{2}{3}\sin^2\theta_W\right)\right],\\ \epsilon^{m\,e}_{\alpha\beta} &= \frac{v^2}{16\pi^2\Lambda^2}\lambda^e_{\alpha\beta}\log\frac{\Lambda}{m_{\rm EW}}\left[\frac{8}{3}e^2(C_1 - C_e + 3C_3 - 2C_{\ell\ell})\right.\\ &\left.-12\lambda^u_{33}y_t^2(C_1 + C_3)\left(-\frac{1}{2} + 2\sin^2\theta_W\right)\right].\end{aligned} \tag{3.34}$$

Then we need to specify the parameters that are present in these expressions, we can safely put that $y_t \simeq \lambda^u_{33} \simeq 1$, $v = 246$ GeV and assume the scale of NP to be $\Lambda \simeq 1$ TeV. As a result, the parameters $\epsilon^m_{\alpha\beta}$, defined in 3.21, and $\epsilon^{s,d}_{\alpha\beta}$ defined by 3.19 become

- Source/Detector parameter

$$\epsilon^s_{\alpha\beta} \simeq 6\times10^{-3}\left(\frac{1\,\text{TeV}}{\Lambda}\right)^2 C_3\lambda^e_{\alpha\beta}\,. \tag{3.35}$$

- Matter parameter

$$\epsilon^m_{\alpha\beta} \simeq 10^{-3}\left(\frac{1\,\text{TeV}}{\Lambda}\right)^2[-(0.01)(C_e + C_{\ell\ell}) + (C_1 + C_3)]\lambda^e_{\alpha\beta}\,, \tag{3.36}$$

where lower order corrections have been neglected.

Some comments are needed:

- the magnitude of the two NSI parameters is comparable, even if, as it will be exposed in the following, their effect in the modified conservation and transition probability is different,
- the Wilson coefficients associated to leptonic operators ($C_{\ell\ell}$ and C_e) are suppressed with respect to $C_{1,3}$ of a factor 10^{-2}. Assuming that all the C_i's are of the same order ($\approx \mathcal{O}(1)$), this means that semi-leptonic interactions give a greater contribution to NSIs.

In any case, this parametrization is in agreement with the current experimental bounds on the NP parameters ϵ_i, whose best fit is nowadays fixed by 3.13.

In order to better understand the extent and the relevance of those parameters in the modification of the observable at stake at IceCube, a specified overview for the case of the IC detector properties is requested.

MODIFIED OSCILLATION PROBABILITY AT ICECUBE Having calculated the general expression for the modified conservation and transition probability (3.28 and 3.29), it is instructive to specify such a general result in the case in exam, i.e. with the energies and the experimental set up of the IceCube Observatory.

The IceCube detector, as already mentioned, investigates a flux of neutrinos and antineutrinos along the Zenith direction, in the energy range $E_\nu = [10, 200]$ GeV. The parameters at stake are then

- the Zenith angle corresponds to $\cos\theta_z = -1$,
- the average potential along the Earth profile can be assumed to be $V_d \simeq 9 \times 10^{-13}$ eV,
- then, $V_d L \simeq 62$ that for $L \simeq d_\oplus = 1.27 \times 10^4$ km.

Having fixed this set of parameters, it is clear that, with reference to 3.29, the NC NSIs are enhanced with respect to CC NSI of a factor $V_d L$. Consequently, even if the magnitude of $\epsilon^{s/d}_{\alpha\beta}$ (3.35) is comparable with $\epsilon^m_{\alpha\beta}$ (3.36), for long baseline experiments, such as IceCube, we can neglect the effect of CC NSIs and focus only on the matter NSI parameters $\epsilon^m_{\mu\mu}$, $\epsilon^m_{\tau\tau}$ and $\epsilon^m_{\mu\tau}$.

Standard matter effects and NSIs can be distinguished using the energy and arrival direction distributions of observed flavor-violating transitions. The neutrino flavor oscillations due to the well-established mass differences have been observed from atmospheric neutrinos predominately at energies initially below 10 GeV and recently up to 56 GeV.
The observation of atmospheric neutrino oscillations at different energy ranges, but at the same baseline-energy ratio (L/E) highlights the complementarity of neutrino experiments at different energy ranges. Moreover, the signal predicted for the dominant $\nu_\mu \to \nu_\tau$ NSIs, parametrized by the coupling $\epsilon^m_{\mu\tau}$, can be seen over a larger range of energies, as shown in fig. 3.3.
The importance of the IceCube experiment in this case is that, its energy range extends to higher energies than that of previous studies, thus giving greater sensitivity. Moreover, with the future IceCube upgrade, PINGU, it will be possible to perform a low energy study, $E_\nu < 5$ GeV, in order to further extend the sensitivity of the experiment.

Another interesting issue is that, in general, Čerenkov detectors cannot distinguish neutrino from antineutrinos. In fact, the standard conservation probability P_0 is the same for both ν_μ and $\bar{\nu}_\mu$. The primary neutrino source for this type of analysis is provided by atmospheric neutrinos and, at the South Pole, the flux ratio $\nu_\mu/\bar{\nu}_\mu \simeq 1$ at 10 GeV but it increases with energy. It also slightly depends on the Zenith angle, with small seasonal variations (35). It is striking to notice, though, that when introducing NSI modifications, the conservation probability is

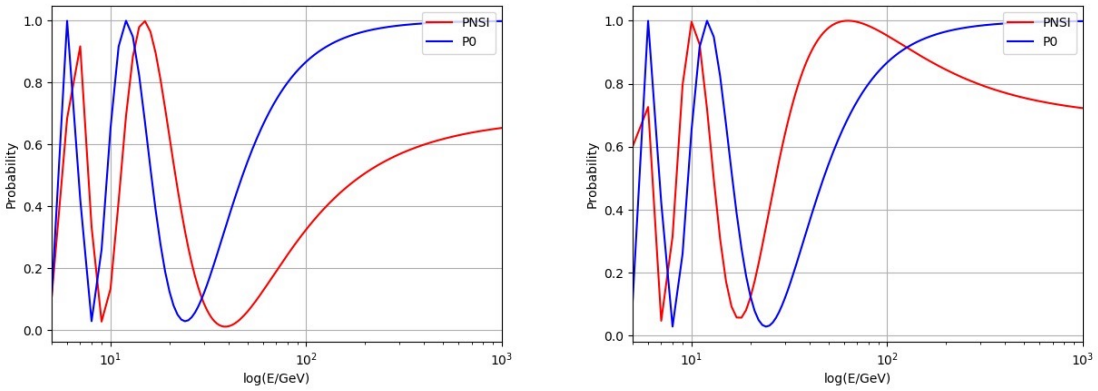

Figure 3.3: ν_μ(left) and $\bar{\nu}_\mu$(right) survival probability at zenith angle $\cos(\theta_z) = -1$, corresponding to vertically up going neutrinos that traverse the entire diameter of the Earth, for standard oscillations (blue) and $\epsilon^m_{\mu\tau} = 10^{-2}$ NSI modification (red).

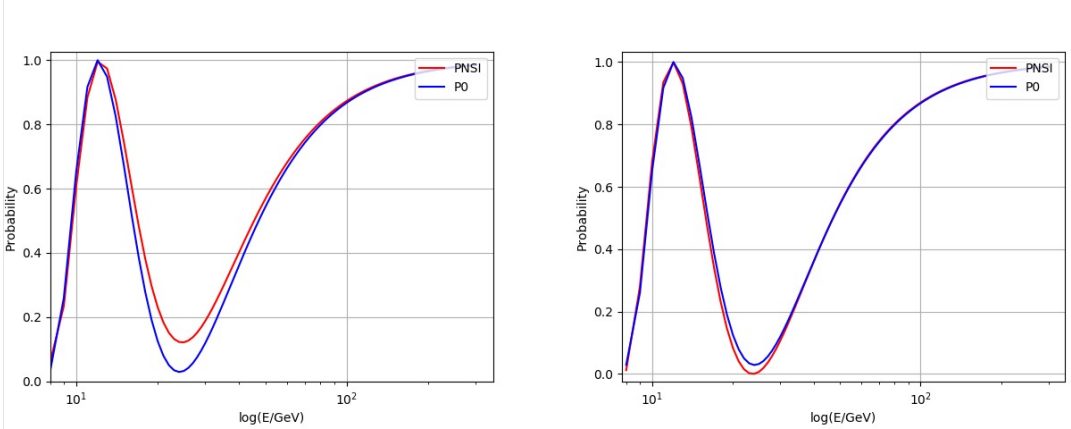

Figure 3.4: ν_μ(left) and $\bar{\nu}_\mu$(right) survival probability at zenith angle $\cos(\theta_z) = -1$, corresponding to vertically up going neutrinos that traverse the entire diameter of the Earth, for standard oscillations (blue) and $\epsilon^m_{\mu\mu} - \epsilon^m_{\tau\tau} = 10^{-2}$ NSI modification (red).

different from particle to antiparticle, in particular in its behavior around 50 GeV.

For completeness, it is interesting to show the modified NSI conservation probability when it is parametrized by the difference $\epsilon^m_{\mu\mu} - \epsilon^m_{\tau\tau}$. The magnitude of NSIs with respect to the standard conservation probability, in the energy range $E_\nu = [5, 300]$ GeV, is shown in fig. 3.4.

It is instructive to make a comparison with the case where $\nu_\mu \to \nu_\tau$ NSIs are parametrized by $\epsilon' = \epsilon^m_{\mu\mu} - \epsilon^m_{\tau\tau}$.

- *Region of interest* - In 3.3 NSI effects are visible in the full neutrino energy range, while in 3.4 NSI effects are visible only in the oscillation minimum around 25 GeV.

- *Magnitude* - The ratio P_{NSI}/P_0 in the energy range of interest for the conservation probability, i.e. $E_\nu \simeq 25$ GeV, is larger when NSIs are parametrized

by $\epsilon^m_{\mu\tau}$ and analogously in the energy range of interest in the oscillation probability, i.e. $E_\nu > 100$ Gev.

- *ν_μ and $\bar{\nu}_\mu$* - While P_{NSI} parametrized by ϵ' shows a little discrepancy between the neutrino and anti-neutrino survival probability, which are actually different only in the $E_\nu \simeq 25$ GeV minimum, the discrepancy becomes quite relevant for NSIs parametrized by $\epsilon^m_{\mu\tau}$.

Therefore, we can conclude that the optimal method for searching for an NSI signal is to use a large range of neutrino energies, where one expects a combined effect of the NSI survival probability in the low-energy region, $E_\nu \simeq 25$ GeV, and an exclusively NSI oscillation signal in the high-energy region. In this context, the scenario of NSI parametrized by $\epsilon^m_{\mu\tau}$ seems more promising.
Moreover, it is an important result that the constraints derived in our setup, in particular 3.36, are compatible with the best fit $-0.0067 < \epsilon^m_{\mu\tau} < 0.0081$ at a 90% C.L., found by (33).

3.4 THE DUNE PROJECT

In order to push even further the sensitivity and precision of neutrino experiments, many next-generation projects have been planned. Among them, one of the most promising is the DUNE project.

The Deep Underground Neutrino Experiment (DUNE) is an international project, whose aim is to study neutrino physics BSM. The main fields of interest span from the innermost of particle physics to the urgent issues of modern cosmology. For these reasons DUNE will focus on the study of neutrino oscillation, the observation of supernova neutrinos originating from black holes and the search for proton decay.

The experiment, that is planned to start operating in 2027, will be made up of two detectors: a *near detector* at the Fermi National Accelerator Laboratory in Illinois and a *far detector* at the Sanford Underground Research Laboratory in South Dakota. They will be placed in the world's most intense neutrino beam. One detector will record particle interactions near the source of the beam, in order to provide constraints on the systematic uncertainties in oscillation studies; the other will be installed more than 1,300 kilometers downstream the source and 1.4 km underground, protected from muons and cosmic rays. These detectors will enable scientists to search for new subatomic phenomena and potentially transform our understanding of neutrinos and their role in the universe.

THE PHYSICS PROGRAM The technologies and the configuration of the planned detectors offer excellent sensitivity to a range of physics processes. Among the other, the most important features are represented by the following items.

- The muon-neutrino beam produced at FermiLab has a peak flux at 2.5 GeV, which, coupled with a baseline of $1,300$ km to the fare detector gives a very good sensitivity to Non Standard neutrino effects.

- The near detector located downstream of the neutrino beam at Fermilab will enable high-precision long-baseline oscillation measurements, which will allow a precise determination of the oscillation parameters still undetermined. Given the configuration, a huge number of events is expected, providing data for a rich program of neutrino interaction physics.
- Liquid argon as a target material provides unique sensitivity to the electron-neutrino (ν_e) component, relevant in many observables at stake.

With the facilities provided by Fermilab and the detectors provided by DUNE, the DUNE Collaboration proposes to mount a focused attack on the puzzle of neutrinos, with particular attention to neutrino oscillation parameters and NSIs. For this reason this program represents one of the most interesting prospect in neutrino physics.

3.5 NSIS AT DUNE

The unprecedented neutrino flux that will be studied at DUNE offers a huge opportunity to greatly improve the current limits on Wilson coefficients. As will be seen, in fact, the constraints that we will be able to produce on the parameters of NP are $1-2$ orders of magnitude more strict then the previous ones.
In the following the possible consequences of the DUNE neutrino experiment on constraining NSI parameters are analyzed. In order to understand the extent of such impact one needs to quantify the DUNE sensitivity to dimension-6 operators in the EFT Lagrangian, by analyzing the expected number of events that affect the observables at stake.

In general, the predicted number of events can be calculated using

$$N = \text{time} \times \#\text{targets} \times \text{efficiency} \times \int_{E_i}^{E_f} \mathrm{d}E_\nu \frac{\mathrm{d}\phi(E_\nu}{\mathrm{d}E_\nu} \sigma(E_\nu)\,, \tag{3.37}$$

where the parameters involved have been chosen as follows

- the span of time considered for the operation is 3 years, which is a period of time perfectly consistent with other long-baseline experimental runs,
- the target is calculated for 1.1×10^{21} proton on target, with a 120 GeV proton beam,
- the neutrino energy is assumed to range from $0.25\ \text{GeV} < E_\nu < 8.25\ \text{GeV}$, since the contribution from higher energies would be negligible,
- the neutrino flux ϕ is simulated following (36),
- the cross section σ is to be calculated depending on the relevant observable at DUNE for the trident production and neutrino scattering off electrons and nuclei.

Since the cross sections could be, in principle, modified by NSI effects, the comparison with the expected number of events could allow us to put constraints

on some of the coefficients. For the following we assumed the number of events predicted by (37).
Let us focus on the different processes separately. In general they would involve leptonic (trident production, neutrino scattering off electrons) and semi-leptonic (neutrino scattering off nuclei) processes. All the cross sections involved have been calculated explicitly in Appendix D.

TRIDENT PRODUCTION Neutrino trident events are processes where a neutrino impacting on a heavy nucleus produces a lepton pair: $\nu_\alpha N \to \nu_\beta e^+ e^- N$. For what concerns the experimental side, the observable process are $\nu_\mu \to \nu_\mu \mu^- \mu^+$ and $\nu_e \to \nu_e \mu^- \mu^+$. The best choice is represented by $\nu_\mu \to \nu_\mu \mu^- \mu^+$, since the total SM cross section is bigger and consequently the number of events would be more notable. The explicit calculation of the cross section is given in Appendix D and the modification due to NSIs can be obtained by expanding the couplings at first order.

The ratio between the SM and NSI-modified cross section reads

$$R_t = \frac{\sigma(\nu_\mu \to \nu_\mu \mu^- \mu^+)}{\sigma_{\rm SM}(\nu_\mu \to \nu_\mu \mu^- \mu^+)} = 1 + \underbrace{2\frac{g_L^{2222}\epsilon_L^{2222} + g_R^{2222}\epsilon_R^{2222}}{(g_L^{2222})^2 + (g_R^{2222})^2}}_{\delta R_t}, \tag{3.38}$$

where g_L^{2222} and g_R^{2222} are the SM couplings to Z defined in 2.27 and $\epsilon_{L,R}^{2222}$ are the NSI couplings to $(\bar{\nu}_\mu \gamma_\mu P_L \nu_\mu)(\bar{\mu}\gamma^\mu P_L \mu)$ and $(\bar{\nu}_\mu \gamma_\mu P_L \nu_\mu)(\bar{\mu}\gamma^\mu P_R \mu)$ respectively.

Those couplings need to be specified in terms of Wilson coefficients after the running of the Λ scale Lagrangian. In our context, having implemented the G_F modifications, they read

$$\begin{aligned}
\epsilon_L^{2222} =& \frac{v^2}{16\pi^2\Lambda^2}\log\frac{\Lambda}{m_{\rm EW}}\lambda_e^{22}\left(\frac{4}{3}e^2(C_1 - C_e + 3C_3 - 2C_{\ell\ell})\right. \\
& \left. -12\lambda_{33}y_t^2(C_1 + C_3)\left(-\frac{1}{2} + s_W^2\right) - 3C_3 y_t^2 \lambda_e^{22}\lambda_{33}^u\right), \\
\epsilon_R^{2222} =& \frac{v^2}{16\pi^2\Lambda^2}\log\frac{\Lambda}{m_{\rm EW}}\lambda_e^{22}\left(\frac{4}{3}e^2(C_1 - C_e + 3C_3 - 2C_{\ell\ell})\right. \\
& \left. -12\lambda_{33}y_t^2(C_1 + C_3)s_W^2 - 3C_3 y_t^2 \lambda_e^{22}\lambda_{33}^u\right),
\end{aligned} \tag{3.39}$$

where sub-leading terms have been neglected.

Then, one can translate the total number of events calculated with 3.37 to forecast the NSI coefficients. Specifying all the parameters at stake, imposing

$y_t^2 = \lambda_{33}^u = 1$, $\lambda_{22}^e \simeq 0.1$ and the scale of NP to be $\Lambda = 1$ TeV, the following constraints were obtained

$$\begin{aligned} -0.039 <& 1.3 \times 10^{-3} \left(\frac{1\text{TeV}}{\Lambda}\right)^2 \times \\ & \times \left(\frac{\lambda_e^{22}}{0.1}\right) [(0.01)(C_e - 2C_{\ell\ell}) + (0.02)C_1 + (0.1)C_3)] < 0.039\,, \end{aligned} \tag{3.40}$$

where higher order corrections have been neglected.
Assuming that all the Wilson coefficients are approximately of the same order, it is straightforward to see that all the different parameters scale approximately with the same power, so there is no enhancement of a particular class of them. Moreover, the δR_t predicted by the model, setting $\Lambda = 1$, $\lambda_{22}^e = 0.1$ and $C_i = \mathcal{O}(1)$ in 3.40, falls within the interval allowed by the forecast constraint, which is in agreement with the bounds previously found in literature. In this case, in fact, the number of events that can be seen at DUNE is not much greater than the previous experiments', producing bounds that are not stricter.

NEUTRINO SCATTERING OFF ELECTRONS Neutrino scattering off electrons can be both a CC or NC process. For what concerns CC processes, like $\nu_\mu e^- \to \nu_e \mu^-$, they can be neglected since their threshold ($E_\nu \simeq 10.9$ GeV) is larger then the neutrino energy in DUNE ($0.25 \div 8.25$ GeV). Only the cross section from NC processes like $\nu_\mu e^- \to \nu_\mu e^-$ and its conjugate, then, would be calculated. The explicit calculation for the cross section of interest can be found in Appendix D. The interesting ratio, this time, differs form neutrino to anti neutrino events and, after having implemented G_F modifications inside ϵ_L^{2211}, reads

$$R_e = 2\frac{x_i\sigma_{\text{NSI}}^{\nu} + \bar{x}_i\sigma_{\text{NSI}}^{\bar{\nu}}}{x_i\sigma_{\text{SM}}^{\nu} + \bar{x}_i\sigma_{\text{SM}}^{\bar{\nu}}} = 1 + \underbrace{2\frac{(1+2x_i)(g_L^{2211}\epsilon_L^{2211}) + (3-2x_i)g_R^{2211}\epsilon_R^{2211}}{(1+2x_i)(g_L^{2211})^2 + (3-2x_i)(g_R^{2211})^2}}_{\delta R_e}\,, \tag{3.41}$$

where x_i stands for the abundance of neutrinos and antineutrinos in the beam, which can be approximately taken to be $x_\nu = 0.9$, $\bar{x}_\nu = 0.1$, since the neutrino beam consists of approximately 90% neutrinos and 10% antineutrinos. The NSI coefficients $\epsilon_{L,R}^{2211}$ need to be specified in terms of Wilson coefficients after the running of the Λ scale Lagrangian. In our context, having added the contribution from the G_F modification, they read

$$\begin{aligned} \epsilon_L^{2211} =& \frac{v^2}{16\pi^2\Lambda^2}\frac{1}{2}\Bigg[\lambda_e^{22}\left(\frac{4}{3}e^2(C_1 - C_e + 3C_3 - 2C_{\ell\ell})\right. \\ & \left. -12\lambda_{33}y_t^2(C_1 + C_3)\left(-\frac{1}{2} + s_W^2\right)\right) - \frac{9}{0.87}C_3 y_t^2 \lambda_e^{22}\lambda_{33}^u\Bigg] \log\frac{\Lambda}{m_{\text{EW}}}\,, \end{aligned} \tag{3.42}$$

$$\epsilon_R^{2211} = \frac{v^2}{16\pi^2\Lambda^2}\frac{1}{2}\left[\lambda_e^{22}\left(\frac{4}{3}e^2(C_1 - C_e + 3C_3 - 2C_{\ell\ell}) - 12\lambda_{33}y_t^2(C_1 + C_3)s_W^2\right)\right] \log\frac{\Lambda}{m_{\text{EW}}}\,, \tag{3.43}$$

where sub-leading terms have been neglected.

Then, specifying all the parameters at stake, imposing $y_t^2 = \lambda_{33}^u = 1$, $\lambda_{22}^e \simeq 0.1$ and the scale of NP to be $\Lambda = 1$ TeV, and comparing the result with the total number of events calculated with 3.37, one obtains the following forecast on the NSI coefficients:

$$-8.0 \times 10^{-4} < 2.6 \times 10^{-3} \left(\frac{1\,\text{TeV}}{\Lambda}\right)^2 \left(\frac{\lambda_e^{22}}{0.1}\right) \times \\ \times [(-0.4)(C_1 + 3C_3) + (0.05)(C_e - C_{\ell\ell})] < 8.0 \times 10^{-4}, \tag{3.44}$$

where higher order corrections have been neglected.
Given those stringent constraints, we can safely assume that DUNE is expected to dramatically improve the existing constraints, which are listed by (1). This is due the great number of events that DUNE will be able to observe, according to (37), thanks to its improved sensibility.
Moreover, it is straightforward to see, assuming that all the Wilson coefficients are approximately of the same order, that the semi-leptonic parameters C_1 and C_3 are enhanced with respect to the leptonic coefficients $C_{\ell\ell}$ and C_e of a factor 10. Semi-leptonic processes will then seem to give a stronger contribution to NP.
What it is interesting to notice is that, the dependence of the predicted δR_e with respect to the Λ scale of NP, highlights an important feature. In fact, as can be seem in fig. 3.5, the prediction of our model is in agreement with the experimental forecast only for $\Lambda \geq 4$ TeV. For smaller energy, it falls outside the allowed interval, even if abundantly inside the more loose bounds found in literature until now.
This further confirms the strictness of DUNE bounds, which allow to put more stringent bounds on the Λ scale of NP.

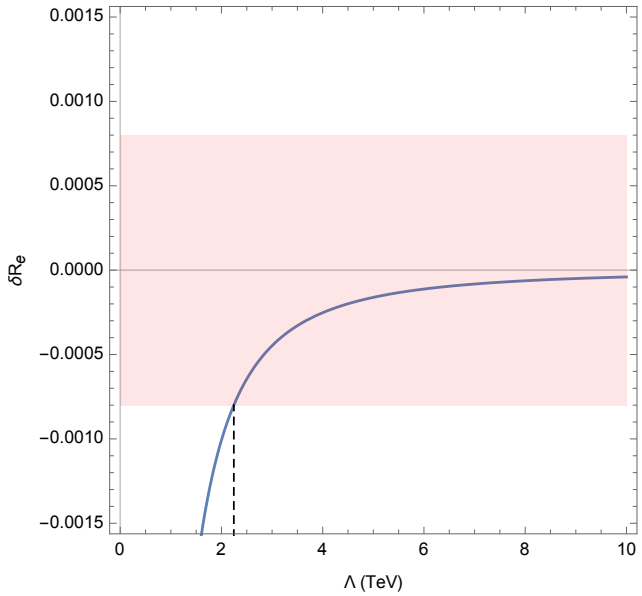

Figure 3.5: Dependance of δR_e with respect to the Λ scale of NP, following 3.44 where we set $\lambda_{22}^e = 0.1$ and $C_i = \mathcal{O}(1)$. The red region corresponds to the forecast bounds that are expected from the DUNE experiment. It can be seen that the predicted value of δR_e in our setup falls inside the allowed region for $\Lambda \geq 4$ TeV.

NEUTRINO SCATTERING OFF NUCLEI Neutrino scattering off nuclei are typically CC processes like $\nu_\alpha N \to e_\alpha^- N^+$ and NC processes like $\nu_\alpha N \to \nu_\alpha N$.
The observable that is usually considered in those cases is the ratio among CC and NC quantities, which, in the SM framework can in turn be expressed in term of only the CC cross section as showed in (38). It reads

$$R_N^{SM} = \frac{x\sigma^{NC} + \bar{x}\bar{\sigma}^{NC}}{x\sigma^{CC} + \bar{x}\bar{\sigma}^{CC}} = (g_L^\nu)^2 + \underbrace{\frac{\bar{x}\sigma_{CC} + x\bar{\sigma}_{CC}}{x\sigma_{CC} + \bar{x}\bar{\sigma}_{CC}}}_{r_\nu^{-1}} (g_R^\nu)^2 \,, \tag{3.45}$$

then, the observable of interest at DUNE reads

$$R_N = R_N^{\rm SM}(1 + \delta R_N) \tag{3.46}$$

where

$$\delta R_N = -\delta V_{ud} - \epsilon_{CC} + 2\frac{g_L^\nu \epsilon_L^\nu + r_\nu^{-1} g_R^\nu \epsilon_R^\nu}{(g_L^\nu)^2 + r_\nu^{-1}(g_R^\nu)^2} \,, \tag{3.47}$$

where, in the case of a beam of neutrinos, r_ν has been estimated to be $\simeq 2.5$ and $x = 0.9$.
In order to take into account δV_{ud} and ϵ_{CC} the coefficients can be re-expressed in the relation

$$\begin{aligned} g_L^\nu \epsilon_L^\nu &= (g_{LL}^{\nu u}\epsilon_{LL}^{\nu u} + g_{LL}^{\nu d}\epsilon_{LL}^{\nu d}) - (g_{LL}^{\nu u} + g_{LL}^{\nu d})^2(\epsilon_L^{CC} + \delta V_{ud}) \,, \\ g_R^\nu \epsilon_R^\nu &= (g_{LR}^{\nu u}\epsilon_{LR}^{\nu u} + g_{LR}^{\nu d}\epsilon_{LR}^{\nu d}) - (g_{LR}^{\nu u} + g_{LR}^{\nu d})^2(\epsilon_L^{CC} + \delta V_{ud}) \,, \end{aligned} \tag{3.48}$$

where $\epsilon_{L,R}^{\nu q=u,d}$ are NSI the couplings to $(\bar{\nu}_\alpha \gamma_\mu P_L \nu_\beta)(\bar{q}\gamma^\mu P_{L,R} q)$, while ϵ_L^{CC} is the NSI coupling to $(\bar{\nu}_\alpha \gamma_\mu P_L \ell_\beta)(\bar{d}\gamma^\mu P_L u)$ and δV_{ud} was extracted in 3.12.
Once again, we give the explicit expression for those couplings in terms of the Wilson coefficients that emerged in the running from the Λ scale Lagrangian:

$$\begin{aligned} \epsilon_{LL}^{\nu u} =& \frac{v^2}{16\pi^2\Lambda^2} \log\frac{\Lambda}{m_{\rm EW}} \frac{\lambda_e^{22}}{2} \left[\frac{8}{9}e^2(C_e - 3C_3 + 2C_{\ell\ell} - C_1) - 12\lambda_u^{33} y_t^2 (C_1 + C_3)\left(\frac{1}{2} - \frac{2}{3}s^2\theta_W\right)\right] \,, \\ \epsilon_{LL}^{\nu d} =& \frac{v^2}{16\pi^2\Lambda^2} \log\frac{\Lambda}{m_{\rm EW}} \frac{\lambda_e^{22}}{2} \left[\frac{4}{9}e^2(C_1 + 3C_3 - 2C_{\ell\ell} - C_e) - 12\lambda_u^{33} y_t^2 (C_1 + C_3)\left(-\frac{1}{2} + \frac{1}{3}s^2\theta_W\right)\right] \,, \\ \epsilon_{LR}^{\nu u} =& \frac{v^2}{16\pi^2\Lambda^2} \log\frac{\Lambda}{m_{\rm EW}} \frac{\lambda_e^{22}}{2} \left[\frac{8}{9}e^2(C_e - 3C_3 + 2C_{\ell\ell} - C_1) + 8\lambda_u^{33} y_t^2 (C_1 + C_3)(s^2\theta_W)\right] \,, \\ \epsilon_{LR}^{\nu d} =& \frac{v^2}{16\pi^2\Lambda^2} \log\frac{\Lambda}{m_{\rm EW}} \frac{\lambda_e^{22}}{2} \left[\frac{4}{9}e^2(C_1 + 3C_3 - 2C_{\ell\ell} - C_e) - 4\lambda_u^{33} y_t^2 (C_1 + C_3)\right] \,, \end{aligned}$$

$$\begin{aligned} \epsilon_L^{CC} =& \frac{v^2}{16\pi^2\Lambda^2}\frac{1}{2} \log\frac{\Lambda}{m_{\rm EW}} [\lambda_e^{22}\lambda_{ud}^{11}(-12g_2^2 C_1 + 4(6g_2^2 + g_1^2)C_3) + \lambda_e^{22} V_{ud}(-12\lambda_u^{33} y_t^2 C_3] \,, \\ \delta V_{ud} =& \frac{v^2}{16\pi^2\Lambda^2}\left(3C_3 y_t^2 \lambda_e^{22}\lambda_{33}^u \log\left(\frac{\Lambda}{m_{EW}}\right)\right) \end{aligned}$$

where sub-leading terms have been neglected.

Then, specifying all the parameters at stake, imposing $y_t^2 = \lambda_{33}^u = 1$, $\lambda_{22}^e \simeq 0.1$ and the scale of NP to be $\Lambda = 1$ TeV, and comparing the result with the total number of events calculated with 3.37, one obtains the following constraints on the NSI coefficients

$$-9.6 \times 10^{-5} < 2.9 \times 10^{-3} \left(\frac{1\text{TeV}}{\Lambda}\right)^2 \left(\frac{\lambda_e^{22}}{0.1}\right) \times \\ \times [(-0.5)(C_1 + C_3) + (0.005)(C_e + 2C_{\ell\ell})] < +9.6 \times 10^{-5} \tag{3.49}$$

where higher order corrections have been neglected.

Given those stringent constraints, we can safely assume that DUNE is expected to dramatically improve the existing constraints, even better that in the case of neutrino scattering off electrons. Moreover, it is straightforward to see that, assuming all the Wilson coefficients to be approximately of the same order, the semi-leptonic parameters C_1 and C_3 are enhanced with respect to the leptonic coefficients $C_{\ell\ell}$ and C_e of a factor 10^2. As already observed in the previous cases, semi-leptonic processes will again seem to give a stronger contribution to NP, even more decisive that in the previous case.

What it is important to stress in this case, as was already done in the case of scattering off electrons, is that, in order to accomplish the new predicted bounds, it will be necessary to consider a slightly greater Λ scale of NP. In fact, as can be seen in fig. 3.6, δR_N falls inside the allowed region for $\Lambda \geq 5.5$ TeV.

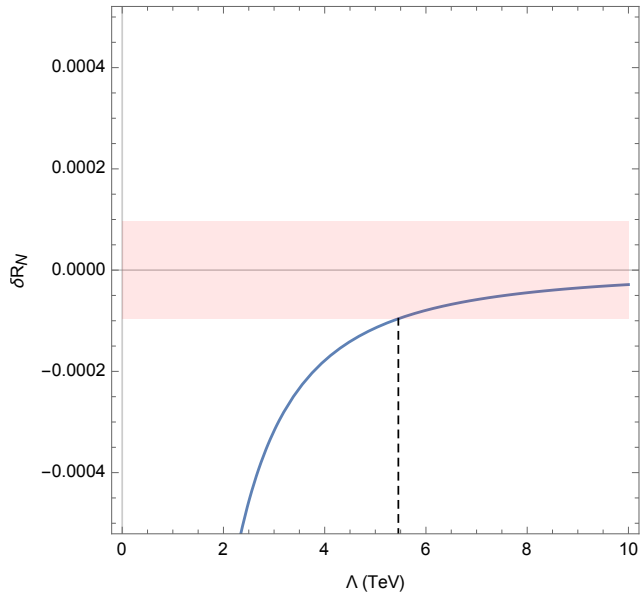

Figure 3.6: Dependance of δR_N with respect to the Λ scale of NP, following 3.49 where we set $\lambda_{22}^e = 0.1$ and $C_i = \mathcal{O}(1)$. The red region corresponds to the forecast bounds that are expected from the DUNE experiment. It can be seen that the predicted value of δR_N in our setup falls within the allowed region for $\Lambda \geq 5.5$ TeV.

Given this discussion, it is clear that DUNE is going to dramatically improve the constraints on the parameters at stake in the its observables, giving us a deeper knowledge of neutrino NSIs in the prospect of searching for NP BSM.
Even if the assumption that the DUNE errors will be dominated by statistics is clearly very optimistic, one can reach an $\mathcal{O}(10^4)$ relative precision for ν couplings to muons and light quarks, and for some semi-leptonic operators. This is beyond the direct reach of the LHC or near-future colliders, as well as beyond the indirect reach of electroweak precision measurements at LEP, as stated by (37). Without the DUNE input, the expected precision is typically an order of magnitude worse.
Obviously, with less optimistic assumptions about the systematic errors achievable in DUNE, projections are degraded, but this must be just an encouragement for future efforts to reduce experimental and theoretical sources of these errors.

CONCLUSIONS

The nature of neutrino masses and mixing represents one of the most compelling hints in the flavor sector of the Standard Model, addressing to New Physics.
In the beginning, neutrino peculiar properties were identified as the only source of lepton flavor violation in the SM, but it became clear that it was possible to introduce extra lepton flavor violation sources when introducing new and dimension-six operators in the Lagrangian, using the tools provided by the Effective Field Theory approach. Such interactions, called Non-Standard Neutrino Interactions (NSIs) can affect neutrino oscillation experiments, modifying the propagation of neutrinos in matter. NSIs can also affect the production and the detection processes, directly at the source and at the detector, producing wrong flavor neutrinos, without oscillation.
On the experimental side, current oscillation data from solar and atmospheric neutrino experiments leave room for the existence of sub-leading effects, induced by NSIs, as it has been proved in a great number of experimental analyses, for example using data from the IceCube Telescope, one of the most promising experiment at work nowadays. Future, high precision, experiments may shed further light on the strength of such interactions as motivated in the analysis of the DUNE project, that should start operating in 2027.

In the present MSc thesis we analyzed the most interesting observables at stake in NSI experiments in a model-independent way, assuming New Physics to originate at a scale $\Lambda \simeq 1$TeV.
In order to perform such a study, we have started by building the NP Lagrangian at the scale Λ in terms of 2 six-dimensional leptonic and 5 six-dimensional semi-leptonic operators. Then, we have derived the low-energy effective Lagrangian extensively: we have addressed running effects from Λ to the EW scale by employing one-loop RGEs in the limit of exact electroweak symmetry, and, after integrating out heavy degrees of freedom, we have described the evolution down to 1 GeV using RGEs dominated by the electromagnetic interaction.
In the last part of our work, we have studied the most relevant phenomenological consequences of the derived Lagrangian. In particular, we focused on the observables at stake in two of the most promising among the present and future neutrino experiment, IceCube and DUNE.

For what concerns the IceCube experiment we focused on the modification to oscillation probability. Specifying the Wilson coefficients enclosed in the NP parameters ϵ^m and $\epsilon^{s/d}$, we could be able to state that the coefficients associated to leptonic operators ($C_{\ell\ell}$ and C_e) are suppressed with respect to $C_{1,3}$ of a factor 10^2. Assuming that all the C_i's are of the same order ($\simeq \mathcal{O}(1)$), this means that semi-leptonic interactions give a greater contribution to NSIs. Moreover, we were able to confirm that our parametrization was in agreement with the current ex-

perimental bounds on the NP parameters and constituted a stricter bound with respect to the ones found in the literature. Moreover, we chose to analyze the ratio P_{NSI}/P_0 in the energy range of interest, specifying all the parameters according to the experimental set up, in order to be able to understand the extent and the relevance of those parameters in the modification of the observables at stake at IceCube.

Regarding the DUNE project, we also parametrized the modifications to the observables at stake, due to NP corrections. For what concerns trident production observable, we were able to state that this observable is not going to increase our knowledge on the NP parameters, since the constraints are of the same order of the ones found in the literature. Studying scattering off electrons and off nuclei observables instead, has been much more instructive. The rate of events that we expect will produce stricter bounds on the NP parameters than the ones found until now. In particular, they both impose to increase the chosen scale of NP, of a factor 2-3, assuming $\Lambda \gtrsim 5$ TeV.
In the end, all the three observables showed a predominance of the effect of the semi-leptonic coefficients with respect to the leptonic ones, implying that semi-leptonic interactions give a greater contribution to NSIs.

The chosen Λ scale Lagrangian was able to successfully describe NSIs. Moreover, even if the constraints given by IceCube were promising, it is very likely that DUNE will be the first probe of effective neutrino couplings, at least in scattering off electrons and nuclei.

A

DIMENSION SIX OPERATORS

In this section we list the $SU(3) \times SU(2) \times U(1)$ invariant dimension-six operators that can be used to build any EFT Lagrangian.

X^3		ϕ^6 and $\phi^4 D^2$		$\psi^2\phi^3$	
Q_G	$f^{ABC} G^{A\nu}_{\mu} G^{B\rho}_{\nu} G^{C\mu}_{\rho}$	Q_ϕ	$(\phi^\dagger\phi)^3$	$Q_{e\phi}$	$(\phi^\dagger\phi)(\bar{\ell}_p e_r \phi)$
$Q_{\tilde{G}}$	$f^{ABC} \tilde{G}^{A\nu}_{\mu} G^{B\rho}_{\nu} G^{C\mu}_{\rho}$	$Q_{\phi\Box}$	$(\phi^\dagger\phi)\Box(\phi^\dagger\phi)$	$Q_{u\phi}$	$(\phi^\dagger\phi)(\bar{q}_p u_r \tilde{\phi})$
Q_W	$\epsilon^{IJK} W^{I\nu}_{\mu} W^{J\rho}_{\nu} W^{K\mu}_{\rho}$	$Q_{\phi D}$	$(\phi^\dagger D^\mu \phi)^*(\phi^\dagger D_\mu \phi)$	$Q_{d\phi}$	$(\phi^\dagger\phi)(\bar{q}_p d_r \phi)$
$Q_{\tilde{W}}$	$f^{IJK} \tilde{W}^{I\nu}_{\mu} W^{J\rho}_{\nu} W^{K\mu}_{\rho}$				

$X^2\phi^2$		$\psi^2 X\phi$		$\psi^2\phi^2 D$	
$Q_{\phi G}$	$\phi^\dagger\phi G^A_{\mu\nu} G^{A\mu\nu}$	Q_{eW}	$(\bar{\ell}_p \sigma^{\mu\nu} e_r)\tau^I \phi W^I_{\mu\nu}$	$Q^{(1)}_{\phi\ell}$	$(\phi^\dagger i D_\mu \phi)(\bar{\ell}_p \gamma^\mu \ell_r)$
$Q_{\phi\tilde{G}}$	$\phi^\dagger\phi \tilde{G}^A_{\mu\nu} G^{A\mu\nu}$	Q_{eB}	$(\bar{\ell}_p \sigma^{\mu\nu} e_r)\phi B_{\mu\nu}$	$Q^{(3)}_{\phi\ell}$	$(\phi^\dagger i D^I_\mu \phi)(\bar{\ell}_p \tau^I \gamma^\mu \ell_r)$
$Q_{\phi W}$	$\phi^\dagger\phi W^I_{\mu\nu} W^{I\mu\nu}$	Q_{uG}	$(\bar{q}_p \sigma^{\mu\nu} T^A u_r)\tilde{\phi} G^A_{\mu\nu}$	$Q_{\phi e}$	$(\phi^\dagger i D_\mu \phi)(\bar{e}_p \gamma^\mu \ell_r)$
$Q_{\phi\tilde{W}}$	$\phi^\dagger\phi \tilde{W}^I_{\mu\nu} W^{I\mu\nu}$	Q_{uW}	$(\bar{q}_p \sigma^{\mu\nu} u_r)\tau^I \tilde{\phi} W^I_{\mu\nu}$	$Q^{(1)}_{\phi q}$	$(\phi^\dagger i D_\mu \phi)(\bar{q}_p \gamma^\mu q_r)$
$Q_{\phi B}$	$\phi^\dagger\phi B_{\mu\nu} B^{\mu\nu}$	Q_{uB}	$(\bar{q}_p \sigma^{\mu\nu} u_r)\tilde{\phi} B_{\mu\nu}$	$Q^{(3)}_{\phi q}$	$(\phi^\dagger i D^I_\mu \phi)(\bar{q}_p \tau^I \gamma^\mu q_r)$
$Q_{\phi\tilde{B}}$	$\phi^\dagger\phi \tilde{B}_{\mu\nu} W^{\mu\nu}$	Q_{dG}	$(\bar{q}_p \sigma^{\mu\nu} T^A u_r)\tau^I \phi G^A_{\mu\nu}$	$Q_{\phi u}$	$(\phi^\dagger i D_\mu \phi)(\bar{u}_p \gamma^\mu u_r)$
$Q_{\phi WB}$	$\phi^\dagger\tau^I\phi W^I_{\mu\nu} B^{\mu\nu}$	Q_{dW}	$(\bar{q}_p \sigma^{\mu\nu} d_r)\tau^I \phi W^I_{\mu\nu}$	$Q_{\phi d}$	$(\phi^\dagger i D_\mu \phi)(\bar{d}_p \gamma^\mu d_r)$
$Q_{\phi\tilde{W}B}$	$\phi^\dagger\tau^I\phi \tilde{W}^I_{\mu\nu} B^{\mu\nu}$	Q_{dB}	$(\bar{q}_p \sigma^{\mu\nu} d_r)\phi B_{\mu\nu}$	$Q_{\phi ud}$	$(\phi^\dagger i D_\mu \phi)(\bar{u}_p \gamma^\mu d)$

$(\bar{L}L)(\bar{L}L)$		$(\bar{R}R)(\bar{R}R)$		$(\bar{L}L)(\bar{R}R)$	
$Q_{\ell\ell}$	$(\bar{\ell}_p \gamma_\mu \ell_r)(\bar{\ell}_s \gamma^\mu \ell_t)$	Q_{ee}	$(\bar{e}_p \gamma_\mu e_r)(\bar{e}_s \gamma^\mu e_t)$	$Q_{\ell e}$	$(\bar{\ell}_p \gamma_\mu \ell_r)(\bar{e}_s \gamma^\mu e_t)$
$Q^{(1)}_{qq}$	$(\bar{q}_p \gamma_\mu q_r)(\bar{q}_s \gamma^\mu q_t)$	Q_{uu}	$(\bar{u}_p \gamma_\mu u_r)(\bar{u}_s \gamma^\mu u_t)$	$Q_{\ell u}$	$(\bar{\ell}_p \gamma_\mu \ell_r)(\bar{u}_s \gamma^\mu u_t)$
$Q^{(3)}_{qq}$	$(\bar{q}_p \gamma_\mu \tau^I \ell_r)(\bar{q}_s \gamma^\mu \tau^I q_t)$	Q_{dd}	$(\bar{d}_p \gamma_\mu d_r)(\bar{d}_s \gamma^\mu d_t)$	$Q_{\ell d}$	$(\bar{\ell}_p \gamma_\mu \ell_r)(\bar{d}_s \gamma^\mu d_t)$
$Q^{(1)}_{\ell q}$	$(\bar{\ell}_p \gamma_\mu \ell_r)(\bar{q}_s \gamma^\mu q_t)$	Q_{eu}	$(\bar{e}_p \gamma_\mu e_r)(\bar{u}_s \gamma^\mu u_t)$	Q_{qe}	$(\bar{q}_p \gamma_\mu q_r)(\bar{e}_s \gamma^\mu e_t)$
$Q^{(3)}_{\ell q}$	$(\bar{\ell}_p \gamma_\mu \tau^I \ell_r)(\bar{\ell}_s \gamma^\mu \tau^I \ell_t)$	Q_{ed}	$(\bar{e}_p \gamma_\mu e_r)(\bar{d}_s \gamma^\mu d_t)$	$Q^{(1)}_{qu}$	$(\bar{q}_p \gamma_\mu q_r)(\bar{u}_s \gamma^\mu u_t)$
		$Q^{(1)}_{ud}$	$(\bar{u}_p \gamma_\mu u_r)(\bar{d}_s \gamma^\mu d_t)$	$Q^{(8)}_{qu}$	$(\bar{q}_p \gamma_\mu T^A q_r)(\bar{u}_s \gamma^\mu T^A u_t)$
		$Q^{(8)}_{ud}$	$(\bar{u}_p \gamma_\mu T^A u_r)(\bar{d}_s \gamma^\mu T^A d_t)$	$Q^{(1)}_{qd}$	$(\bar{q}_p \gamma_\mu q_r)(\bar{d}_s \gamma^\mu d_t)$
				$Q^{(8)}_{qd}$	$(\bar{q}_p \gamma_\mu T^A q_r)(\bar{d}_s \gamma^\mu T^A d_t)$

$(\bar{L}R)(\bar{R}L)$ and $(\bar{L}R)(\bar{L}R)$	
$Q_{\ell edq}$	$(\bar{\ell}^j_p e_r)(\bar{d}_s q^j_t)$
$Q^{(1)}_{quqd}$	$(\bar{q}^j_p u_r)\epsilon_{jk}(\bar{q}^k_s d_t)$
$Q^{(8)}_{quqd}$	$(\bar{q}^j_p T^A u_r)\epsilon_{jk}(\bar{q}^k_s T^A d_t)$
$Q^{(1)}_{lequ}$	$(\bar{\ell}^j_p e_r)\epsilon_{jk}(\bar{q}^k_s u_t)$
$Q^{(3)}_{lequ}$	$(\bar{\ell}^j_p \sigma_{\mu\nu} e_r)\epsilon_{jk}(\bar{q}^k_s \sigma^{\mu\nu} u_t)$

B

USEFUL RELATIONS AND CONVENTIONS

B.1 FEYNMAN RULES

In this section we list all the Feynman rules that were used in the calculation of Feynman amplitudes.

- Photon Propagator:

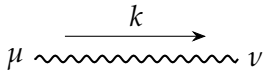

$$= \frac{-ig_{\mu\nu}}{k^2 + i\epsilon} \tag{B.1}$$

- Charged boson Propagator:

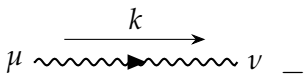

$$= \frac{-ig_{\mu\nu}}{k^2 - M^2 + i\epsilon} \tag{B.2}$$

- Gluon Propagator:

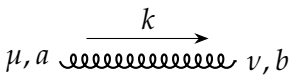

$$= \frac{-i\delta^{ab} g_{\mu\nu}}{k^2 + i\epsilon} \tag{B.3}$$

- Lepton Propagator:

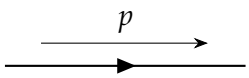

$$= \frac{i}{\not{p} - m_f + i\epsilon} \tag{B.4}$$

- Quark Propagator

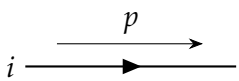

$$= \frac{i\delta^i_j}{\not{p} - m_f + i\epsilon} \tag{B.5}$$

- Boson Vertex

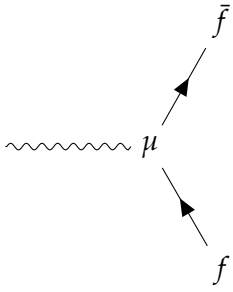

(B.6)

- Yukawa Vertex

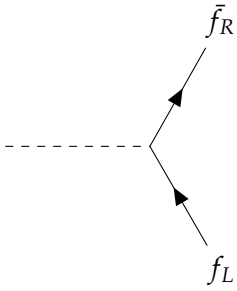

(B.7)

- Gluon Vertex

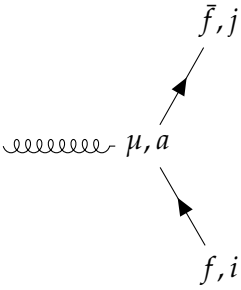

(B.8)

B.2 MANIPULATION OF DIRAC STRUCTURES

In this section we review the properties of Pauli and Dirac matrices in order to obtain useful relation to manipulate Dirac structure.

PAULI MATRICES

$$\sigma_1 = \begin{pmatrix} 0 & 1 \\ 1 & 0 \end{pmatrix} \quad \sigma_2 = \begin{pmatrix} 0 & -i \\ i & 0 \end{pmatrix} \quad \sigma_3 = \begin{pmatrix} 1 & 0 \\ 0 & -1 \end{pmatrix} \tag{B.9}$$

$$[\sigma_i, \sigma_j] = 2i\epsilon^{ijk}\sigma_k \quad \{\sigma_i, \sigma_j\} = 2\delta_{ij} \tag{B.10}$$

$$\sum_i (\sigma_i)_{ab}(\sigma_i)_{cd} = 2\left(\delta_{bc}\delta_{ad} - \frac{1}{2}\delta_{ab}\delta_{cd}\right) \tag{B.11}$$

DIRAC MATRICES

In the Dirac representation they read

$$\gamma_0 = \begin{pmatrix} \mathbb{1} & 0 \\ 0 & -\mathbb{1} \end{pmatrix} \quad \gamma_i = \begin{pmatrix} 0 & \sigma \\ -\sigma & 0 \end{pmatrix} \quad \gamma_5 = \begin{pmatrix} 0 & \mathbb{1} \\ \mathbb{1} & 0 \end{pmatrix} \tag{B.12}$$

$$\text{Contractions} \begin{cases} \{\gamma^\mu, \gamma^\nu\} = 2g^{\mu\nu} \\ [\gamma^\mu, \gamma^\nu] = \frac{1}{2}\sigma^{\mu\nu} \\ \gamma^\mu\gamma^\nu\gamma_\mu = -2\gamma^\nu \\ \gamma^\mu\gamma^\nu\gamma^\rho\gamma_\mu = 4g^{\nu\rho} \\ \gamma^\mu\gamma^\nu\gamma^\rho\gamma^\sigma\gamma_\mu = -2\gamma^\sigma\gamma^\rho\gamma^\nu \\ \gamma_\mu\gamma_\alpha\gamma_\nu = g_{\mu\alpha}\gamma_\nu - g_{\alpha\nu}\gamma_\mu - g_{\mu\nu}\gamma_\alpha + i\epsilon_{\mu\alpha\nu\sigma}\gamma^\rho\gamma^5 \end{cases} \tag{B.13}$$

$$\text{Traces} \begin{cases} \mathrm{Tr}[\gamma^\mu\gamma^\nu] = 4g^{\mu\nu} \\ \mathrm{Tr}[\gamma^\mu\gamma^\nu\gamma^\rho\gamma^\sigma] = 4(g^{\mu\nu}g^{\rho\sigma} - g^{\mu\rho}g^{\nu\sigma} + g^{\mu\sigma}g^{\nu\rho}) \\ \mathrm{Tr}\left[\gamma^\mu\gamma^\nu\gamma^\rho\gamma^\sigma\gamma^5\right] = -4i\epsilon^{\mu\nu\rho\sigma} \\ \mathrm{Tr}\left[\gamma^\mu\gamma^\nu\gamma^5\right] = \mathrm{Tr}\left[\underbrace{\gamma^\mu\gamma^\nu\ldots}_{odd}\gamma^5\right] = \mathrm{Tr}\left[\underbrace{\gamma^\mu\gamma^\nu\ldots}_{odd}\right] = 0 \end{cases} \tag{B.14}$$

FIERZ IDENTITIES Let $\Gamma_S = 1$, $\Gamma_V = \gamma_\mu$, $\Gamma_T = \sigma_{\mu\nu}$, $\Gamma_A = \gamma_\mu\gamma_5$ and $\Gamma_P = \gamma_5$. Then $\sum_i g_i(\Gamma_i)_{\alpha\beta}(\Gamma_i)_{\gamma\delta} = \sum_j \hat{g}_j(\Gamma_j)_{\alpha\delta}(\Gamma_j)_{\gamma\beta}$, where $(i,j) = \{S,V,T,A,P\}$ and the g_i are related to the $\hat{g}_j$ by

$$\begin{pmatrix} \hat{g}_S \\ \hat{g}_V \\ \hat{g}_T \\ \hat{g}_A \\ \hat{g}_P \end{pmatrix} = \frac{1}{4}\begin{pmatrix} 1 & 4 & 12 & -4 & 1 \\ 1 & -2 & 0 & -2 & -1 \\ \frac{1}{2} & 0 & -2 & 0 & \frac{1}{2} \\ -1 & -2 & 0 & -2 & 1 \\ 1 & -4 & 12 & 4 & 1 \end{pmatrix}\begin{pmatrix} g_S \\ g_V \\ g_T \\ g_A \\ g_P \end{pmatrix} \tag{B.15}$$

SPINOR IDENTITIES

$$\begin{aligned} &(\bar{v}\gamma^\alpha\gamma^\beta P_{L/R}u)(\bar{u}\gamma_\alpha\gamma_\beta P_{L/R}v) = 4(\bar{v}P_{L/R}u)(\bar{u}P_{L/R}v) - (\bar{v}\sigma^{\alpha\beta}P_{L/R}u)(\bar{u}\sigma_{\alpha\beta}P_{L/R}v) \\ &(\bar{v}\gamma^\alpha\gamma^\beta P_{L/R}u)(\bar{u}\gamma_\alpha\gamma_\beta P_{R/L}v) = 4(\bar{v}P_{L/R}u)(\bar{u}P_{R/L}v) \\ \\ &(\bar{v}\gamma^\alpha\gamma^\beta P_{L/R}u)(\bar{u}\gamma_\beta\gamma_\alpha P_{L/R}v) = 4(\bar{v}P_{L/R}u)(\bar{u}P_{L/R}v) + (\bar{v}\sigma^{\alpha\beta}P_{L/R}u)(\bar{u}\sigma_{\alpha\beta}P_{L/R}v) \\ &(\bar{v}\gamma^\alpha\gamma^\beta P_{L/R}u)(\bar{u}\gamma_\beta\gamma_\alpha P_{R/L}v) = 4(\bar{v}P_{L/R}u)(\bar{u}P_{R/L}v) \\ \\ &(\bar{v}\gamma^\alpha\gamma^\beta\gamma^\delta P_{L/R}u)(\bar{u}\gamma_\alpha\gamma_\beta\gamma_\delta P_{L/R}v) = 16(\bar{v}\gamma^\alpha P_{L/R}u)(\bar{u}\gamma_\alpha P_{L/R}v) \\ &(\bar{v}\gamma^\alpha\gamma^\beta\gamma^\delta P_{L/R}u)(\bar{u}\gamma_\alpha\gamma_\beta\gamma_\delta P_{R/L}v) = 4(\bar{v}\gamma^\alpha P_{L/R}u)(\bar{u}\gamma_\alpha P_{R/L}v) \end{aligned} \tag{B.16}$$

B.3 DIMENSIONAL REGULARIZATION

In this section we summarize all the relation that have been used in the calculation of dimensional regularized integrals which appear in the calculation of loop amplitudes.

FEYNMAN PARAMETRIZATION

$$\begin{aligned}\frac{1}{AB} &= \int_0^1 \mathrm{d}x\, \frac{1}{[Ax + B(1-x)]^2} \\ \frac{1}{ABC} &= \int_0^1 \mathrm{d}x\, \mathrm{d}y\, \mathrm{d}z\, \delta(x+y+z-1) \frac{2}{[xA + yB + zC]^3}\end{aligned} \tag{B.17}$$

REGULARIZED INTEGRALS

$$\begin{aligned}\mathcal{I}_{0,2} &= \int \frac{\mathrm{d}^D k}{(2\pi)^D} \mu^{4-D} \frac{1}{(k^2 - \Delta + i\epsilon)^2} = \frac{i}{16\pi^2}\left(\frac{2}{\epsilon} + \ln\frac{4\pi\mu^2}{\Delta} - \gamma + \mathcal{O}(\epsilon)\right) \\ \mathcal{I}_{1,2} &= \int \frac{\mathrm{d}^D k}{(2\pi)^D} \mu^{4-D} \frac{k^2}{(k^2 - \Delta + i\epsilon)^2} = \frac{2i}{16\pi^2}\Delta\left(\frac{2}{\epsilon} + \ln\frac{4\pi\mu^2}{\Delta} + \gamma - 1 + \mathcal{O}(\epsilon)\right) \\ \mathcal{I}_{1,3} &= \int \frac{\mathrm{d}^D k}{(2\pi)^D} \mu^{4-D} \frac{k^2}{(k^2 - \Delta + i\epsilon)^3} = \frac{i}{16\pi^2}\left(\frac{2}{\epsilon} + \ln\frac{4\pi\mu^2}{\Delta} - \gamma + \mathcal{O}(\epsilon)\right)\end{aligned} \tag{B.18}$$

C

EXPLICIT CALCULATIONS OF ONE-LOOP MATRIX ELEMENTS $\mathcal{M}$

C.1 CANCELLATION OF THE μ SCALE

The explicit cancellation of the μ scale is checked explicitly in the following example, calculating the W boson decay in leptons, $W^+ \to e_L^+ \nu_L$.
The involved diagrams are

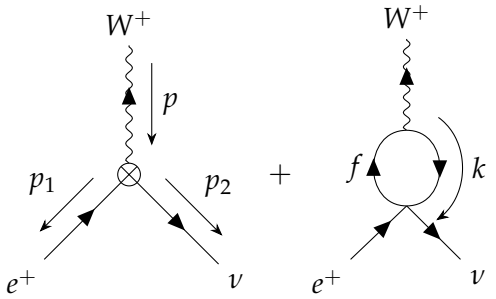

(C.1)

The amplitude for the formal tree level diagram reads

$$\mathcal{M}_a = \mathcal{M}_{\text{SM}} + \Delta\mathcal{M}_\ell = -i\frac{g_2}{\sqrt{2}}\bar{u}_i \not{\epsilon}(g_l + \Delta g^l)_{ij} P_L v_j \tag{C.2}$$

where

$$\Delta\mathcal{M}_\ell = -i\frac{g_2}{\sqrt{2}}v^2\frac{L}{(4\pi)^2\Lambda^2}\left[-\frac{2}{3}g_2^2 C_{\ell\ell} - 2g_2^2 C_3 + 6\lambda_{33}^u y_t^2 C_3\right](\bar{u}_i \not{\epsilon} P_L \lambda_{ij}^e v_j). \tag{C.3}$$

The four fermions operators contributing to the one loop diagram amplitude $\mathcal{M}_{\text{loop}} = \mathcal{M}_{\text{loop}}^{(1)} + \mathcal{M}_{\text{loop}}^{(2)}$ are

$$\begin{aligned} &(1) \quad \frac{2C_{\ell\ell}}{\Lambda^2}(\bar{e}_L\gamma_\mu\lambda_e\nu_L)(\bar{\nu}_L\gamma^\mu\lambda_e e_L) \\ &(2) \quad \frac{2C_3}{\Lambda^2}(\bar{e}_L\gamma_\mu\lambda_e\nu_L)(\bar{u}_L\gamma^\mu\lambda_{ud} d_L) \end{aligned} \tag{C.4}$$

The result of the computation of $\mathcal{M}_{\text{loop}} + \Delta\mathcal{M}_\ell$ should not depend on the renormalization scale μ, as will be proven in the following.
All conventions on Feynman rules, Feynman parametrization, trace calculation and solutions of renormalized integrals are listed in the Appendix B.

Let k^μ be the loop momentum and p^μ the W momentum such that $p^2 = m_W^2$, i.e. W is on shell; using Feynman rules, the one loop amplitude with operator (1) inserted reads

$$\mathcal{M}^{(1)}_{\text{loop}} = \frac{2C_{\ell\ell}}{\Lambda^2}\frac{g_2}{\sqrt{2}}(\bar{u}_i\gamma^\mu P_L\lambda^e_{ij}v_j)\epsilon^\nu\sum_e\lambda^e_{ij}\int\frac{\mathrm{d}^4k}{(2\pi)^4}\frac{\mathrm{Tr}\left[\gamma_\mu P_L(\not{k}+m_e)\gamma_\nu P_L(\not{k}+\not{p})\right]}{(k^2-m_e^2)(k+p)^2}. \quad \text{(C.5)}$$

The integral diverges for large k like k^2, hence it must be dimensionally regularized.
In order to do so the integration measure must be modified so that

$$\int\frac{\mathrm{d}^4k}{(2\pi)^4}\to\int\frac{\mathrm{d}^Dk}{(2\pi)^D}\mu^{4-D}\equiv\int_k\mu^{4-D}. \quad \text{(C.6)}$$

Using *Gammology* the trace can be easily calculated, so the numerator becomes

$$N^{(1)}_{\mu\nu} = 4[g_{\mu\rho}g_{\nu\sigma} - g_{\mu\nu}g_{\rho\sigma} + g_{\mu\sigma}g_{\nu\rho} + i\epsilon_{\mu\rho\nu\sigma}]k^\rho(k+p)^\sigma\,, \quad \text{(C.7)}$$

while, using *Feynman parametrization* and shifting the loop momentum $k\to k+px$, the denominator becomes

$$\frac{1}{(k^2-m_e^2)(k+p)^2} = \int_0^1\mathrm{d}x\,\frac{1}{[k^2-\Delta]^2} \quad \text{with} \quad \Delta = (m_e^2-p^2x)(1-x)\,. \quad \text{(C.8)}$$

Given shift eventually modifies the numerator. Moreover, some properties are used in order to further simplify the numerator, such as

- only even powers of k^μ give non zero contribution, all the terms of the form $k^\alpha p^\beta$ or $k\cdot p$ cancel,
- contraction of symmetric and anti-symmetric indices gives $\epsilon_{\mu\rho\nu\sigma}k^\rho k^\sigma = 0$,
- use of Dirac equation, which makes $p_\mu p_\nu = 0$ when contracting with $\bar{u}_i$ and v_j for the conservation of momentum $p_e^\mu + p_\nu^\mu = p^\mu$
- use of properties of the metric like $k_\mu k_\nu = \frac{k^2}{D}g_{\mu\nu}$

In the end, after all these manipulations, the regularized integral becomes

$$\mathcal{I}^{(R)}_\ell = \int_0^1\mathrm{d}x\,2g_{\mu\nu}\left[\underbrace{\int_k\mu^{4-D}\left(\frac{2}{D}-1\right)\frac{k^2}{(k^2-\Delta)^2}}_{\mathcal{I}_{1,2}} + p^2x(1-x)\underbrace{\int_k\frac{1}{(k^2-\Delta)^2}}_{\mathcal{I}_{0,2}}\right] \quad \text{(C.9)}$$

Working in the $\overline{MS}$ scheme in the leading logarithms approximation, the solution of $\mathcal{I}_{1,2}$ and $\mathcal{I}_{0,2}$ are well known. Plugging then C.9 into C.5 one obtains

$$\mathcal{M}^{(1)}_{\text{loop}} = \frac{4i}{(4\pi)^2\Lambda^2}C_{\ell\ell}\frac{g_2}{\sqrt{2}}(\bar{u}_i\not{\epsilon}P_L\lambda^e_{ij}v_j)\int_0^1\mathrm{d}x\,m_W^2x(1-x)\ln\frac{\mu^2}{\Delta} \quad \text{(C.10)}$$

Where the assumption that lepton masses are negligible with respect to m_W^2 have been made, so that $\Delta \to m_W^2(x-1)$.

An analogous calculation must be followed in order to obtain $\mathcal{M}^{(2)}_{\text{loop}}$, noticing that $\lambda_{ud} = \lambda_u V_{\text{CKM}}$

$$\begin{aligned}\mathcal{M}^{(2)}_{\text{loop}} =& \frac{3\cdot 2C_3}{\Lambda^2}\frac{g_2}{\sqrt{2}}(\bar{u}_i\gamma^\mu P_L\lambda^e_{ij}v_j)\epsilon^\nu\sum_u \lambda^u_{ij}V_{\text{CKM}}\times \\ &\times\int\frac{\mathrm{d}^4k}{(2\pi)^4}\frac{\mathrm{Tr}\left[\gamma_\mu P_L(\not{k}+m_u)\gamma_\nu P_L(\not{k}+\not{p})+m_d\right]}{(k^2-m_u^2)((k+p)^2-m_d^2)}\,,\end{aligned} \tag{C.11}$$

which can be simplified by noticing that

- The numerator in the integral of C.11 is just the same as C.7, the one in C.5,
- The denominator is different but the shift is the same and the the Feynman parametrization gives
  $\Delta' = p^2x(x-1) + m_u^2(1-x) + m_d^2x$,
- In the end, the renormalized integrals are formally the same as C.9.

Plugging all this information in C.11, assuming that all quark masses are negligible with respect to m_W^2, with the exception of the top mass m_t, thanks to the strong hierarchy between the CKM matrix elements $(\lambda^u V_{\text{CKM}})_{33} \sim \lambda^u$, one obtains

$$\begin{aligned}\mathcal{M}^{(2)}_{\text{loop}} =& \frac{12i}{(4\pi)^2\Lambda^2}C_3\frac{g_2}{\sqrt{2}}\int_0^1\mathrm{d}x\left[\lambda^u_{33}\left(m_t^2(x-1)+2m_W^2x(1-x)\right)\ln\frac{\mu^2}{\Delta'}\right. \\ &\left.+\,(1-\lambda^u_{33})(2m_W^2x(1-x))\ln\frac{\mu^2}{\Delta}\right](\bar{u}_i\not{\epsilon}P_L\lambda^e_{ij}v_j)\,.\end{aligned} \tag{C.12}$$

In conclusion, summing C.10 and C.12 one obtains

$$\begin{aligned}\mathcal{M}_{\text{loop}} =& \frac{4i}{(4\pi)^2\Lambda^2}\frac{g_2}{\sqrt{2}}(\bar{u}_i\not{\epsilon}P_L\lambda^e_{ij}v_j)[(2C_{\ell\ell}+6C_3)m_W^2\mathcal{I}_2^\mu - 3m_t^2\lambda_3 3C_3\mathcal{I}_1^\mu + \\ &+6m_t^2C_3\lambda_{33}\mathcal{I}_3]\,,\end{aligned} \tag{C.13}$$

where

$$\begin{aligned}\mathcal{I}_1^\mu &= \int_0^1\mathrm{d}x\,(1-x)\ln\frac{\mu^2}{\Delta'} \\ \mathcal{I}_2^\mu &= \int_0^1\mathrm{d}x\,x(1-x)\ln\frac{\mu^2}{\Delta} \\ \mathcal{I}_3 &= \int_0^1\mathrm{d}x\,x(1-x)\ln\frac{\Delta}{\Delta'}\,.\end{aligned} \tag{C.14}$$

In order to check explicitly the cancellation of μ, C.2 should be rewritten using some useful relations

$$\begin{gathered} m_W^2 = \frac{v^2 g_2^2}{4}, \quad m_t^2 = \frac{v^2 y_t^2}{2} \\ \int_0^1 \mathrm{d}x\,(1-x) = \frac{1}{2}, \quad \int_0^1 \mathrm{d}x\, x(1-x) = \frac{1}{6} \\ L = \ln\frac{\Lambda}{\mu} = \frac{1}{2}\ln\frac{\Lambda^2}{\mu^2}\,. \end{gathered} \tag{C.15}$$

In the end, summing C.2, rewritten using C.15, and C.13 the μ dependence cancels, and the total amplitudes reads

$$\mathcal{M}_a + \mathcal{M}_{\text{loop}} = \frac{i}{(4\pi)^2\Lambda^2} v^2 \frac{g_2}{\sqrt{2}} (\bar{u}_i \not{\epsilon} P_L \lambda^e_{ij} v_j)[(2g_2^2 C_{\ell\ell} + 6g_2^2 C_3)\mathcal{I}_2 - 6\lambda_{33} y_t^2 C_3 \mathcal{I}_1 + 6g_2^2 C_3 \lambda_{33} \mathcal{I}_3]$$

where

$$\begin{aligned} \mathcal{I}_1 &= \int_0^1 \mathrm{d}x\,(1-x)\ln\frac{\Lambda^2}{\Delta'} \\ \mathcal{I}_2 &= \int_0^1 \mathrm{d}x\, x(1-x)\ln\frac{\Lambda^2}{\Delta} \end{aligned} \tag{C.16}$$

do not depend on the fictitious scale μ, concluding the demonstration.
Similar procedures can be followed to prove cancellation of μ scale in any other process.

C.2 CURRENT-CURRENT DIAGRAMS

With reference with the one loop diagrams listed in 2.4, we give an explicit calculation of the amplitude involved in the determination of the RGE parameters. With reference to diagram (7), which is equivalent to (8), the associated amplitude reads

$$\begin{aligned} \mathcal{M}_{(7)} =& (-ieq_f)(-ieq_g) i \frac{C_i}{\Lambda^2} M^f_{ij} M^g_{ij} \int \frac{\mathrm{d}^D k}{(2\pi)^D}\, \mu^{4-D} \frac{-ig_{\nu\rho}}{k^2 - m_\gamma^2} \times \\ &\times \frac{(k-p)^\alpha (k-p)^\beta (\bar{v}\gamma_\mu \gamma_\alpha \gamma^\rho P u)(\bar{u}\gamma^\mu \gamma^\beta \gamma^\nu P v)}{(k-p)^4}\,, \end{aligned} \tag{C.17}$$

being $q_{f/g}$ the charge of the fermion, k^α the momentum of the photon, m_γ the mass regulator of the photon and p^α the external momentum.
Since the external momentum is arbitrary and we expect the result to be dimensionless, one is allowed to put $p^\alpha = 0$ in order to simplify the calculations.

Moreover, using the property $k^\alpha k^\beta = \frac{k^2}{D} g^{\alpha\beta}$ and the relations of the Appendix B, plus Feynman parametrization with $A = (k^2 - m_\gamma^2)$ and $B = k^2$, one obtains

$$\mathcal{M}_{(7)} = \pm 4e^2 q_f q_g \frac{C_i}{\Lambda} M_{ij}^f M_{ij}^g \int_0^1 \mathrm{d}x \underbrace{\int_k \frac{1}{(k^2 - m_\gamma^2 x)^2}}_{I_{0,2}} (\bar{v}\gamma_\mu P u)(\bar{u}\gamma^\mu P v) \tag{C.18}$$

where the $+$ sign stands if Q_{CC} has a chiral structure $(LL)(RR)$ or $(RR)(LL)$, while the $-$ sign stands when Q_{CC} is $(LL)(LL)$ or $(RR)(RR)$, as a consequence of the spinor current contractions properties.
All is left to do is the integration of $I_{0,2}$, which is a well known regularized integral, and consequently the integration over $\mathrm{d}x$.
Considering only the part of the amplitude that shows a μ dependence, one obtains

$$\mathcal{M}_{(7)}^\mu = \frac{i}{16\pi^2\Lambda^2} (\pm 4e^2 q_f q_g C_i) \ln \mu^2 M_{ij}^f M_{ij}^g (\bar{v}\gamma_\mu P u)(\bar{u}\gamma^\mu P v) \tag{C.19}$$

The calculation of $\mathcal{M}_{(9)}$, which is equivalent to diagram (10), is completely analogous and the associated amplitude reads

$$\begin{aligned} \mathcal{M}_{(9)} =& (-ieq_f)(-ieq_g) i \frac{C_i}{\Lambda^2} M_{ij}^f M_{ij}^g \int \frac{\mathrm{d}^D k}{(2\pi)^D} \mu^{4-D} \frac{-ig_{\nu\rho}}{k^2 - m_\gamma^2} \times \\ & \times \frac{(k-p)^\alpha (k-p)^\beta (\bar{v}\gamma^\nu \gamma^\alpha \gamma^\mu P u)(\bar{u}\gamma_\mu \gamma^\beta \gamma_\rho P v)}{(k-p)^4} \end{aligned} \tag{C.20}$$

where the only difference lies in the Dirac structure of the numerator.
Using the relations listed in App. B, and following the same steps that led to the calculation of $\mathcal{M}_{(7)}$, one obtains

$$\mathcal{M}_{(9)}^\mu = \frac{i}{16\pi^2\Lambda^2} (\mp e^2 q_f q_g C_i) \ln \mu^2 M_{ij}^f M_{ij}^g (\bar{v}\gamma_\mu P u)(\bar{u}\gamma^\mu P v)\,. \tag{C.21}$$

Then, inserting C.19 and C.21 in 2.60, one obtains the sector of the one loop amplitude with μ dependence

$$\mathcal{M}_{\text{loop}}^\mu = \frac{i}{16\pi^2\Lambda^2} (\pm 6e^2 q_f q_g C_i) \ln \mu^2 M_{ij}^f M_{ij}^g (\bar{v}\,\gamma_\mu P u)(\bar{u}\gamma^\mu P v)\,. \tag{C.22}$$

Comparing this result with the RGE amplitude it is possible to extract the coefficients needed for the RGE flow.

Scalar vertices

Scalar operators need to be analyzed separately since the different vertex Dirac structure modifies the calculations with respect to the vector operators.
Scalar operators of the form $Q_S = (\bar{f} A^i P_{L/R} f)(\bar{g} A_i P_{R/L} g)$ are modified at one loop by the insertion of Q_S itself with vertex corrections, where the mediator is the photon. It is not possible to construct Penguin operators since those Q_S involve chiral currents, that don't couple with the photon.
The main difference with respect to the Vector case is that the different Dirac

structures of the vertex do not assure the validity of the Ward identity. In this case then, one needs to calculate the contributions from all (1) to (10) diagrams.

Let's consider a generic process $\bar{f'}_i f_j \to \bar{g'}_k g_l$, that receive contribution only by the insertion of Q_S itself. The involved diagrams are just the same that the one of the vector case.

Diagrams (1) and (2) have the same structure, the only difference is represented by the different charges $q_{f,f'}$ and $q_{g,g'}$. The amplitude reads:

$$\mathcal{M}_{(1,2)} = q_p q'_p \frac{C_i}{\Lambda^2}(\bar{u}A_i v)\int \frac{\mathrm{d}^D k}{(2\pi)^D}\mu^{4-D}\frac{(\bar{v}\gamma^\rho(-\not{k}-\not{p}+m_u)B^i(\not{p}'+\not{k}+m_d)\gamma_\rho u}{(k^2-\lambda^2)[(k+p)^2-m_u^2][(k+p')^2-m_d^2]}\,.$$

where k_μ is the loop momentum, λ is the mass regulator of the photon, p_μ and p'_μ are the external momenta, the p in q_p^2 stands for f or g alternatively, and A_i and B_i stand for the different Dirac structure of the vertex, associated to the $C_i = \{C_s, C_s^1, C_s^3\}$, as follows:

$$(A_i)(B^i) = \{(P_L)(P_R), (P_L)(P_L), (\sigma^{\mu\nu}P_L)(\sigma_{\mu\nu}P_L)\}\,. \tag{C.23}$$

Solving for the different Dirac structures, one finds for the part proportional to $\ln\mu$ of $\mathcal{M}_{(1)}+\mathcal{M}_{(2)}$

$$\begin{aligned}\mathcal{M}_{Q_s,Q_s^1} &= -4(q_f q'_f + q_g q'_g)\frac{i\,C_i}{16\pi^2\Lambda^2}\ln\mu^2(\bar{v}A_i P u)(\bar{u}A_i P v)\\ \mathcal{M}_{Q_s^3} &= 0\,.\end{aligned} \tag{C.24}$$

For what concerns the diagrams from (3) to (6), the contribution is independent on the Vertex structure, since it is directly proportional to the wave function counterterm Z_2.
The part proportional to $\ln\mu$ of the sum of the four diagram reads

$$\mathcal{M}_{Q_i} = i\frac{q_f^2+q_{f'}^2+q_g^2+q_{g'}^2}{2}\frac{C_i Q_i}{16\pi^2\Lambda^2}\mathrm{I}_1\ln(\mu)(\bar{v}A_i P u)(\bar{u}A_i P v)\,, \tag{C.25}$$

where an additional $\frac{1}{2}$ term is due as a symmetry factor and I_1 is the result of the integration over x of the non divergent part.

Diagrams (7) and (8) have the same structure, just like the vector case, but are modified by the vertex structure. Their amplitude reads:

$$\mathcal{M}_{(7),(8)} = q_p q_{p'}\frac{C_i}{\Lambda^2}\int\frac{\mathrm{d}^D k}{(2\pi)^D}\mu^{4-D}\frac{\bar{v}\gamma^\rho(-\not{k}+\not{p}+m_u)A_i u)(\bar{u}\gamma_\rho(\not{k}-\not{p}'+m_\mu)B^i v}{(k^2-\lambda^2)[(k-p)^2-m_u^2][(k-p')^2-m_d^2]}\,.$$

It is important to notice that, in the calculation, a mixing between $Q^1_{\ell equ}$ and $Q^3_{\ell equ}$ arises.

The amplitude for diagrams (9) and (10) is completely analogous and reads:

$$\mathcal{M}_{(9),(10)} = q_p q_{p'} \frac{C_i}{\Lambda^2} \int \frac{\mathrm{d}^D k}{(2\pi)^D} \mu^{4-D} \frac{\bar{v}\gamma^\rho(-\not{k}+\not{p}+m_d)A_i u)(\bar{u}B_i(\not{k}-\not{p}'+m_\mu)\gamma_\rho v}{(k^2-\lambda^2)[(k-p)^2-m_u^2][(k-p')^2-m_d^2]} .$$

The part proportional to $\ln\mu$ of the sum of amplitudes (7) to (10) reads

$$\mathcal{M}_{Q_S} = (q_f q_g - q_f q_{g'} + q_{f'} q_g - q_{f'} q_{g'}) \frac{iC_S}{16\pi\Lambda^2} \ln\mu^2 (\bar{v}P_L u)(\bar{u}P_R v)$$

$$\begin{aligned}\mathcal{M}_{Q_S^1} = &\left[(q_f q_g + q_{f'} q_{g'}) \frac{i(C_S^1 - 12C_S^3)}{16\pi^2\Lambda^2} - (q_f q_{g'} + q_{f'} q_g) \frac{i(C_S^1 + 12C_S^3)}{16\pi^2\Lambda^2}\right] \times \\ &\times \ln\mu^2 (\bar{v}P_L u)(\bar{u}P_L v)\end{aligned} \tag{C.26}$$

$$\begin{aligned}\mathcal{M}_{Q_S^3} = &\left[(q_f q_g + q_{f'} q_{g'}) \frac{i(3C_S^3 - \frac{1}{4}C_S^1)}{16\pi^2\Lambda^2} - (q_f q_{g'} + q_{f'} q_g) \frac{i(3C_S^3 + \frac{1}{4}C_S^1)}{16\pi^2\Lambda^2}\right] \times \\ &\times \ln\mu^2 (\bar{v}\sigma^{\mu\nu}P_L u)(\bar{u}\sigma_{\mu\nu}P_L v) .\end{aligned}$$

Then, summing C.24, C.25 and C.26 one gets

$$\begin{aligned}\mathcal{M}_{Q_S} = &\left[\frac{q_f^2 + q_{f'}^2 + q_g^2 + q_{g'}^2}{2} \mathrm{I}_1 - 4(q_f q_f' + q_g q_g') + (q_f q_g - q_f q_{g'} + q_{f'} q_g - q_{f'} q_{g'})\right] \times \\ &\times \frac{iC_S}{16\pi\Lambda^2} \ln\mu^2 (\bar{v}P_L u)(\bar{u}P_R v)\end{aligned}$$

$$\begin{aligned}\mathcal{M}_{Q_S^1} = &\left[\frac{q_f^2 + q_{f'}^2 + q_g^2 + q_{g'}^2}{2} \mathrm{I}_1 - 4(q_f q_f' + q_g q_g'))C_S^1 + (q_f q_g + q_{f'} q_{g'}) i(C_S^1 - 12C_S^3)\right. \\ &\left. - (q_f q_{g'} + q_{f'} q_g) i(C_S^1 + 12C_S^3)\right] \frac{1}{16\pi^2\Lambda^2} \ln\mu^2 (\bar{v}P_L u)(\bar{u}P_L v)\end{aligned}$$

$$\begin{aligned}\mathcal{M}_{Q_S^3} = &\left[\frac{q_f^2 + q_{f'}^2 + q_g^2 + q_{g'}^2}{2} \mathrm{I}_1 C_S^3 + (q_f q_g + q_{f'} q_{g'}) i(3C_S^3 - \frac{1}{4}C_S^1) - (q_f q_{g'} + q_{f'} q_g) i(3C_S^3 + \frac{1}{4}C_S^1)\right] \times \\ &\times \frac{1}{16\pi^2\Lambda^2} \ln\mu^2 (\bar{v}\sigma^{\mu\nu}P_L u)(\bar{u}\sigma_{\mu\nu}P_L v) .\end{aligned}$$

Comparing this result with the RGE amplitude it is possible to extract the coefficients needed for the RGE flow.

C.3 PENGUIN DIAGRAMS

With reference to the diagram in 2.4, the one loop amplitude reads *Semi-leptonic penguin*

$$\mathcal{M}_P^H = (-ieq_l)(-ieq_e)\frac{iC_P}{\Lambda^2}\sum_i \lambda^e_{ii}\left(-\frac{ig_{\mu\nu}}{l^2}\right)\int \frac{\mathrm{d}^D k}{(2\pi)^D}\,\mu^{4-D}\frac{\mathrm{Tr}\left[(\gamma_\rho \not{k})\gamma_\nu P(\not{k}+\not{l})\right]}{(k^2-m_\ell^2)(k+l)^2}\times \\ \times M^q_{ij}(\bar{v}\gamma_\rho P u)(\bar{u}\gamma_\mu v)\,, \tag{C.27}$$

where l is the momentum of the photon and k, $k+l$ the momenta running in the loop.

Using Gammology properties and Feynman parametrization with $\Delta = l^2 x(1-x) + m_l^2$) one gets

$$\mathcal{M}_P^H = 4e^2 q_l q_e)\frac{C_P}{\Lambda^2}\sum_i \lambda^e_{ii}\int_0^1 \mathrm{d}x\int_k \mu^{4-D}\frac{x(1-x)}{(k^2-\Delta^2)^2}\,M^q_{ij}(\bar{v}\gamma_\rho P u)(\bar{u}\gamma_\mu v)\,, \tag{C.28}$$

Concluding, imposing $l^2 = 0$ and solving the integral in $\mathrm{d}x$, after the usual integration of $I_{0,2}$, one gets

$$\mathcal{M}_P^{\mu,H} = \frac{i}{16\pi^2\Lambda^2}\left(-\frac{2}{3}e^2 q_l q_e C_P\right)\sum_i \lambda^e_{ii}\ln\mu^2 M^q_{ij}(\bar{v}\gamma_\rho P u)(\bar{u}\gamma_\mu v)\,, \tag{C.29}$$

where only the part with a μ dependence was outlined.
Comparing this result with the RGE amplitude it is possible to compute the coefficients for every semi leptonic Q_P^H operator.

Leptonic penguin

With reference to the diagram in 2.4, associated to the generic process $\bar{\ell}_i\ell_j \to \bar{f}_k f_k$, we calculate, for example, the case of charged leptons running in the loop. In that case, the one loop amplitude reads

$$\mathcal{M}_P^L = -(ieq_g)(ieq_\ell)\left(-\frac{ig_{\mu\nu}}{l^2}\right)\frac{C_\ell}{\Lambda^2}\sum_i \lambda^e_{ii}\int \frac{\mathrm{d}^D k}{(2\pi)^D}\frac{\mathrm{Tr}\left[\gamma_\rho \not{k}\gamma_\nu P(\not{k}+\not{l})\right]}{(k^2-m_f^2)((k+l)^2-m_f^2)}\times \\ \times M^e_{ij}(\bar{v}\gamma_\mu P u)(\bar{u}\gamma^\mu v)\,, \tag{C.30}$$

where l is the momentum of the photon and k and $k+l$ the momenta running in the loop.

Using Gammology properties, Feynman parametrization and consequently integrating in $\mathrm{d}x$ the integral becomes

$$\int \frac{\mathrm{d}^D k}{(2\pi)^D}\frac{\mathrm{Tr}\left[\gamma_\rho \not{k}\gamma_\nu P(\not{k}+\not{l})\right]}{(k^2-m_f^2)((k+l)^2-m_f^2)} \to \frac{4}{6}\frac{i}{16\pi^2}\ln\frac{\mu^2}{m_f^2}\,. \tag{C.31}$$

It is straightforward to notice that the integral result does not depend on the chirality (P), nor on the nature of the fermion running in the loop[1].

Summing all the contributions, considering only the dependence on μ, one gets

$$\mathcal{M}_P^L = -\frac{2ie^2}{16\pi^2\Lambda^2}\left[\frac{2}{3}q_e(C_L^e\sum_i\lambda_{ii}^e + C_R^e\sum_i\Gamma_{ii}^e) + q_uC_L^u\sum_j\lambda_{jj}^u + q_dC_L^d\sum_k\lambda_{kk}^d\right]\times \\ \times \ln\mu^2 M_{ij}^e(\bar{v}\gamma_\mu Pu)(\bar{u}\gamma^\mu v)\,. \tag{C.32}$$

This time the amplitude is modified in the different energy ranges and one needs to be vary careful when comparing this result with the RGE amplitude.

C.4 PION DECAY RATE

In the following we state the procedure to calculate the Pion decay rate.

In order to calculate the decay width of the pion into leptons we can generally state that the matrix element reads

$$\mathcal{M} = \langle\mu\nu_\mu|\,\mathcal{L}_{\text{int}}\,|\pi^-\rangle\,, \tag{C.33}$$

where $\mathcal{L}_{\text{int}}$ is the interaction Lagrangian and $|\pi^-\rangle$, $|\mu\nu_\mu\rangle$ are respectively the initial and the final state.
The interaction Lagrangian reads

$$\mathcal{L}_{\text{int}} = \frac{G_F}{\sqrt{2}}V_{ud}\Big[(1+\epsilon_L)(\nu\gamma^\mu P_L\bar{\mu})(\bar{u}\gamma_\mu P_L d) + \epsilon_S^R(\nu P_L\bar{\mu})(\bar{u}P_R d) \\ +\epsilon_S^L(\nu P_L\bar{\mu})(\bar{u}P_L d) + \epsilon_T(\nu\sigma^{\mu\nu}P_L\bar{\mu})(\bar{u}\sigma_{\mu\nu}P_L d)\Big]\,, \tag{C.34}$$

Along with the definition of the interaction Lagrangian, in order to deal with $|\pi^-\rangle$ which is not an asymptotic state, one needs to define the elements of the Hilbert space

$$|\psi\rangle = |\text{leptons}\rangle\,|\text{hadrons}\rangle\,, \tag{C.35}$$

so that

$$|\pi^-\rangle = |0\rangle_L\,|\pi\rangle_H\,, \qquad |\mu^-\nu\rangle = |\mu^-\nu\rangle_L\,|0\rangle_H\,. \tag{C.36}$$

Then, in order to calculate C.33, one needs to define how the operators act on the states.
For what concerns the leptonic part, one can simply use the well known Feynman rules based on the annihilation and creation operators, since at low energies the perturbative approach is preserved.
For the hadronic part, instead, one needs to use symmetry properties, for example, imposing the parity transformation of a vector.

1 When considering quark running in the loop one needs to carefully consider the color, multiplying by three.

This approach leads to some well known relation, the so called Partially Conserved Axial Current (PCAC) relations, which must be implemented in the calculations.
They read

$$\begin{aligned} \langle 0|_L\, \bar{u}(0)\gamma^\mu d(0)\,|\pi(p)\rangle = 0\,, \quad \langle 0|_L\, \bar{u}(0)\gamma^\mu\gamma^5 d(0)\,|\pi(p)\rangle = i f_\pi p^\mu\,, \\ \langle 0|_L\, \bar{u}(0)\gamma^5 d(0)\,|\pi(p)\rangle = -i f_\pi \frac{m_\pi^2}{m_d + m_u}\,. \end{aligned} \tag{C.37}$$

By making use of C.37 one obtains

$$\begin{aligned} \mathcal{M} = -\,i f_\pi \frac{G_F}{\sqrt{2}} V_{ud} \Big[(1+\epsilon_L) p^\mu (\bar{u}(p^\mu)\gamma^\mu(1-\gamma_5)v(p_v)) \\ - (\epsilon_S^L - \epsilon_S^R)\frac{m_\pi^2}{m_d+m_u}(\bar{u}(p^\mu)(1-\gamma_5)v(p_v))\Big]\,. \end{aligned} \tag{C.38}$$

Then, using the Dirac equation $\bar{u}(p_\mu)\not{p}_\mu = \bar{u}(p_\mu)m_\mu$ the amplitude becomes

$$\mathcal{M} = -i f_\pi \frac{G_F}{\sqrt{2}} V_{ud}\, m_\mu \left[1 + \epsilon_L - (\epsilon_S^L - \epsilon_S^R)\frac{m_\pi^2}{m_\mu(m_d+m_u)}\right] (\bar{u}(p^\mu)(1-\gamma_5)v(p_v))\,. \tag{C.39}$$

The differential decay width reads

$$\begin{aligned} d\Gamma &= \frac{1}{32\pi^2}\frac{|p_\nu|}{m_\pi^2}\sum_{\text{spin}}|\mathcal{M}|^2 \\ &= \frac{1}{16\pi^2}\frac{|p_\nu|}{m_\pi^2} G_F^2 m_\pi^2 V_{ud}^2 f_\pi^2 (m_\pi^2 - m_\mu^2)\left|1 + \epsilon_L - (\epsilon_S^L - \epsilon_S^R)\frac{m_\pi^2}{m_\mu(m_d+m_u)}\right|^2 \end{aligned} \tag{C.40}$$

and, integrating over the solid angle, the total decay rate is obtained.

D

EXPLICIT CALCULATIONS OF SCATTERING AMPLITUDES

In the following we expose explicit results of scattering amplitudes of those processes that are of interest in neutrino physics experiments and will be of particular interest since they represent the main observables for the determination of NSI constraints at DUNE.

D.1 TRIDENT PRODUCTION

Trident events are processes where a neutrino impacting on a nucleus produces a lepton pair in the final state.

$$\nu_\mu N \to \nu_\mu \mu^+ \mu^- N \tag{D.1}$$

The process is rather difficult and involve the exchange of a virtual photon. The complete and general amplitude can be estimated by applying Feynman rules to the following Feynman diagram

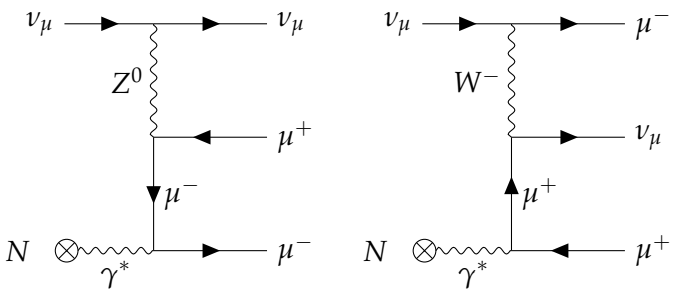

(1) (2)

but, since at DUNE are involved low energy neutrinos, the vector boson propagator can be neglected and the Feynman diagram reduces to

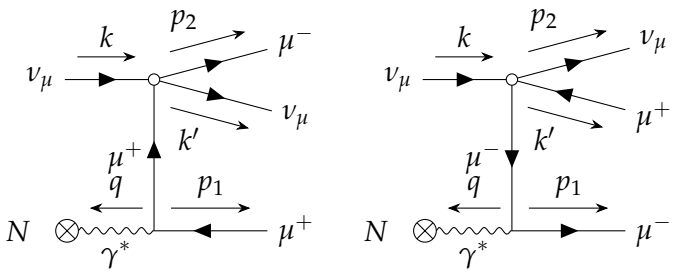

which corresponds in good approximation to the process

$$\nu_\mu \gamma^* \to \nu_\mu \mu^+ \mu^- \tag{D.2}$$

Using Feynman rules one gets the following expression for the matrix element

$$\begin{aligned}\mathcal{M} =& \frac{G_F}{\sqrt{2}} e\ \bar{u}(p_2)\epsilon_\mu \gamma^\mu \left[\frac{1}{p_2 - q - m_\mu} \gamma_\alpha g_R (1+\gamma_5) \right. \\ &\left. + \gamma_\alpha g_R (1+\gamma_5) \frac{1}{-p_1 + q - m_\mu} \right] \epsilon_\nu \gamma^\nu v(p_1) \cdot \bar{u}(k') \gamma^\alpha g_L (1-\gamma_5) u(k)\end{aligned} \tag{D.3}$$

the unpolarized squared amplitude, obtained by calculating traces of gamma matrices, reads

$$\begin{aligned}|\mathcal{M}|^2 =& 4e^2 G_F^2 (g_L^2 + g_R^2) \frac{(p_1 \cdot q)(k \cdot q)(p_2 \cdot k')}{[(p_1 - q)^2 - m_\mu^2]^2} + \frac{(p_2 \cdot q)(k' \cdot q)(p_1 \cdot k)}{[(p_2 - q)^2 - m_\mu^2]} \\ &+ \frac{(2p_1 \cdot p_2 - p_1 \cdot q - p_2 \cdot q)(p_1 \cdot k)(p_2 \cdot k') - (p_1 \cdot p_2)(p_1 \cdot k)(q. \cdot k')}{[(p_1 - q)^2 - m_\mu^2][(p_2 - q)^2 - m_\mu^2]} \\ &- \frac{(p_1 \cdot p_2)(p_2 \cdot k')(q \cdot k) + (q \cdot p_1)(k \cdot p_2)(k' \cdot p_2) + (q \cdot p_2)(p_1 \cdot k)(p_1 \cdot k')}{[(p_1 - q)^2 - m_\mu^2][(p_2 - q)^2 - m_\mu^2]}\end{aligned} \tag{D.4}$$

where the terms proportional to m_μ^2 were neglected.
Then, the differential cross section can be evaluated, being the flux $v_{\text{rel}} E_1 E_2 = k \cdot q$ and, leaving unspecified the phase space, it reads

$$\mathrm{d}\sigma = \frac{1}{(2\pi)^5 (k \cdot q)} |\mathcal{M}|^2 \delta^4(k + q - k' - p_1 - p_2) \frac{\mathrm{d}^3 p_1}{E_1} \frac{\mathrm{d}^3 p_2}{E_2} \frac{\mathrm{d}^3 k'}{E'} \tag{D.5}$$

Integrating D.5 as done in (39), one can obtain the following expression in the logarithm approximation of the total cross section

$$\sigma \simeq \frac{G_F^2}{9\pi^2} \alpha_{\text{em}} (g_L^2 + g_R^2) s \log \frac{s}{4m_\mu^2} \simeq 1 s/\text{MeV}^2 \tag{D.6}$$

where $s = (k+q)^2$ is the center of mass energy and the numerical value is in units of 10^{-46}cm^2.

D.2 NEUTRINO-ELECTRON ELASTIC SCATTERING

Low energy neutrinos (and antineutrinos) interact with electrons through an elastic scattering process whose sole effect is a redistribution of the total energy and momentum of the involved particles. The process reads

$$\nu_\alpha e^- \to \nu_\alpha e^- \tag{D.7}$$

and the general expression of the matrix element is similar for the different species of neutrinos α interacting with the electron.
Let's consider first of all the process of interest at DUNE which is the one for $\alpha = \mu$ which is mediated by the neutral Z boson. The amplitude for this process is obtained using Feynman rules from the diagram

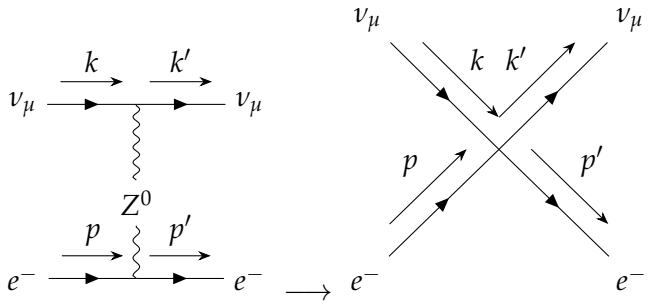

where, for low energy neutrinos the effects of the Z propagator can be neglected. We will refer then to the diagram on the right. The matrix element for this process reads

$$\mathcal{M} = \frac{G_F}{\sqrt{2}}[\bar{u}(k')g_L^\nu\gamma_\mu(1-\gamma_5)u(k)][\bar{u}(p')(g_L^e\gamma^\mu(1-\gamma_5)+g_R^e\gamma^\mu(1+\gamma_5))u(p)] \tag{D.8}$$

Summing over the final spin, averaging over the initial electron spin and performing the traces over gamma matrices one gets to the following squared amplitude

$$|\mathcal{M}|^2 = (16G_F^2)^2(g_L^\nu)^2[(g_L^e)^2(k\cdot p)^2 + (g_R^e)^2(k'\cdot p)^2] \tag{D.9}$$

where the term proportional to lepton masses have been neglected.
Consequently the differential cross-section is simply given by

$$\mathrm{d}\sigma = \frac{1}{4E_\nu m_e v_{\mathrm{rel}}}\frac{1}{(2\pi)^2}|\mathcal{M}|^2\delta^4(k+p-k'-p')\frac{\mathrm{d}^3k'}{2E_\nu}\frac{\mathrm{d}^3p'}{2E_e} \tag{D.10}$$

Easily integrating the phase space and expressing it in terms of a conventional scaling variable $y = E_e/E_\nu = [0,1]$ we get

$$\frac{\mathrm{d}\sigma}{\mathrm{d}y} = \frac{8G_F^2}{\pi}m_e E_\nu (g_L^\nu)^2[(g_L^e)^2 + (g_R^e)^2(1-y)^2] \tag{D.11}$$

and integrating over y the total cross section becomes

$$\sigma(\nu_\mu e) = \frac{G_F^2 s}{4\pi}\left[(g_L^e)^2 + \frac{1}{3}(g_R^e)^2\right]. \tag{D.12}$$

where $s = 2m_e E_\nu$ is the center-of-mass energy squared of the collision.

Notice that, the cross section for the anti-neutrino process

$$\bar{\nu}_\mu e^- \to \bar{\nu}_\mu e^- \tag{D.13}$$

can be inferred in complete analogy, in fact the matrix element reads

$$\mathcal{M} = \frac{G_F}{\sqrt{2}}[\bar{u}(k')g_L^\nu\gamma_\mu(1-\gamma_5)u(k)][\bar{u}(p')(g_L^e\gamma^\mu(1+\gamma_5) + g_R^e\gamma^\mu(1-\gamma_5))u(p)] \tag{D.14}$$

which correspond to shifting $g_L^e \to g_R^e$. The cross section then becomes

$$\sigma(\bar{\nu}e) = \frac{G_F^2 s}{4\pi}\left[(g_R^e)^2 + \frac{1}{3}(g_L^e)^2\right]. \tag{D.15}$$

For what concerns the scattering involving electron neutrinos, $\alpha = e$, one need to consider both the neutral and the charged current. But, thanks to a Fierz transformation it is possible to rewrite the charged current as a neutral one. The total amplitude, which corresponds to the sum of the neutral and charged current reads

$$\begin{aligned}\mathcal{M} =& \frac{G_F}{\sqrt{2}}[\bar{u}(k')g_L^\nu\gamma_\mu(1-\gamma_5)u(k)][\bar{u}(p')((g_L^e\gamma^\mu(1-\gamma_5) + g_R^e\gamma^\mu(1+\gamma_5))u(p)] \\ &+ \frac{G_F}{\sqrt{2}}[\bar{u}(k')g_L^\nu\gamma_\mu(1-\gamma_5)u(k)][\bar{u}(p')\gamma^\mu(1-\gamma_5)u(p)]\,.\end{aligned} \tag{D.16}$$

Summing the neutral and the charged current then, can be seen as a shift of $g_L \to g_L + 1$ and the total cross section can be inferred from D.12 and reads

$$\sigma(\nu_e e) = \frac{G_F^2 s}{4\pi}\left[(g_L^e + 1)^2 + \frac{1}{3}(g_R^e)^2\right]. \tag{D.17}$$

Consequently, the cross section for the conjugated scattering can be obtained in analogy to the $\nu_\mu e$ scattering.

It is now possible to make a comparison between the different neutrino-electron elastic cross sections in order to get a better acknowledgment of the phenomenon.

Table D.1: Total neutrino-electron elastic scattering cross-section. The numerical values are in units of 10^{-46}cm^2 and given by (40).

Process	Total cross-section
$\nu_e + e^-$	$\frac{G_F^2 s}{4\pi}[(g_L^e+1)^2 + \frac{1}{3}(g_R^e)^2] \simeq 93s/\text{MeV}^2$
$\bar{\nu}_e + e^-$	$\frac{G_F^2 s}{4\pi}[(g_R^e)^2 + \frac{1}{3}(g_L^e+1)^2] \simeq 39s/\text{MeV}^2$
$\nu_\mu + e^-$	$\frac{G_F^2 s}{4\pi}[(g_L^e)^2 + \frac{1}{3}(g_R^e)^2] \simeq 15s/\text{MeV}^2$
$\bar{\nu}_\mu + e^-$	$\frac{G_F^2 s}{4\pi}[(g_R^e)^2 + \frac{1}{3}(g_L^e)]^2 \simeq 13s/\text{MeV}^2$

D.3 NEUTRINO-NUCLEUS QUASI-ELASTIC SCATTERING

At the energies at stake at DUNE $E_\nu \lesssim m_N$ so, in this energy regime the deep inelastic scattering is excluded. The interaction is in a quasi-elastic regime and involves proton and neutron can be both NC and CC

$$\nu_\mu n \to \nu_\mu n \qquad \nu_\mu n \to \mu^- p \tag{D.18}$$

and analogously for the antineutrino.
The observable at DUNE will be the ration between the NC and CC cross section but, since as showed by Lewellyn-Smith(38) it is possible to express this ratio only in term of the CC cross section we provide an explicit calculation of that one only.
The Feynman diagram reads

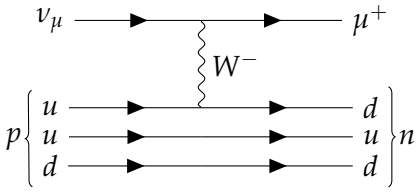

from it is possible to calculate the matrix element, which is build taking into account the relevant form factors that are related to the inner hadronic structure. In this case, being at low energy, we can assume the form factors do not vary with the transferred momentum and we take them to be constant. The matrix element, containing the most general Lorentz structure then reads

$$\mathcal{M} = \frac{G_F V_{ud}}{\sqrt{2}}\left[\bar{u}_n(\gamma_\mu(g_V - g_A) - \frac{iF_2}{2M}\sigma_{\mu\nu}q^\nu)u_p\right]\,[\bar{v}_\nu\gamma^\mu(g_V - g_A)v_e] \tag{D.19}$$

where F_2 is the anomalous nucleon isovector magnetic moment, defined as $F_2 = \mu_p - \mu_n = 3.706$.
Then, the differential decay width reads

$$\mathrm{d}\sigma = \frac{1}{4E_\nu m_\mu v_{\text{rel}}}\frac{1}{(2\pi)^2}|\mathcal{M}|^2\delta^4(k+p-k'-p')\frac{\mathrm{d}^3k'}{2E_\nu}\frac{\mathrm{d}^3p'}{2E_\mu} \tag{D.20}$$

by expressing it in terms of the angular variation one gets, following (41)

$$\frac{\mathrm{d}\sigma}{\mathrm{d}\cos\theta} = \frac{G_F^2|V_{ud}|^2}{\pi}\left[(g_V^2 + 3g_A^2 + (g_V^2 - g_A^2)\frac{p_e}{E_e}\cos(\theta)\right] E_e p_e \tag{D.21}$$

and integrating over the angle a standard expression for the total cross section is obtained

$$\sigma_{CC} \simeq \frac{G_F^2|V_{ud}|^2}{\pi}(g_V^2 + 3g_A^2)E_e p_e \simeq 30 \times s/\mathrm{MeV}^2 \tag{D.22}$$

and evaluated in unit of $10^{-46}\mathrm{cm}^2$.
The expression for the conjugated process is just analogous with the only exception that $g_A \to -g_A$.

BIBLIOGRAPHY

1. Y. Farzan, M. Tortola, "Neutrino oscillations and Non-Standard Interactions", *Front. in Phys.* **6**, 10 (2018).
2. G. 't Hooft *et al.*, "Recent Developments in Gauge Theories. Proceedings, Nato Advanced Study Institute, Cargese, France, August 26 - September 8, 1979", *NATO Sci. Ser. B* **59**, pp.1–438 (1980).
3. G. Jungman, M. Kamionkowski, K. Griest, "Supersymmetric dark matter", *Phys. Rept.* **267**, 195–373 (1996).
4. A. Crivellin *et al.*, "Lepton-flavour violating B decays in generic Z' models", *Phys. Rev. D* **92**, 054013 (2015).
5. M. Knecht, "The Muon Anomalous Magnetic Moment", *Nucl. Part. Phys. Proc.* **258-259**, 235–240 (2015).
6. M. S. Turner, "Windows on the Axion", *Phys. Rept.* **197**, 67–97 (1990).
7. C. Biggio, M. Blennow, E. Fernandez-Martinez, "General bounds on non-standard neutrino interactions", *JHEP* **08**, 090 (2009).
8. O. G. Miranda, H. Nunokawa, "Non standard neutrino interactions: current status and future prospects", *New J. Phys.* **17**, 095002 (2015).
9. P. A. R. Ade *et al.*, "Planck 2013 results. XVI. Cosmological parameters", *Astron. Astrophys.* **571**, A16 (2014).
10. P. Langacker, N. Polonsky, "Uncertainties in coupling constant unification", *Phys. Rev.D* **47**, 4028–4045 (1993).
11. B. Pontecorvo, "Neutrino Experiments and the Problem of Conservation of Leptonic Charge ", *JETP* **26**, 984 (1968).
12. J. Beringer *et al.*, "Review of Particle Physics", *Phys. Rev. D* **86**, 010001 (1 July 2012).
13. J. Schechter, J. W. F. Valle, "Neutrino masses in SU(2) $\times$ U(1) theories", *Phys. Rev. D* **22**, 2227–2235 (9 Nov. 1980).
14. B. T. Cleveland *et al.*, "Measurement of the Solar Electron Neutrino Flux with the Homestake Chlorine Detector", *The Astrophys. J.* **496**, 505–526 (Mar. 1998).
15. W. Hampel *et al.*, "GALLEX solar neutrino observations: Results for GALLEX IV", *Phys. Lett. B* **447**, 127–133 (1999).
16. A. J. N., S. collaboration, "Results from SAGE (the Russian-American gallium solar neutrino experiment)", *Phys. Let. B* **328**, ed. by E. Science, 234–248, ISSN: 0370-2693 (1994).
17. Q. R. Ahmad *et al.*, "Measurement of the rate of $\nu_e + d \rightarrow p + p + e^-$ interactions produced by ^8B solar neutrinos at the Sudbury Neutrino Observatory", *Phys. Rev. Lett.* **87**, 071301 (2001).

18. S. P. Rosen, J. M. Gelb, "Mikheyev-Smirnov-Wolfenstein enhancement of oscillations as a possible solution to the solar-neutrino problem", **34**, 969–979 (Aug. 1986).
19. Y. Fukuda *et al.*, "Evidence for oscillation of atmospheric neutrinos", *Phys. Rev. Lett.* **81**, 1562–1567 (1998).
20. M. G. Aartsen *et al.*, "IceCube-Gen2: A Vision for the Future of Neutrino Astronomy in Antarctica", *PoS* **FRAPWS2016**, 004 (2017).
21. W. Buchmuller, D. Wyler, "Effective Lagrangian Analysis of New Interactions and Flavor Conservation", *Nucl. Phys. B* **268**, 621–653 (1986).
22. B. Grzadkowski, M. Iskrzynski, M. Misiak, J. Rosiek, "Dimension-Six Terms in the Standard Model Lagrangian", *JHEP* **10**, 085 (2010).
23. A. V. Manohar, M. B. Wise, *Heavy Quark Physics* (Cambridge University Press, 2000).
24. M. Neubert, presented at the Physics in $D \geq 4$. Proceedings, Theoretical Advanced Study Institute in elementary particle physics, TASI 2004, Boulder, USA, June 6-July 2, 2004, pp. 149–194, arXiv: `hep-ph/0512222 (hep-ph)`.
25. B. Bellazzini, Y. Grossman, I. Nachshon, P. Paradisi, "Non-Standard Neutrino Interactions at One Loop", *JHEP* **06**, 104 (2011).
26. F. Feruglio, P. Paradisi, A. Pattori, "On the Importance of Electroweak Corrections for B Anomalies", *JHEP* **09**, 061 (2017).
27. E. E. Jenkins, A. V. Manohar, M. Trott, "Renormalization Group Evolution of the Standard Model Dimension Six Operators I: Formalism and lambda Dependence", *JHEP* **10**, 087 (2013).
28. E. E. Jenkins, A. V. Manohar, M. Trott, "Renormalization Group Evolution of the Standard Model Dimension Six Operators II: Yukawa Dependence", *JHEP* **01**, 035 (2014).
29. R. Alonso, E. E. Jenkins, A. V. Manohar, M. Trott, "Renormalization Group Evolution of the Standard Model Dimension Six Operators III: Gauge Coupling Dependence and Phenomenology", *JHEP* **04**, 159 (2014).
30. R. D. C. Miller, B. H. J. McKellar, "Anomalous-dimension matrices of four-quark operators", *Phys. Rev. D* **28**, 844–855 (4 Aug. 1983).
31. J. C. Collins, *Renormalization: An Introduction to Renormalization, the Renormalization Group and the Operator-Product Expansion* (Cambridge University Press, 1984).
32. M. Gonzalez-Alonso, J. Martin Camalich, K. Mimouni, "Renormalization-group evolution of new physics contributions to (semi)leptonic meson decays", *Phys. Lett. B* **772**, 777–785 (2017).
33. M. G. Aartsen *et al.*, "Search for Nonstandard Neutrino Interactions with IceCube DeepCore", arXiv: `1709.07079 (hep-ex)` (2017).
34. J. Salvado, O. Mena, S. Palomares-Ruiz, N. Rius, "Non-standard interactions with high-energy atmospheric neutrinos at IceCube", *JHEP* **01**, 141 (2017).

35. M. Honda, M. Sajjad Athar, T. Kajita, K. Kasahara, S. Midorikawa, "Atmospheric neutrino flux calculation using the NRLMSISE-00 atmospheric model", *Phys. Rev. D* **92**, 023004 (2015).

36. T. Alion *et al.*, "Experiment Simulation Configurations Used in DUNE CDR", arXiv: 1606.09550 (physics.ins-det) (2016).

37. A. Falkowski, G. Grilli di Cortona, Z. Tabrizi, "Future DUNE constraints on EFT", arXiv: 1802.08296 (hep-ph) (2018).

38. C. Smith, "On the determination of $\sin^2\theta_w$ in semi-leptonic neutrino interactions", *Nucl. Phys. B* **228**, 205–215, ISSN: 0550-3213 (1983).

39. R. Belusevic, J. Smith, "W-Z interference in ν-nucleus scattering", *Phys. Rev. D* **37**, 2419–2422 (9 May 1988).

40. C. Giunti, C. W. Kim, *Fundamentals of Neutrino Physics and Astrophysics* (Oxford University Press, 2007).

41. P. Vogel, J. F. Beacom, "Angular distribution of neutron inverse beta decay, $\bar{\nu}_e + p \to e^+ + n$", *Phys. Rev. D* **60**, 053003 (1999).

42. C. Cornella, F. Feruglio, P. Paradisi, "Low-energy Effects of Lepton Flavour Universality Violation", arXiv: 1803.00945 (hep-ph) (2018).

43. L. B. Okun, *Leptons and Quarks* (World Scientific Press, 1986).

44. S. Bilenky, *Introduction to the Physics of Massive and Mixed Neutrinos* (Springer Heidelberg, 2010).

45. J. Valle, J. Romao, *Neutrinos in High Energy and Astroparticle Physics* (Wiley-VCH, 2015).

46. N. Fornengo, M. Maltoni, R. Tomas, J. W. F. Valle, "Probing neutrino non-standard interactions with atmospheric neutrino data", *Phys. Rev. D* **65**, 013010 (2002).

47. M. C. Gonzalez-Garcia, M. Maltoni, "Atmospheric neutrino oscillations and new physics", *Phys. Rev. D* **70**, 033010 (2004).

48. M. Gonzalez-Alonso, J. Martin Camalich, "Global Effective-Field-Theory analysis of New-Physics effects in (semi)leptonic kaon decays", *JHEP* **12**, 052 (2016).

49. P. F. de Salas, D. V. Forero, C. A. Ternes, M. Tortola, J. W. F. Valle, "Status of neutrino oscillations 2017", arXiv: 1708.01186 (hep-ph) (2017).

50. T. Ohlsson, H. Zhang, S. Zhou, "Effects of nonstandard neutrino interactions at PINGU", *Phys. Rev. D* **88**, 013001 (2013).

51. M. Day, I. Collaboration, "Non-standard neutrino interactions in IceCube", *J.l of Phys.: Conference Series* **718**, 062011 (2016).